

OUT-OF-PLANE SEISMIC BEHAVIOR OF BRICK AND PUMICE
CONCRETE INFILL WALLS BUILT INTO THE RC FRAME

A THESIS SUBMITTED TO
THE GRADUATE SCHOOL OF NATURAL AND APPLIED SCIENCES
OF
MIDDLE EAST TECHNICAL UNIVERSITY

BY

SAİME SELİN AKTAŞ

IN PARTIAL FULFILLMENT OF THE REQUIREMENTS
FOR
THE DEGREE OF MASTER OF SCIENCE
IN
EARTHQUAKE STUDIES

JANUARY 2023

Approval of the thesis:

**OUT-OF-PLANE SEISMIC BEHAVIOR OF BRICK AND PUMICE
CONCRETE INFILL WALLS BUILT INTO THE RC FRAME**

submitted by **Saime Selin Aktaş** in partial fulfillment of the requirements for the degree of Master of Science in Earthquake Studies, **Middle East Technical University** by,

Prof. Dr. Halil Kalıpçılar
Dean, Graduate School of **Natural and Applied Sciences**

Prof. Dr. Ayşegül Askan
Head of the Department, **Earthquake Studies**

Prof. Dr. Erdem Canbay
Supervisor, **Civil Engineering, METU**

Examining Committee Members:

Prof. Dr. Barış Binici
Civil Engineering, METU

Prof. Dr. Erdem Canbay
Civil Engineering, METU

Prof. Dr. Ahmet Yakut
Civil Engineering, METU

Prof. Dr. Kağan Tuncay
Civil Engineering, METU

Assoc. Prof. Dr. Alper Aldemir
Civil Engineering, Hacettepe University

Date: 27.01.2023

I hereby declare that all information in this document has been obtained and presented in accordance with academic rules and ethical conduct. I also declare that, as required by these rules and conduct, I have fully cited and referenced all material and results that are not original to this work.

Name Last name: Saime Selin Aktaş

Signature:

ABSTRACT

OUT-OF-PLANE SEISMIC BEHAVIOR OF BRICK AND PUMICE CONCRETE INFILL WALLS BUILT INTO THE RC FRAME

Aktaş, Saime Selin
Master of Science, Earthquake Studies
Supervisor: Prof. Dr. Erdem Canbay

January 2023, 106 pages

Unreinforced infill walls are widely used non-structural elements in structures worldwide for architectural and engineering disciplines. The seismic capacity and response of unreinforced infill walls have been ignored until realizing the importance of these members during many seismic events and their aftermaths. Thus, the out-of-plane behavior of infill walls has become a topic that has been popular to investigate in the last decades for civil engineers especially. Although different infill materials are used to construct, traditional clay brick is the most preferred infill material. However, as new infill materials are discovered and developed, improving knowledge has become a necessity for different infill materials. Pumice concrete blocks are one of the popular infill materials used in recent years. This infill material is chosen due to its high thermal insulation, aesthetic concerns, and acoustic advantages. However, its seismic behavior, one of the characteristics of the pumice concrete infill walls, has not been discussed in detail in the literature. This study focuses on the out-of-plane behavior of clay brick and pumice concrete infill walls and their comparison. In addition, the presence of openings and different opening sizes were simulated for both clay brick and pumice concrete infill walls and tested under out-of-plane loading. Demand and design thickness estimation for both clay

brick and pumice concrete infill walls were investigated for different spectral accelerations and story numbers of reinforced concrete structures.

Keywords: Infill walls, Out-of-plane, Experimental study, Yield line analysis, Seismic behavior

ÖZ

BETONARME ÇERÇEVE İÇİNE ÖRÜLEN TUĞLA VE BİMS DOLGU DUVARLARIN DÜZLEM DIŐI SİSMİK DAVRANIŐI

Aktaő, Saime Selin
Yüksek Lisans, Deprem Çalıőmaları
Tez Yöneticisi: Prof. Dr. Erdem Canbay

Ocak 2023, 106 sayfa

Donatısız dolgu duvarlar, mimari ve mühendislik disiplinlerinde tüm dünyada yapılar da yaygın olarak kullanılan yapısal olmayan elemanlardır. Donatısız dolgu duvarların sismik kapasitesi ve tepkisi, birçok sismik olay ve sonrasında bu elemanların önemi fark edile kadar göz ardı edilmiştir. Bu yüzden dolgu duvarların düzlem dıőı davranıőı, özellikle inőaat mühendisleri için son yıllarda araőtırılması yaygın olan bir konu haline gelmiştir. İnőası için farklı dolgu malzemeleri kullanılsa da, geleneksel kil tuęla en çok tercih edilen dolgu malzemesidir. Bununla birlikte, yeni dolgu malzemeleri keőfedilip geliőtirildikçe, farklı dolgu malzemeleri için bilgi birikiminin artırılması bir gereklilik haline gelmiştir. Bims beton bloklar son yıllarda kullanılan yaygın dolgu malzemelerinden birisidir. Bu dolgu malzemesi, yüksek ısı yalıtımı, estetik kaygılar ve akustik avantajları nedeniyle sečilmektedir. Ancak bims beton dolgu duvarların özelliklerinden biri olan sismik davranıőı literatürde detaylı olarak ele alınmamıştır. Bu bağlamda, bu çalışmada kil tuęla ve bims beton dolgu duvarların düzlem dıőı davranıőları ve birbirleriyle karşılaştırılması üzerinde durulmuőtur. Ek olarak, dolgu duvarlardaki boşlukların varlıęı ve farklı boşluk boyutları hem kil tuęla hem bims beton dolgu duvarlar için simüle edilmiş ve düzlem dıőı yük altında test edilmiştir. Betonarme yapıların farklı spektral ivmelerine ve kat

sayılarına göre hem kil tuđla hem de bims beton dolgu duvarlar için talep ve tasarım kalınlık tahmini alıřılmıřtır.

Anahtar Kelimeler: Dolgu duvar, Deneysel alıřma, Akma izgisi analizi, Sismik davranıř

To my dear family

To the memory of dear uncle Bedri ...

ACKNOWLEDGMENTS

I want to express my deepest gratitude to my supervisor Prof. Dr. Erdem Canbay, for supporting, guiding, trusting, and believing in me starting from my undergraduate years to the end of the graduate program. I want to thank him for encouraging me and for everything he taught me patiently over and over again. I am grateful to him for teaching me how to conduct an experiment in the laboratory. Finally, I thank him for accepting me as a master's student.

I am deeply grateful to Prof. Dr. Barış Binici for believing in me in any circumstances. I thank him for the things he taught me and for spending time with me without hesitating. I am grateful to him for teaching me how to improve my knowledge.

I want to thank Prof. Dr. Ahmet Yakut for helping me during this study and spending his time explaining what I ask, even if he is busy. I am so grateful for the motivation he gave in the times I lost my motivation.

I want to thank the technicians of the Uğur Ersoy Structural Laboratory for helping me in the preparation of the test set-up for each test I conducted. I also want to thank them for sharing their experiences in the laboratory.

I am grateful to Salim Azak for sharing his knowledge and helping me in the laboratory.

Finally, I would like to thank my dear mother and sister for supporting me and believing in me during those times, even though I did not believe in myself and thought of giving up. I am so grateful to my friends for supporting me and giving me strength and hope when it is difficult to bear.

This work is partially funded by Turkey Disaster and Management Authority (AFAD) under grant number UDAP-G-20-04.

TABLE OF CONTENTS

ABSTRACT.....	v
ÖZ	vii
ACKNOWLEDGMENTS	x
TABLE OF CONTENTS.....	xi
LIST OF TABLES	xiii
LIST OF FIGURES	xiv
CHAPTERS	
1 INTRODUCTION	1
1.1 General.....	1
1.2 Literature Review.....	2
1.2.1 On the Out-of-Plane Behavior of Infill Walls.....	3
1.2.2 Related Codes	11
1.3 Motivation and Objective.....	14
2 EXPERIMENTAL WORK.....	17
2.1 Introduction.....	17
2.2 Test Setup and Instrumentation	17
2.3 Testing on Infill Constituents.....	25
2.4 Test Specimens	27
2.5 Test Results	28

2.5.1	Wall WBHN	31
2.5.2	Wall WBVN1	32
2.5.3	Wall WBVN2	35
2.5.4	Wall WBVW	38
2.5.5	Wall WBVD	41
2.5.6	Wall WPVN.....	43
2.5.7	Wall WPVW.....	46
2.5.8	Wall WPVD.....	49
2.6	Comparisons of Test Results	56
3	ANALYSIS	61
3.1	Out-of-Plane Capacity of Infill Walls	61
3.1.1	Yield Line Analysis of Test Specimens	61
3.1.2	Demand Calculation of Infill Walls	73
3.2	Design Thickness of Infill Walls	83
4	CONCLUSION	93
	REFERENCES	97
	APPENDIX	
A.	Yield Line Analysis Solutions for Infill Walls Without Opening	103

LIST OF TABLES

TABLES

Table 2.1 Capacities and Places of LVDTs	25
Table 2.2 Detailed Information of Tested Specimens.....	28
Table 2.3 Mechanical Properties of Mortar and Plasters	29
Table 2.4 Maximum Load and Corresponding Deflections of the Specimens	60
Table 3.1 Comparison of Test Results with Yield Line Analysis for Infill Walls Without Opening.....	67
Table 3.2 Comparison of Test Results with Yield Line Analysis for Infill Walls With Window Opening	68
Table 3.3 Comparison of Test Results with Yield Line Analysis for Infill Walls with Door Opening	69
Table 3.4 One-Way Failure Assumption	70
Table 3.5 Suggested C_0 Values	75
Table 3.6 Suggested C_2 values	75
Table 3.7 Design Wall Thickness for 0.2 MPa Flexural Strength	89
Table 3.8 Design Wall Thickness for 0.4 MPa Flexural Strength	89
Table 3.9 Design Wall Thickness for 0.6 MPa Flexural Strength	90
Table 3.10 Design Wall Thickness for 0.8 MPa Flexural Strength	90
Table 3.11 Design Wall Thickness for 1.0 MPa Flexural Strength	91

LIST OF FIGURES

FIGURES

Figure 2.1. Dimension Details of Reinforced Concrete Frame	18
Figure 2.2. Reinforcement Details of Reinforced Concrete Frame	19
Figure 2.3. Infill Wall Materials	20
Figure 2.4. In Details of Test Setup	21
Figure 2.5. Instruments of Test Setup	22
Figure 2.6. The Placement of LVDTs	23
Figure 2.7. Cube and Prismatic Specimens of Constituents	26
Figure 2.8. Built WBHN Without Plaster on i	31
Figure 2.9. Deflected Shape of WBHN Before Failure	32
Figure 2.10. Load-Deflection Relation of Specimen WBHN	32
Figure 2.11. Built WBVN1 Without Plaster on it	33
Figure 2.12. Deflected Shape of WBVN1 Before the Failure	33
Figure 2.13. Crack Path of WBVN1 Experiment	34
Figure 2.14. Load-Deflection Relation of Specimen WBVN1	35
Figure 2.15. Built WBVN2 Without Plaster on it	36
Figure 2.16. Deflected Shape of WBVN2 Before the Failure	36
Figure 2.17. Crack Path of WBVN2 Experiment	37
Figure 2.18. Load-Deflection Relation of Specimen WBVN2	38
Figure 2.19. Built WBVW Without Plaster on it	38
Figure 2.20. Deflected Shape of WBVW Before the Failure	39
Figure 2.21. Crack Path of WBVW Experiment	39
Figure 2.22. Load-Deflection Relation of Specimen WBVW	40
Figure 2.23. Built WBVD Without Plaster on it	41
Figure 2.24. Deflected Shape of WBVD Before the Failure	41
Figure 2.25. Crack Path of WBVD Experiment	42
Figure 2.26. Load-Deflection Relation of Specimen WBVD	43

Figure 2.27. Built WPVN Without Plaster on it	44
Figure 2.28. Deflected Shape of WPVN Before the Failure.....	44
Figure 2.29. Crack Path of WPVN Experiment.....	45
Figure 2.30. Load-Deflection Relation of Specimen WPVN	46
Figure 2.31. Built WPVW Without Plaster on it	47
Figure 2.32. Deflected Shape of WPVW Before the Failure.....	47
Figure 2.33. Crack Path of WPVW Experiment.....	48
Figure 2.34. Load-Deflection Relation of Specimen WPVW	49
Figure 2.35. Built WPVD Without Plaster on it	50
Figure 2.36. Deflected Shape of WPVD Before the Failure.....	50
Figure 2.37. Crack Path of WPVD	51
Figure 2.38. Load-Deflection Relation of Specimen WPVD	52
Figure 2.39. The Corresponding Loads of Cracks for WBVN1	53
Figure 2.40. The Corresponding Loads of Cracks for WBVN2	53
Figure 2.41. The Corresponding Loads of Cracks for WBVW	54
Figure 2.42. The Corresponding Loads of Cracks for WBVD	54
Figure 2.43. The Corresponding Loads of Cracks for WPVN	55
Figure 2.44. The Corresponding Loads Of Cracks for WPVW.....	55
Figure 2.45. The Corresponding Loads of Cracks for WPVD	56
Figure 2.46. Load-Deflection Relation of Clay Brick Infill Walls	58
Figure 2.47. Load-Deflection Relation of Pumice Concrete Infill Walls	58
Figure 2.48. Load-Deflection Relation of Infill Walls Without Opening.....	59
Figure 2.49. Load-Deflection Relation of Infill Walls With Door Opening.....	59
Figure 2.50. Load-Deflection Relation of Infill Walls with Window Opening.....	60
Figure 3.1. Assumed Yield Pattern for Four Sided fixed Supported Infill Wall	62
Figure 3.2. Assumed Yield Pattern for One-Way Bending for Infill Wall.....	63
Figure 3.3. Yield Line Patterns for Four Sides Fixed-End Boundary Conditions..	64
Figure 3.4. Yield Line Patterns for Three Sides Fixed + One Side Simply Supported Boundary Conditions	64

Figure 3.5. Yield Line Patterns for both Fixed-End and Simply Supported Boundary Conditions of One-Way Infill Walls.....	65
Figure 3.6. Failure State of Clay Brick Infill Walls	71
Figure 3.7. Failure State of Pumice Concrete Infill Walls	72
Figure 3.8. Demand and Story Number Relation of İstanbul Using FEMA356	77
Figure 3.9. Demand and Story Number Relation of Ankara Using FEMA356	78
Figure 3.10. Comparison of Demand Capacities Using FEMA356 and TEC2018.	79
Figure 3.11. Comparison of Demand Capacities Using FEMA356 and TEC2018 for Ankara.....	80
Figure 3.12. Demand and Capacity Comparison of the Infill Walls	81
Figure 3.13. Design Thickness of Clay Brick Infill Walls	85
Figure 3.14. Design Thickness of Pumice Concrete Infill Walls	87

CHAPTER 1

INTRODUCTION

1.1 General

Structures contain various numbers of members for different purposes. These members can be listed under two main groups structural and non-structural members. Infill walls (IW) are considered non-structural or secondary structural elements used to infill reinforced concrete or steel frames. They are widely used members in frame structures in developing countries (Yu et al., 2019). These walls are mostly preferred for fire resistance as well as thermal and acoustic insulation. Infill walls are also used for architectural concerns and aesthetic purposes.

Extreme pressure events such as earthquakes, strong winds, or explosive loads may generate an out-of-plane collapse of infill walls. The observations of the failure of unreinforced infill walls prove that the collapse of unreinforced infill walls risks human life and causes economic loss (Akhoundi et al., 2020). Even if the hazard on these walls does not risk human life, any visible damage disturbs the psychology of occupants

The failure of unreinforced infill walls affects not only non-structural issues but also the seismic capacity of the structures. Several studies have investigated the behavior for different purposes and proved the load-bearing capacity of infill walls in many different boundary conditions. [Brown&Maji,2002; Ehsani et al.,1997; Binici et al., 2019; Demirel et al., 2018. Recent earthquakes (e.g., Van 2011, İzmir 2020) have shown the need for appropriate construction and design of infill walls due to their poor seismic response during seismic events. In addition to the poor seismic response of infill walls, their behavior is also critical during an earthquake. Unreinforced infill masonry walls may significantly change the expected structural response by applying forces on parts of the structure that are not designed to resist them (Paulay

& Priestley, 1992). This situation leads to significant hazard that causes fatal damage. Although the seismic capacity of the unreinforced infill walls gained importance, studies are usually about the in-plane behavior of the infill walls. In recent years, however, the out-of-plane capacity and behavior of infill walls have become more critical because the out-of-plane failure of infill walls also affects the in-plane capacity of these elements (Binici et al., 2019b; Ghobarah et al., 2004). It was observed that out-of-plane failure of an infill wall results in losing the infill wall's vertical and lateral seismic bearing capacity(Ghobarah et al., 2004). Moreover, it was observed that out-of-plane loading decreases the drift capacity as a function of the out-of-plane loading (Binici et al., 2019). In that spirit, many studies were performed by combining both in-plane and out-of-plane loading to understand how the loading procedure affects the capacity and behavior of infill wall in both directions (da Porto et al., 2013.; Ghobarah et al., 2004; Xie et al., 2021).

The numerical and experimental studies presented that the out-of-plane capacities of the infill walls cannot be underestimated (Martini, 1998) [Griffith et al., 2009]. As a result, some researchers have started focusing on the infill walls' out-of-plane behavior more than the in-plane behavior (Derakhshan, 1994; Doherty et al., 2002). Different parameters, such as openings, bonding with the frame, loading procedure, etc., have been chosen to examine the behavior and capacity of the infill walls.

1.2 Literature Review

The behavior of composite systems, such as infilled frames under out-of-plane loading, is one of the subjects studied in structural and earthquake engineering, especially in recent years. The various empirical and analytical results are accepted in the literature for masonry infill walls built with different infill materials. The related studies are improved in time in light of the previous studies on this subject. The valuable knowledge obtained from the earlier studies is summarized below.

1.2.1 On the Out-of-Plane Behavior of Infill Walls

Ghobarah and Galal [2004] studied the capacity and failure difference between strengthened and unstrengthened unreinforced masonry walls with different openings on out-of-plane loading. An experimental study that included five full-scale masonry wall experiments was performed to observe the difference between strengthened and unstrengthened masonry walls. The openings of the constructed walls were chosen as a single center window, a wide window, two windows, one window off-center, and a door. The uniformly distributed out-of-plane loading was applied using an air bag for all experiments. The study showed that strengthened masonry walls have the significantly higher load-carrying capacity and behave much more ductile.

Milanesi et al. [2021] focused on verifying the existing formulas and design procedures in the codes for the out-of-plane behavior of strong masonry infills. The strong masonry infills can have a considerable impact on infilled structures. Moreover, since the present codes, such as European seismic codes (EC-Part 1,2004) and Italian Norms of Construction, do not consider masonry infills as structural elements, these codes do not offer adequate design provisions. The authors conducted two tests for strong masonry infills with out-of-plane loading without combining them with any in-plane load to fill some gaps in the currently used codes for masonry infills. Furthermore, they used the result of previous studies in the literature. The results enabled applying and evaluation of the extant formulas in the present codes and literature for computing the fundamental period and out-of-plane capacity. Considering the results of the performed tests, some additional formulations were proposed. Some dimensionless parameters, such as the bidirectional response of the strong masonry infills, second-order effects, the deformability of the RC frame, and the presence of local failure mechanisms like sliding at the frame/infill interface, were introduced to the proposed equations for physical aspects.

Derakhshan et al. [2013] developed an analytical model to characterize the out-of-plane response of one-way spanning unreinforced masonry (URM) walls by analyzing the impact of several parameters. The qualities of the diaphragm support stiffness, the compressive strength of the masonry, and the horizontal crack height were taken into account as variables, and sensitivity analyses were carried out to investigate the effects of these variables on the behavior of cracked masonry infills. The study showed that the wall's instability displacement and lateral resistance are significantly affected by the crack height. Moreover, it was proved that the applied overburden considerably amplifies the decrease in lateral resistance and the instability resistance of the cracked infill due to finite masonry compressive strength. An existing trilinear model to define the out-of-plane response for a broader range of URM walls was improved, and a method for calculating the out-of-plane response envelope was proposed.

Griffith et al. [2003] studied a systematic evaluation of a simplified method for determining how unreinforced masonry (URM) walls may react to out-of-plane seismic excitation. A total of 1248 case studies were evaluated by combining meaningful parameters describing the URM walls and ground motions. The nonlinear force-displacement reaction of a URM wall was modeled using an appropriate tri-linear curve. A nonlinear SDOF dynamic time-history analysis was conducted for each case study. The results of the analyses were accepted as the reference for a simplified “equivalent stiffness” approach. One of the most applicable conclusions of the results indicates that the initial stiffness and initial period are not essential in determining the onset of failure. Furthermore, the vital parameters that affect the collapse are the second and third branches, which are the maximum strength and the ultimate displacement capacity of the tri-linear force-displacement relationship. The study showed that the latter variables, specifically the elastic modulus E and the compressive strength of URM, are moderately sensitive material mechanical properties often impacted by considerable uncertainty while evaluating an existing structure.

Pradhan et al. [2021] tested the accuracy of analytical capacity models for estimating the out-of-plane capacity of unreinforced masonry (URM) infill walls. The results of existing experimental studies were used to check the validity of the currently available models. During the study, two kinds of capacity models were examined. Type I predicts the strength in the undamaged condition, and Type II predicts the strength loss in the in-plane damaged condition. The results of comparisons were shown, and the most suitable model according to the results was suggested. Moreover, estimated models about the impact of orthotropy of unreinforced masonry infill walls in the out-of-plane capacity were discussed. The possibility of applying capacity models in the situations of infill-beam gaps and infill with openings is also underlined in this research. The best capacity model pairs for unreinforced masonry infill walls were proposed to estimate the decrease of the out-of-plane strength according to damaged and undamaged states.

Lönhoff et al. [2017] focused on the inadequate approximation of simplified methods of design codes about the evaluation of the out-of-plane capacity of unreinforced masonry infill walls. It was stated that the out-of-plane capacity of the URM walls is not determined realistically since the fundamental parameters such as vertical loads, dynamic effects, constraints, and geometry were neglected in the simplified methods of design codes. A nonlinear time-history analysis that includes all the mentioned parameters was performed using real-time earthquake history data. The analyses were applied until the URM walls reached failure. Geometry, axial load, and restraint stiffness were altered; thus, the impact of the parameters was observed. The results showed that since the simplified analytical methods use only peak accelerations, boundary conditions, and axial load effects are not considered, these methods give more conservative results, which is uneconomical and unsustainable.

Liberatore et al. [2020] developed an equation to predict the out-of-plane plane strength capacity of masonry infill walls, including openings and boundary conditions. The authors stated that collapse or failure of the masonry infills causes loss of life and limb of occupants considering the real-life seismic event observations. Thus, research that includes analytical and experimental studies were

conducted for the masonry infill walls for the out-of-plane loading. Boundary conditions and slenderness were considered the main parameters that impact the strength capacity of the masonry infill walls. In total, 191 experimental test results were collected from the literature, and noticed that the formulations were inadequate for the masonry infills with the openings (window and door) and the gap between the top beam and infill. Afterward, numerical analyses were performed, and an empirical model was proposed to determine the out-of-plane strength capacity of masonry infills to be used for local equivalent-static verifications.

Pasca et al. [2017] performed a study about the reliability of analytical methods used to estimate the out-of-plane capacity of masonry infills. Although the in-plane behavior of masonry infills is the subject that researchers focus on, it is noticed that out-of-plane failure of the masonry infill walls creates risks and demanding situations for human life and overall structure during and after seismic events. Therefore, the capacity and design of masonry infill walls in the out-of-plane loading gained the attention of the researchers. Due to the increasing interest in searching the out-of-plane behavior of masonry infill walls during a seismic event, the authors found it necessary to explore the out-of-plane response of masonry infills in view of various aspects. As the first step of the study, the effects of previous earthquakes were assessed to identify the significant parameters and the most important configurations. Secondly, the results of 150 experimental tests were thoroughly investigated, concentrating on the effects of geometrical properties, boundary conditions, previous in-plane damage, reinforcing components, and openings. Lastly, the authors concluded the study with a discussion and comparison of various theoretical capacity models and code provisions, focusing on those relying on the arching theory. As a result, it was stated that while the presence of reinforcing elements increases the capacity of the masonry infill, openings in the masonry infill walls are like to decrease the capacity. Furthermore, instead of the tensile strength, the compressive strength ultimately had an impact on the out-of-plane capacity.

Di Domenico et al. [2018] investigated the impact of boundary conditions in terms of stiffness, strength, and displacement capacity of unreinforced masonry (URM)

infill walls with three pseudo-static experiments. Tested URM infill walls were constrained by a reinforced concrete frame along two, three, or four edges. The reinforced concrete frames were 2/3 scaled and designed according to the Italian building code, NTC2008. The strength and secant stiffness values obtained from the prediction methods and the experiments were compared at first micro cracking and the peak load. As a result, the authors stated that considering the boundary conditions, some analytical models and formulations in the literature give satisfactory results with the experimental test results.

Doherty et al. [2002] assessed the behavior of brick masonry infill walls during a seismic event. In order to obtain the most accurate analytical findings, a simplified linearized displacement-based method was described, together with suggestions for selecting a suitable substitute structure. The actual nonlinear force-displacement relationship for unreinforced brick masonry infill walls was described by a trilinear relationship. The findings of experimental tests and nonlinear time-history analyses are evaluated with the predictions made using the linearized displacement-based approach and quasi-static analysis processes. As the results, the authors stated that the displacement-based approach provides considerably more accurate results than the forced-based approach.

Vaculik [2012] examined the behavior of two-way unreinforced masonry infill walls under out-of-plane loading. The purpose of the study was stated as giving a base for the improvement of a reliable displacement-based design approach and offering upgrades to the existing force-based design approaches. Although forced-based design approaches are the most used for unreinforced masonry infill walls, this traditional design procedure started to change to the displacement-based design approach, which accepts the deformation capacity as the design limit. Out-of-plane loading tests gained importance for the development of a displacement-based design approach. This thought was a good idea, especially for two-way spanning walls with high seismic performance, considering the considerable deformation capacity and effective energy dissipation during cyclic response. The author of the study described the out-of-plane behavior of the two-way spanning unreinforced masonry infill walls

through quasistatic cyclic tests and verified the out-of-plane behavior of these walls under realistic seismic loading conditions. He developed an analytical method to predict the load capacity of the masonry infill walls with the presumption that tensile bond strength is zero. Moreover, a model was proposed for the nonlinear inelastic load-displacement behavior of two-way spanning masonry infill walls and implemented the load-displacement model into a simple displacement-based seismic assessment process.

Dizhur et al. [2018] conducted an on-site proof test to investigate the out-of-plane behavior of masonry infill walls. The study includes nineteen fired-clay brick masonry infill wall tests in six different buildings. In addition, the authors declared that the on-site proof tests demonstrated a real-life experiment which is more realistic considering the laboratory experiments. The out-of-plane load was applied by using the airbag. The tests showed that boundary conditions and assumed “arching” action from the building frame may dramatically increase the out-of-plane capacity of unreinforced masonry infill walls. Furthermore, two-way out-of-plane flexure may significantly increase the load capacity of the masonry infills compared to one-way out-of-plane flexure.

Murty and Jain [2000] conducted research on the benefits of unreinforced masonry infill walls of reinforced concrete frame structures during a seismic event. The observations showed that masonry infills cause serious damage, such as the short-column effect, soft-story effect, torsion, and out-of-plane collapse during a seismic event. Therefore, constructing the masonry infills is an issue that is discouraged in seismic design codes for hazardous seismic regions. On the other hand, although many structures that include masonry infill walls were not designed and constructed for seismic forces, they have performed quite well in several minor earthquakes. This observation encouraged the authors to perform an experimental study for the behavior of masonry infill walls within the reinforced concrete frames under seismic load. It was observed that the masonry infills significantly increase lateral stiffness, overall ductility, and capacity for absorbing energy. The authors also suggested anchoring the masonry infills into the reinforced frames to increase the out-of-plane

capacity of masonry infills. Furthermore, since the reinforced frames with masonry infill are used in most multistory projects in developing nations, it was necessary to provide effective seismic design processes for such structures.

Furtado et al. [2016] performed an experimental study to investigate the out-of-plane capacity of the infill masonry walls with and without previous in-plane damage combinations. The reason for investigating the out-of-plane capacity of infill masonry walls was stated as the occurred interaction of infill masonry walls with the surrounding reinforced concrete frames during a seismic event. Since the observations of real-life seismic events showed that the interaction of the infill masonry walls causes different failure modes and load capacities, the authors decided to consider the contribution of infill masonry walls in the structural response assessment of existing buildings. The experimental tests were conducted to develop effective strengthening solutions to avoid collapse, enhance the performance and consequently minimize the seismic hazard of infill masonry walls during future earthquakes. Three experimental (cyclic and monotonic) out-of-plane tests were performed on full-scale infill masonry walls to learn more about the out-of-plane response of infill masonry walls. Hollow bricks were used as infill material for all tests. The results were presented and discussed in terms of damage progress, stiffness degradation, energy loss, and hysteretic force-displacement curves. The test results with and without prior in-plane damage showed a considerable difference. The maximum strength was nearly four times higher when the tests were conducted without prior in-plane damage and with greater out-of-plane drift values. Compared to the other tests, the test with prior in-plane damage demonstrated a considerable decrease in the initial stiffness. A significant maximum strength drop was observed in tests conducted without the prior in-plane damage.

Hak et al. [2014] performed a study to understand better the seismic behavior of masonry infills in recently designed RC buildings. The behavior of the exterior tongue and groove clay masonry infills under out-of-plane loading were investigated using a systematic numerical and experimental study program. Particular consideration was afforded to determining the out-of-plane behavior of infill walls,

associated damage propagation and failure modes, and evaluating the out-of-plane strength as a function of earlier in-plane damage. The experimental study was conducted by applying static cyclic out-of-plane load on fully scaled, single-bay, single-story RC frame specimens. The tested strong masonry infills were designed according to European seismic design criteria. As the results of the study, it was found that the two-directional arching action is the typical out-of-plane failure state for the tested specimens. The observed crack paths start in the midheight horizontally and continue diagonally toward the corners of the walls. Moreover, strength reduction is also observed due to the previous in-plane damage to the infill wall. According to the observations and results of the experiments, a simplified model was proposed to describe the strength reduction in the out-of-plane direction.

Navas-Sanchez and Bravo [2022] suggested an analytical approach obtained from the theoretical analysis to characterize the complete seismic response curve of cantilever infill walls, which are masonry parapets and historical facades, in the out-of-plane direction. Additionally, the authors offer a simple method for developing a simplified trilinear version of mentioned curves using several non-dimensional mathematical formulations. Energy conservation and the minimum quadratic error were taken into account in the simplified formula for the simplified trilinear version of the capacity curves. The ability of the approach to catch the linear and nonlinear behavior of the masonry infill walls under horizontal loads was evaluated by comparing it with the tests in the literature. As the result of the work, the authors stated that the behavior of the element resulted from the relation of two variables which represent the action of the lateral force and the response of the element to it.

In addition to the studies mentioned above, some authors have chosen to conduct their studies by performing a literature review and analyzing the outcomes (Ferreira et al.,2015; Anic et al., 2020).

1.2.2 Related Codes

As stated previously, the authorities decided that it is necessary to have guidelines for unreinforced infill masonry walls after observing that the unreinforced infill masonry walls affect the seismic capacity of the reinforced concrete structures. Therefore, as a result of this point of view, especially the design and the assessment of the unreinforced infill masonry walls were taken into account in the last decades. Moreover, these issues are included in some codes. Examples of some guidelines and codes are introduced in this chapter. These documents have been published to consider and offer seismic out-of-plane design and assessment methods for the unreinforced infill masonry walls with reinforced concrete frames.

1.2.2.1 ASCE/SEI 41-17

The acceptable criteria for URM walls subject to out-of-plane demands are covered under ASCE/SEI 41-17 recommendations. According to ASCE/SEI 41-17, flexural wall cracking is not allowed for the Immediate Occupancy Structural Performance Level. On the contrary, flexural cracking is acceptable for the other two structural performance levels, Life Safety Level and Collapse Prevention, provided that the damaged wall sections stay stable during the seismic excitation. Collapse Prevention Structural Performance Level requires particular slenderness ratios considering the interval of the acceleration at 1-s period. If the slenderness ratio is not higher than eight or the spectral response acceleration variable at 1-s period is less than or equal to the value determined using the code provided equation, the wall is considered stable for the Life Safety Structural Performance Level.

It is also stated that the lower-bound masonry flexural tension strength, which equates to 70% of the estimated tensile strength, should be used to restrict the lower-bound strength of the infill wall if arching action is not taken into account. However, ASCE/SEI 41-17 also contains the equation for determining the strength of the infill

panel, both with and without an opening, for the cases where the arching effect is considered. The equations mentioned are presented as follows:

$$q_{inf,oop}^{solid} = \frac{0.3 \cdot f'_m \cdot R_1 \cdot R_2 \cdot e^{-0.0985 \frac{h_{inf}}{t_{inf}}}}{\frac{h_{inf}}{t_{inf}}} \quad (1.1)$$

$$q_{inf,oop} = \left(1 - \frac{A_{op}}{A_{wtot}}\right) q_{inf,oop}^{solid} \quad (1.2)$$

1.2.2.2 New Zealand Recommendations 2017

New Zealand recommendations 2006 is a worldwide code that considers the seismic assessment of out-of-plane infill walls (Sorrentino et al., 2017). Although this document provides a quick and beneficial overview of seismic assessment techniques for unreinforced infill walls in out-of-plane loading direction, the seismic events that took place later caused the improvement of the New Zealand recommendations. Thus, the updated document was published as the 2017 New Zealand guidelines for seismic assessment (NZSEE in New Zealand Society for Earthquake Engineering, the seismic assessment of existing buildings—technical guidelines for engineering assessments, Wellington, 2017).

The 2017 New Zealand recommendations include three main parts Part A, Part B, and Part C. Part C establishes some approaches for seismic assessment of the structures.

The guideline states that the vertical and horizontal arching motion is the primary out-of-plane resisting mechanism for infill wall systems. The formula that is used to determine the likely out-of-plane strength of an unreinforced infill wall for both with openings and without openings is also presented in the guideline. The formulas for infill walls without opening and with opening are shown in Equation 1.3 and Equation 1.4, respectively.

$$q_{prob} = 730 \cdot \gamma \cdot (f'_m)^{0.75} \cdot t^2 \cdot \left(\frac{\alpha_{arch}}{L_{inf}^{2.5}} + \frac{\beta_{arch}}{h_{inf}^{2.5}} \right) \quad (1.3)$$

$$q_{prob} = q_{prob}^{solid} \cdot \left(1 - \frac{A_{op}}{A_{wtot}} \right) \quad (1.4)$$

where q_{prob} is the probable uniformly distributed lateral load capacity; t is the thicknesses, h_{inf} is the clear height and L_{inf} is the length dimensions of the infill panel; α_{arch} and β_{arch} are the horizontal and vertical arching coefficients, respectively. γ is defined as the in-plane cracking capacity reduction coefficient. q_{prob}^{solid} is probable uniformly distributed lateral load capacity of an equivalent infill panel with no opening; A_{op} and A_{wtot} are the area of the opening in the infill panel and the gross area of the equivalent infill panel with no openings, respectively.

The recommendation offers an alternative solution with no arching effect to calculate the probable out-of-plane capacity in detail. The related chapter of the guideline presents two different methods, which are the force-based method and displacement-based inelastic method, for evaluating the out-of-plane loaded masonry infill walls.

Yield line patterns are also considered in the recommendations. According to Clause 8 of the guideline, it is stated that if the unreinforced masonry walls are joined to the supports on all four sides, previous earthquake observations have demonstrated that they can perform as a two-way spanning panel and generate yield line patterns resembling those of a two-way spanning slab. Moreover, it presents probable crack paths for different boundary conditions.

1.2.2.3 British Standards Institution BS 5628

The British Standard Institution (BSI) is a national and non-governmental standard-developing organization of the United Kingdom. It also offers businesses certification and standards-related procedures in addition to producing technical

standards on various goods and services. BSI published a standard named BS 5628 for masonry walls. BS 5628 includes three parts: Part 1, Part 2, and Part 3. Part 1 is the code of practice for the structural use of unreinforced masonry; Part 2 is the code of practice for the structural use of reinforced and prestressed masonry, and Part 3 is the code of practice for the use of materials, components, and design of masonry. The recommendations in Part 3 are based on knowledge of single-leaf and cavity walls that have and do not have insulation in the cavities. It is stated that the distance between the supports should not exceed 30 times the total thickness of the infill masonry walls with the cavity. The standard also defines the support conditions i.e., fixed-end support and simply support.

Although some guidelines and codes are mentioned in this chapter, there are different national codes and guidelines used worldwide. Canadian Standard Association, Australian Standard, and Italian Technical Standard are examples of guidelines related to masonry infill walls with out-of-plane loading. They are summarized by Sorrentino et al.,2017.

1.3 Motivation and Objective

Many studies were performed to improve knowledge and design criteria by recognizing the importance of the capacity and the behavior of unreinforced infill walls on adjacent framing structures. However, most of the studies focus on only one kind of infill material, which is traditional clay brick. Moreover, most studies do not focus solely on the out-of-plane behavior of the unreinforced infill walls. Nowadays, however, the construction industry has started using different infill materials. Pumice concrete is one of these materials since it provides more sound and heat insulation. Besides determining and understanding both the capacity and behavior of unreinforced infill walls, it is also important to consider and understand that they change according to the type of infill material.

Many experimental studies on infill walls were conducted in Uğur Ersoy Structural Mechanics Laboratory at the Middle East Technical University Civil Engineering Department. Detailed reports of some studies were published by Binici et al., 2019; Canbay et al., 2018; Demirel et al., 2018; Canbay et al. [2003]. Different infill materials, loading procedures, and boundary conditions are applied to the infill walls to investigate the seismic behavior of different kinds of infill walls.

The objective of this study is to assess the effects of openings of various sizes with two different infill materials, clay brick, and pumice concrete. In light of this, a three-stage study was carried out to understand the seismic behavior of infill walls further. The first part consists of eight out-of-plane loading experiments, of which five are brick infill walls and three are pumice concrete infill walls bounded with a half-scaled, one-bay, and one-story reinforced concrete frame. Out-of-plane loading was applied with an airbag to create uniform pressure on the infill walls. Three kinds of infill walls were simulated for both infill materials. The infill walls with the window opening, door opening, and without opening were simulated for both infill materials. In the second part of the study, yield line analysis was performed with different boundary conditions for all kinds of simulated infill walls. Yield line analysis results were compared with the experimental result to understand the behavior of the unreinforced infill walls. In the last step, the maximum displacement capacities of the infill walls were calculated, taking into account the earthquake accelerations and the number of the story of the structure. The researcher performed this study to further understand the behavior of the unreinforced infill walls and improve the design criteria.

The content of this thesis is structured as shown below:

Chapter 2 reports the experimental work of the study. Information on the test setup, instrumentation, and loading system is given in detail in this chapter. The infill wall specimens are introduced with their specific parameters. Moreover, the results of the experiments are given and compared with each other.

Chapter 3 introduces the analysis part of unreinforced infill walls. Firstly, yield line analysis and capacity analysis considering the seismic response of the structure were performed to understand the behavior of infill walls under the out-of-plane loading effect.

Chapter 4 summarizes the work and the outcomes that are obtained from the performed studies in this thesis.

CHAPTER 2

EXPERIMENTAL WORK

2.1 Introduction

The following chapter introduces the experimental studies conducted in the Structural and Earthquake Engineering Laboratory at Middle East Technical University. The experiments were conducted to observe the behavior of the infill walls on the out-of-plane loading. In total, eight infill wall specimens with different properties were examined. The test parameters were chosen as (i) the presence of openings of different sizes in the infill walls and (ii) different infill materials. The infill walls are tested in three parts: without opening and with window and door openings. Three kinds of infill walls for each infill material were built.

All the specimens were examined using the same RC frame and boundary conditions with the same test setup.

2.2 Test Setup and Instrumentation

A one-bay, one-story, and half-scaled reinforced concrete frame was used to build the infill walls. The reinforced concrete frame is a scaled prototype of a three-bay, five-story reinforced concrete building. The column dimensions of the reinforced concrete frame are 200×200 mm, and the beam is modeled as a T-beam with a 150 mm flange thickness to simulate the interaction between the beam and the slab. The planar dimensions of the frame are 2500×1500 mm, and the inner dimension of the frame is 2300×1300 mm. The reinforced concrete frame is designed and built with 8 mm diameter deformed steel bars as longitudinal reinforcements and 6 mm diameter plain steel bars as transverse reinforcements. The yield strength and ultimate strength values of each kind of reinforcement steel are shown in Table 1. The plastic hinging

regions, the critical regions of the columns and beam, are designed as closely spaced stirrup regions. The length of these critical regions for beams and columns are 400 mm and 300 mm, respectively. This half-scaled frame was designed according to the Turkish Earthquake Code (TEC2018) with a high ductility level. The concrete strength of the frame has been approved as 25 MPa by testing the cube concrete specimens. The dimensions and the reinforcement details of the frame are shown in Figure 2.1 and Figure 2.2, respectively.

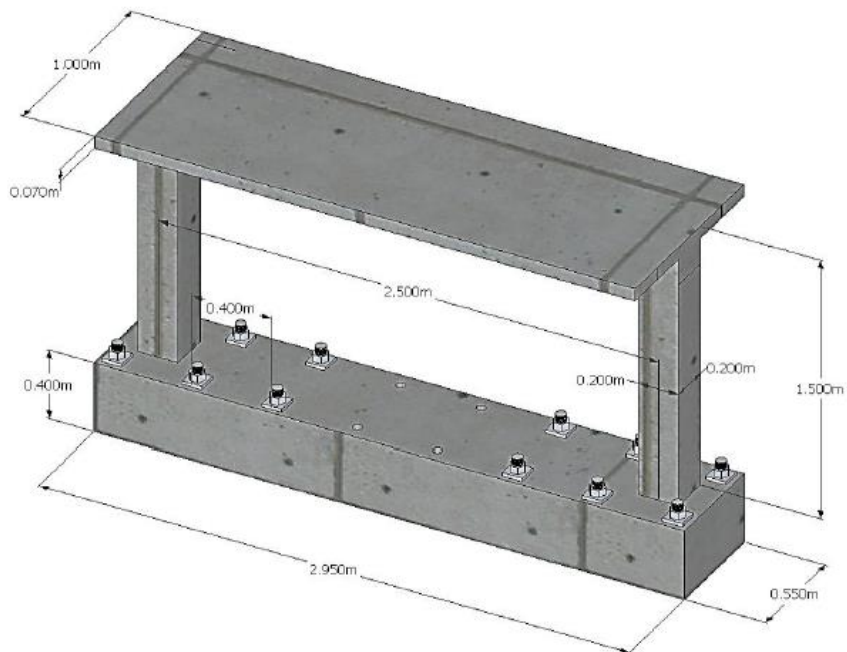


Figure 2.1. Dimension Details of Reinforced Concrete Frame

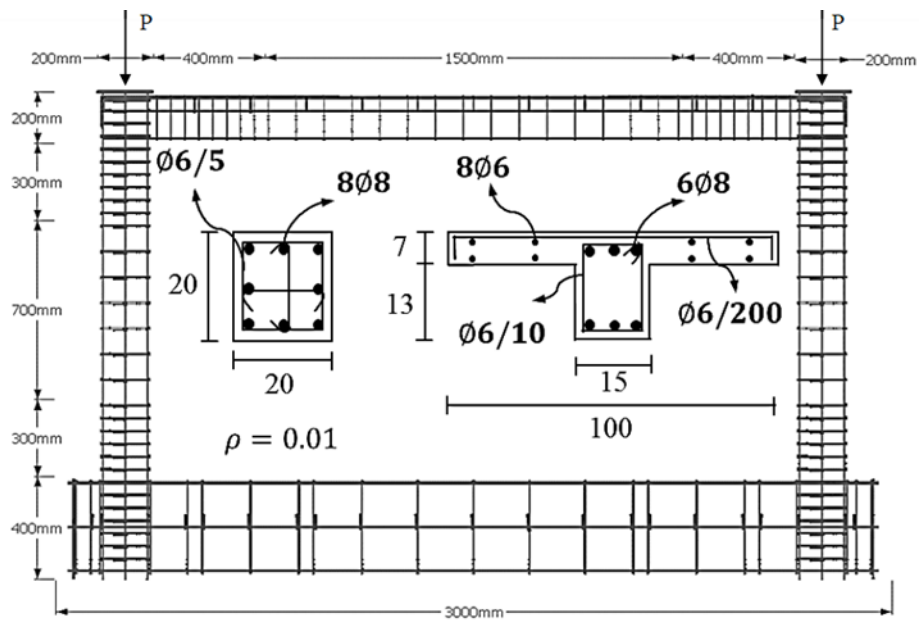


Figure 2.2. Reinforcement Details of Reinforced Concrete Frame

The infill wall materials were 60% hollowed brick, and 71% hollowed pumice concrete. Since the test frame is a 1:2 scaled model, the dimensions of infill materials were also determined to be consistent with the reinforced concrete frame. The clay brick blocks were specially produced, and the pumice concrete blocks were split into two pieces. The dimensions (height: width: length) of the clay brick blocks and pumice concrete blocks were adjusted to 10:10:19 cm and 10:8.5:39 cm, respectively. The pumice concrete blocks used in this experimental study have tongue and groove at side faces. These notches and projections on the side face facilitate laying down the blocks. The horizontal continuity of the blocks may also improve the out-of-plane behavior of the infill walls. A general view of the traditional clay brick and pumice concrete blocks with tongue and groove is given in Figure 2.3. The compressive strength of the infill materials is 3 MPa and 1.8 MPa for clay brick and pumice concrete blocks, respectively. Other tests conducted on infill constituents are given below. The same mixture of ingredients for plaster and mortar was used for each infill wall. The space between the infill materials and the frame surface was filled with mortar.



(a) Traditional Clay Brick Blocks



(b) Pumice Concrete Block

Figure 2.3. Infill Wall Materials

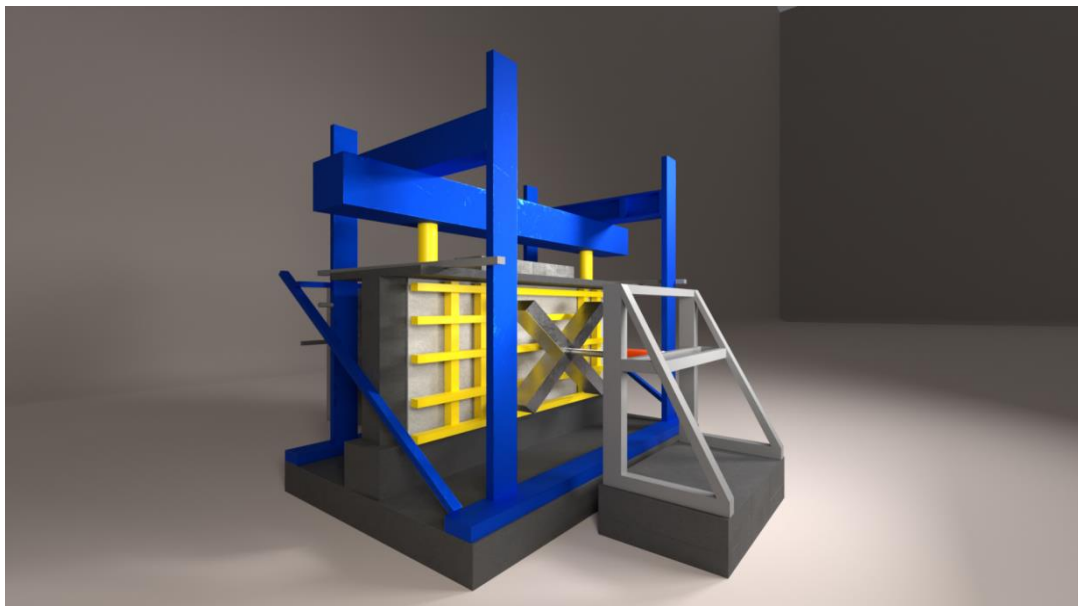
Loading conditions have been designed separately for the RC frame and infill walls, considering the real-life loading conditions. The loading systems are designed to simulate possible loading conditions. As mentioned before, since the RC frame is the half-scaled prototype of a designed structure, the load of upper stories, axial load for columns, and distributed load for the slab have been considered and simulated. 200 kN and 10.25 kN/m load have been applied for the axial load on columns and distributed load on the slab, respectively. The axial load on the columns was applied by using force-controlled hydraulic cylinders. These force-controlled hydraulic cylinders were attached to the rigid steel exterior frame, and column ends.

The out-of-plane loading system was supplied by a force-controlled hydraulic cylinder on the center back side of the infill wall to keep the proximity of the airbag to the infill wall. The load was transferred uniformly to the infill wall through the airbag between the hydraulic cylinder and the infill wall. A 2 mm-thick Teflon sheet was placed between the infill wall and the airbag to prevent the friction forces that are likely to develop between the airbag and the wall. A wooden plate was attached and fixed to the hydraulic cylinder perpendicularly so that as the air pump fills the

airbag with air, the pressure increases inside the airbag. Increased pressure applies the load to the infill wall through a hydraulic cylinder. All the test setup details are shown in Figure 2.4 and Figure 2.5.



a) Front Side of the Test Setup



b) Back Side of the Test Setup

Figure 2.4. In Details of Test Setup



(a) Teflon Sheet



(b) Wooden Plate and out-of-Plane
Load Cell

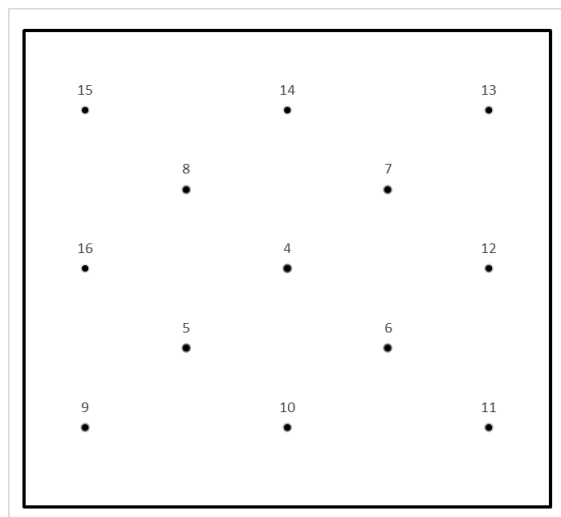


(c) Placed Airbag Between Teflon
Sheet and Wooden Plate

Figure 2.5. Instruments of Test Setup

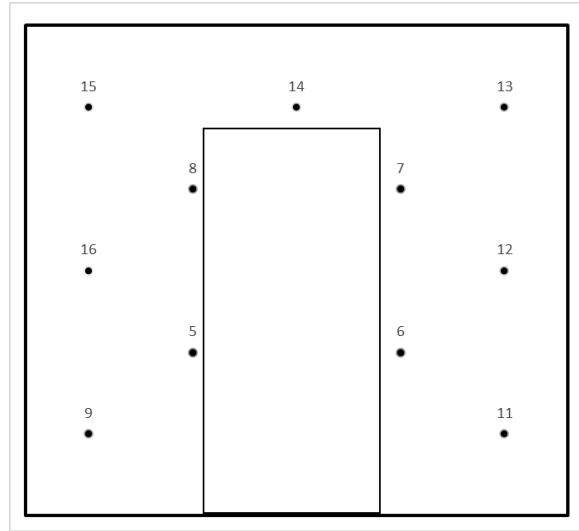
The same measuring systems were used for each test during the experimental studies. Deflection measurements were conducted using different LVDTs for the frame member and the infill wall. The deflection measurements were taken from 13 points for the infill wall without opening, 12 points for the infill wall with the window opening, 11 points for the infill wall with the door opening, and 2 points for the surface of the columns by using the LVDTs with different capacities. The experiments were continued until the infill walls reached failure. In order to take sensitive measurements during the test, different ranged LVDTs were used. The placement scheme of LVDTs for each type of infill wall and the capacities of LVDTs are shown in Figure 2.6. The Placement of LVDTs (continued) and Table 2.1, respectively. The coordinates of the LVDTs are shown, assuming that the origin is the center of the infill wall. The LVDTs were attached to a platform placed 1.5 m away from the infill wall to prevent damage.

The load and deflection measurements were observed with the help of the software StrainSmart. The relation between load and deflection at the measuring points was checked using this software during the experiment. Later, the test data were obtained using the software StrainSmart.

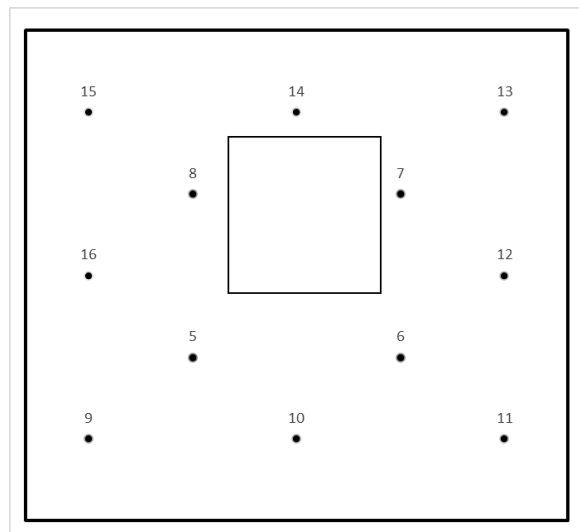


(a) The Placement of the LVDTs for the wall specimens without opening

Figure 2.6. The Placement of LVDTs



(b) The Placement of the LVDTs for the wall specimens with door opening



(c) The Placement of the LVDTs for the wall specimens with window opening

Figure 2.6. The Placement of LVDTs (continued)

Table 2.1 Capacities and Places of LVDTs

ID of LVDT	<i>Measurement</i>		<i>Y Coordinate</i>
	<i>Capacity (mm)</i>	<i>X Coordinate (mm)</i>	<i>(mm)</i>
4	100	0	0
5	100	-383	-217
6	100	383	-217
7	100	383	217
8	100	-383	217
9	50	-767	-433
10	50	0	-433
11	50	767	-433
12	50	767	0
13	50	767	433
14	50	0	433
15	50	-767	433
16	50	-767	0

In total, eight infill walls with different properties were prepared in the Structural and Earthquake Engineering Laboratory at Middle East Technical University. This experimental study aims to observe and understand the behavior of the infill walls with the applied out-of-plane loading.

2.3 Testing on Infill Constituents

The components of the infill walls are the main parts that affect the capacity of the infill wall in this study. Since observing the overall capacity and the behavior of the infill walls are the aims of these experimental studies, the properties of the constituents also were considered while examining the results.

It was decided to use the same ingredients for both mortar and plaster. Lime, cement, and aggregate were mixed with the water to get mortar and plaster. Using lime helps minimize the shrinkage cracks and keeps aggregate and cement together. The mass ratios of the ingredients were chosen as 2:1:6 for the cement, lime, and aggregate, respectively. The only difference between mortar and plaster was only the amount of water. The water amount differed because the plaster needed more water for more workability. During each construction of infill walls, two different kinds of specimens of mortar and plaster were taken and tested immediately after the out-of-plane of infill wall tests. The purpose of these specimens is to obtain the strength and capacity of the mortar and plaster constituents of the infill wall according to ASTM C348-18 and ASTM C109. The cube and prismatic-shaped specimens taken for both mortar and plaster are shown in Figure 2.7. The cube and prismatic specimens were tested to obtain the compression and flexure capacity of the materials, respectively. The dimensions of the cube and prismatic specimens are 50x50x50 mm and 40x40x160 mm, respectively.



Figure 2.7. Cube and Prismatic Specimens of Constituents

2.4 Test Specimens

Detailed information on the eight out-of-plane tests of infill walls is given in Table 2.2. The specimens differ according to the infill materials used, the presence of openings, and the size of the openings. All the experiments have the same boundary conditions. The top and bottom edges of the frame were restrained with the mortar mixture used in the construction of infill walls. Furthermore, all the specimens were covered with a both-sided plaster mixture of 5 mm thickness. It should be noted that above the windows and doors, lintels which are 90 cm long and 12 high are provided, similar to real applications. The infill wall specimens are described below.

WBHN: The plane dimensions of the infill wall were 2300x1300 mm. Brick was used as the infill material. The bricks were placed horizontally. The wall was built without an opening.

WBVN1: The plane dimensions of the infill wall were 2300x1300 mm. Brick was used as the infill material. The brick materials were placed vertically. The wall was built without an opening.

WBVN2: The plane dimensions of the infill wall were 2300x1300 mm. Brick was used as the infill material. The brick infill materials were placed vertically. The wall was built without an opening.

WBVW: The plane dimensions of the infill wall were 2300x1300 mm. Brick was used as the infill material. The brick infill materials were placed vertically. The wall was built with a window opening.

WBVD: The plane dimensions of the infill wall were 2300x1300 mm. Brick was used as the infill material. The brick infill materials were placed vertically. The wall was built with the door opening.

WPVN: The plane dimensions of the infill wall were 2300x1300 mm. Pumice concrete was used as the infill material. The pumice concrete infill materials were placed horizontally. The wall was built without an opening.

WPVW: The plane dimensions of the infill wall were 2300x1300 mm. Pumice concrete was used as the infill material. The pumice concrete infill materials were placed horizontally. The wall was built with a window opening.

WPVD: The plane dimensions of the infill wall were 2300x1300 mm. pumice concrete was used as the infill material. The pumice concrete infill materials were placed horizontally. The wall was built with the door opening.

Table 2.2 Detailed Information of Tested Specimens

Specimen Name	Opening Condition	Infill Material	Loading Protocol
WBHN	Without Opening	Clay Brick	Out-of-Plane
WBVN1	Without Opening	Clay Brick	Out-of-Plane
WBVN2	Without Opening	Clay Brick	Out-of-Plane
WBVW	Window Opening	Clay Brick	Out-of-Plane
WBVD	Door Opening	Clay Brick	Out-of-Plane
WPVN	Without Opening	Pumice Concrete	Out-of-Plane
WPVW	Window Opening	Pumice Concrete	Out-of-Plane
WPVD	Door Opening	Pumice Concrete	Out-of-Plane

2.5 Test Results

The outcomes of the conducted experimental studies are summarized in this section. The mechanical properties of the constituents of each specimen are shown in Table 2.3.

The failure modes of the infill wall specimens under the out-of-loading were illustrated using the software Matlab and presented for each specimen. Since it is the main purpose of these experiments to observe the behavior of infill wall specimens under out-of-plane loading, the occurred crack path of each specimen during the loading process is also given in this chapter. The deflection and load relationships are also shown in the graphs. The load and the deflection capacities σ were compared

at the end of this chapter. The purpose of this chapter is not to analyze but only to show the overall observation and the results of the experiments.

Table 2.3 Mechanical Properties of Mortar and Plasters

Uniaxial Compressive Strength of the Cube Specimens								
<i>Mortar</i>					<i>Plaster</i>			
Specimen Name	<i>n</i>	<i>Avg Mass (gr)</i>	<i>Mean Compression Load (kN)</i>	σ (MPa)	<i>n</i>	<i>Avg Mass (gr)</i>	<i>Mean Compression Load (kN)</i>	σ (MPa)
WBHN	3	230.6	23.5	9.400	3	220.3	12.1	4.800
WBVN1	3	224.3	9.8	3.900	3	213.9	8.2	3.300
WBVN2	3	231.7	24.7	9.900	3	224.0	13.8	5.500
WBVW	3	226.1	18.7	7.500	3	237.0	15.5	6.200
WBVD	3	237.7	17.7	7.100	3	240.5	16.9	6.700
WPVN	4	249.0	29.3	11.700	4	242.7	21.9	8.700
WPVW	3	225.8	22.4	8.900	3	229.1	19.3	7.700
WPVD	3	232.8	23.8	9.500	3	233.0	17.5	7.000

Table 2.3 Mechanical Properties of Mortar and Plasters (continued)

Flexural Strength of the Prismatic Specimens								
<i>Mortar</i>					<i>Plaster</i>			
Specimen Name	<i>n</i>	<i>Avg Mass (gr)</i>	<i>Mean Flexural Load (kN)</i>	σ (MPa)	<i>n</i>	<i>Avg Mass (gr)</i>	<i>Mean Flexural Load (kN)</i>	σ (MPa)
WBHN	3	448.4	0.58	1.376	3	449.0	0.46	1.078
WBVN1	3	422.5	0.45	1.062	3	454.2	0.34	0.797
WBVN2	3	486.5	1.00	2.351	3	451.4	0.52	1.219
WBVW	3	475.3	1.13	2.641	3	469.5	0.73	1.711
WBVD	3	467.3	1.83	4.296	3	474.7	0.75	1.758
WPVN	4	485.1	0.87	2.027	4	480.0	0.73	1.711
WPVW	3	485.9	0.69	1.610	3	467.5	0.60	1.399
WPVD	3	474.7	1.08	2.531	3	477.0	0.66	1.554

Compressive Strength of Prism Halves Fractured in Flexure								
<i>Mortar</i>					<i>Plaster</i>			
Specimen Name	<i>n</i>	<i>Avg Mass (gr)</i>	<i>Mean Compression Load (kN)</i>	σ (MPa)	<i>n</i>	<i>Avg Mass (gr)</i>	<i>Mean Compression Load (kN)</i>	σ (MPa)
WBHN	6	223.5	8.7	5.4	6	223.6	8.1	5.1
WBVN1	6	226.2	5.4	3.4	6	210.2	4.2	2.7
WBVN2	6	243.0	16	9.8	6	224.7	8.3	5.2
WBVW	6	236.8	12.5	7.8	6	234.0	12.4	7.7
WBVD	6	232.3	12.2	7.0	6	235.6	11.1	7.0
WPVN	8	240.0	15	6.0	8	241.3	13.7	8.6
WPVW	6	233.0	13.6	8.5	6	242.0	14.5	9.0
WPVD	6	236.8	14.2	8.9	6	238.1	10.3	6.4

2.5.1 Wall WBHN

Wall WBHN is the only specimen built to observe the effect of the alignment of infill material in a structure. The bricks were established horizontally in this specimen. Although the same construction materials were used, the building alignment of the infill material changes the deflection and the load capacity of wall WBHN.

Specimen WBHN without plaster is shown in Figure 2.8. According to the data acquired, the deflection contour of specimen WBHN just before failure and the load-deflection curve is shown in Figure 2.9 and Figure 2.10, respectively.



Figure 2.8. Built WBHN Without Plaster on i

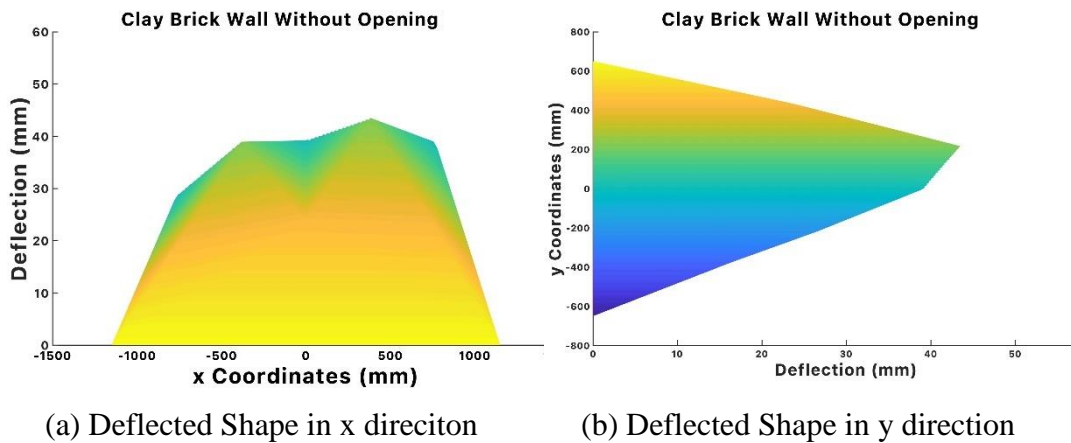


Figure 2.9. Deflected Shape of WBHN Before Failure

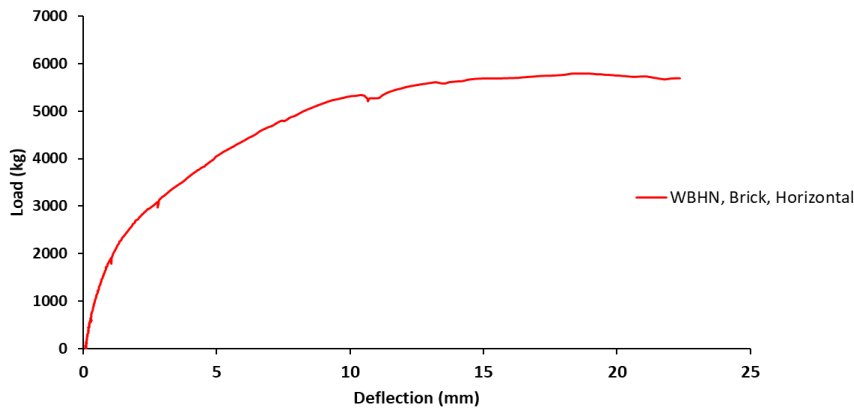


Figure 2.10. Load-Deflection Relation of Specimen WBHN

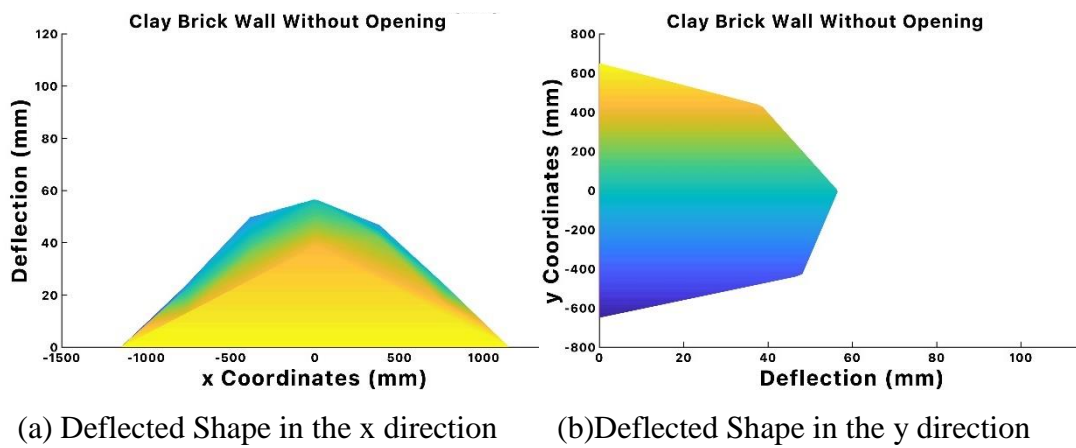
2.5.2 Wall WBVN1

Wall WBVN1 is the second gapless wall that uses brick as infill material. The infill material was constructed with vertical placement. This experiment was conducted to have an opinion and observe the difference between the infill wall using the same material with vertical arrangement. Figure 2.11 shows the wall WBVN1 without plaster on it. The Matlab model of the deflected shape and the crack path of wall

WBVN1 are shown in Figure 2.12 and Figure 2.13, respectively. Load-deflection curve is shown in Figure 2.14.



Figure 2.11. Built WBVN1 Without Plaster on it



(a) Deflected Shape in the x direction (b) Deflected Shape in the y direction

Figure 2.12. Deflected Shape of WBVN1 Before the Failure

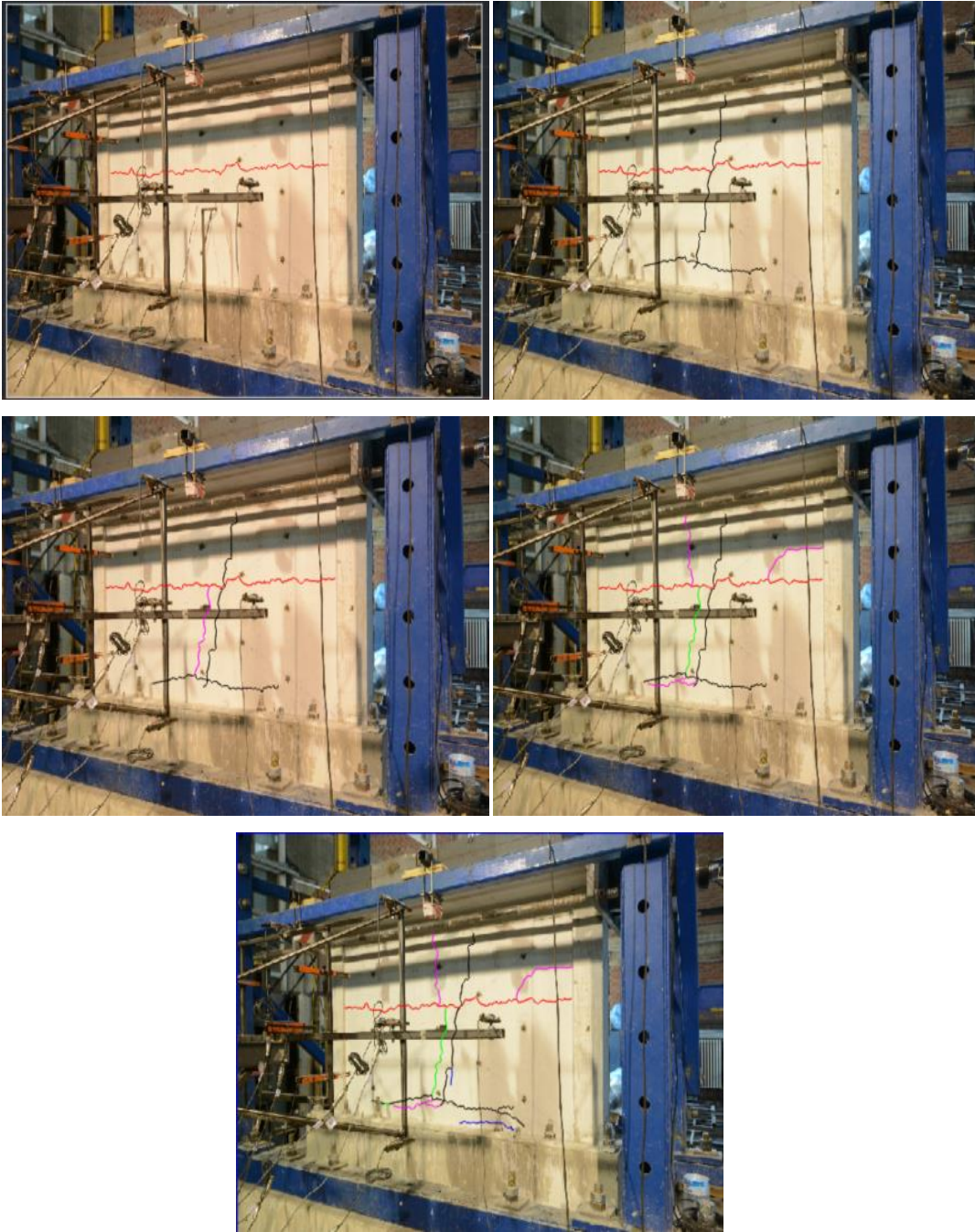


Figure 2.13. Crack Path of WBVN1 Experiment

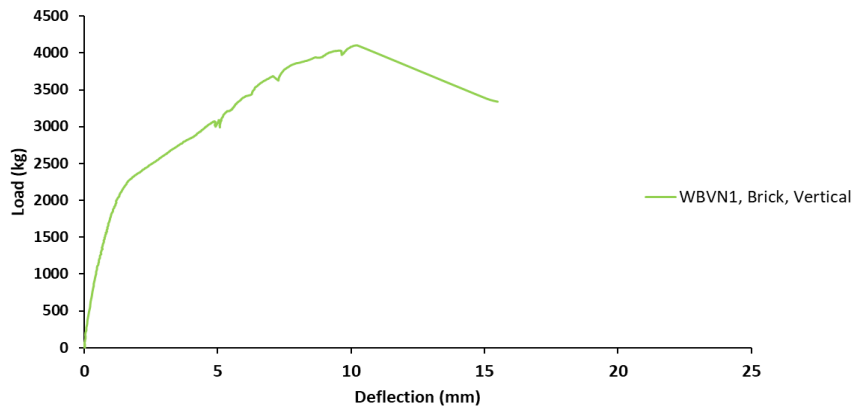


Figure 2.14. Load-Deflection Relation of Specimen WBVN1

2.5.3 Wall WBVN2

Wall WBVN2 is the third gapless wall with clay brick infill. The infill material was constructed with vertical placement. This experiment is a duplicate of the Wall WBVN1 experiment. The reason why wall WBVN1 was repeated is to ensure the experiment was conducted correctly because of the load capacity difference between wall WBHN and wall WBVN1 experiments. The Figure 2.15 shows the wall WBVN2 without plaster on it. The Matlab model of the deflected shape and the crack path of wall WBVN2 are shown in Figure 2.16 and Figure 2.17, respectively. Load-deflection curve is shown in Figure 2.18.



Figure 2.15. Built WBVN2 Without Plaster on it

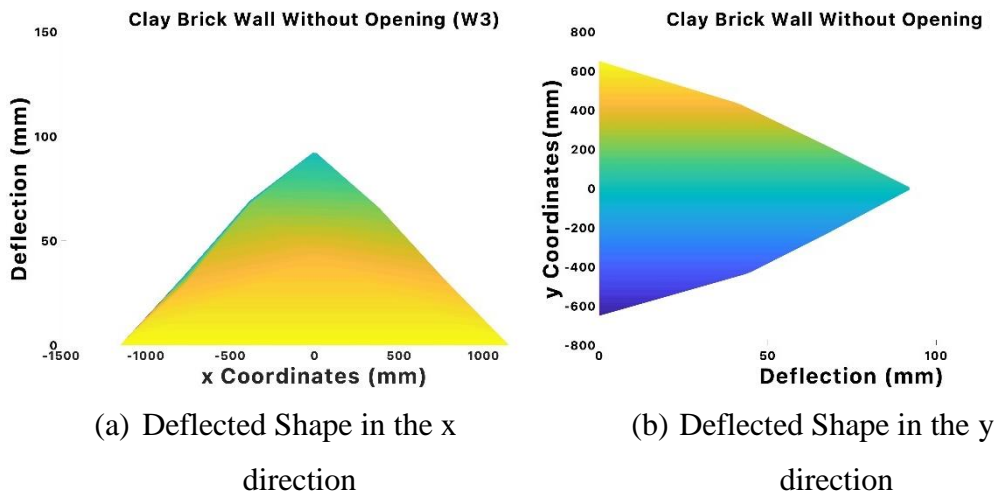


Figure 2.16. Deflected Shape of WBVN2 Before the Failure

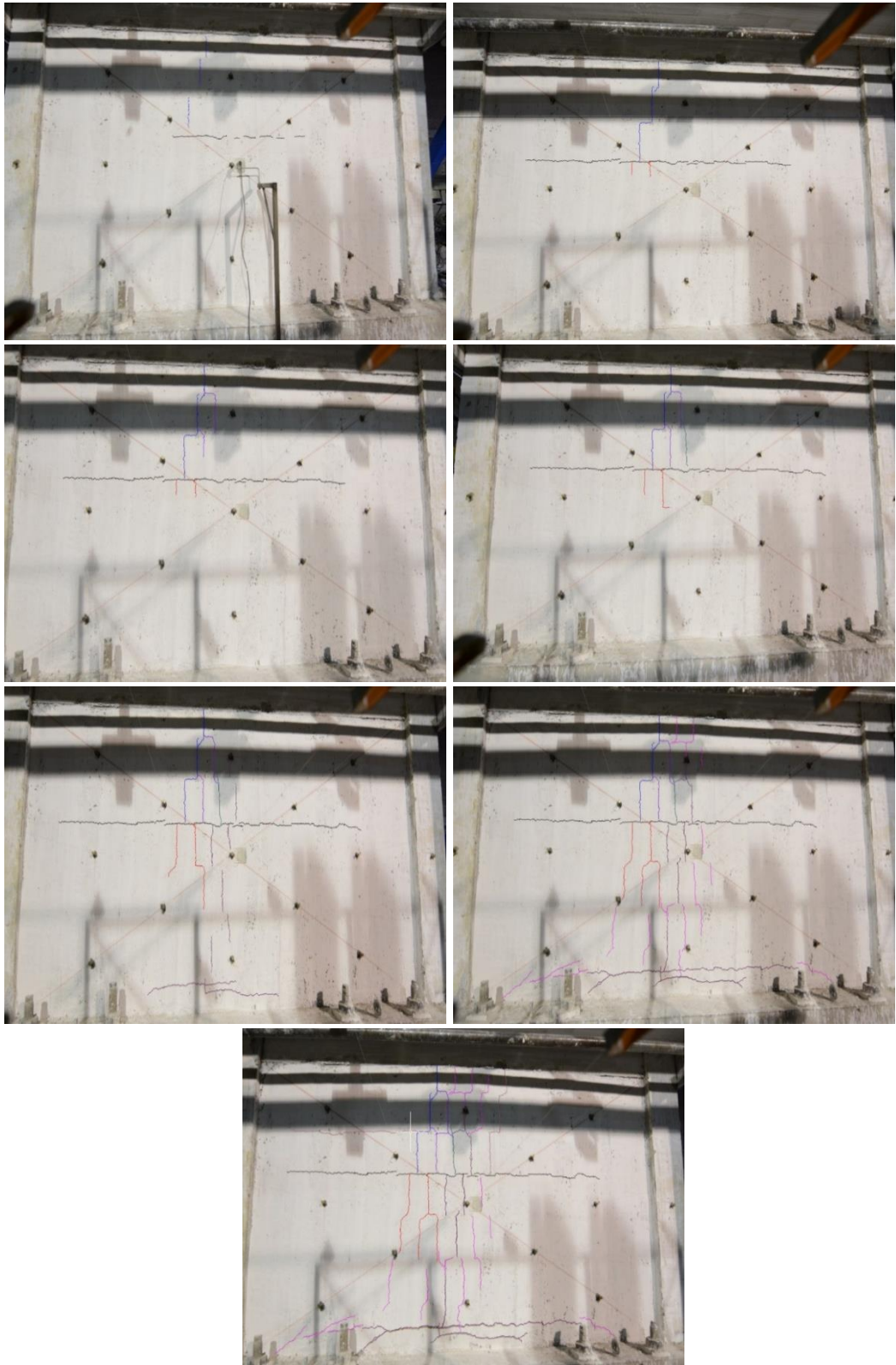


Figure 2.17. Crack Path of WBVN2 Experiment

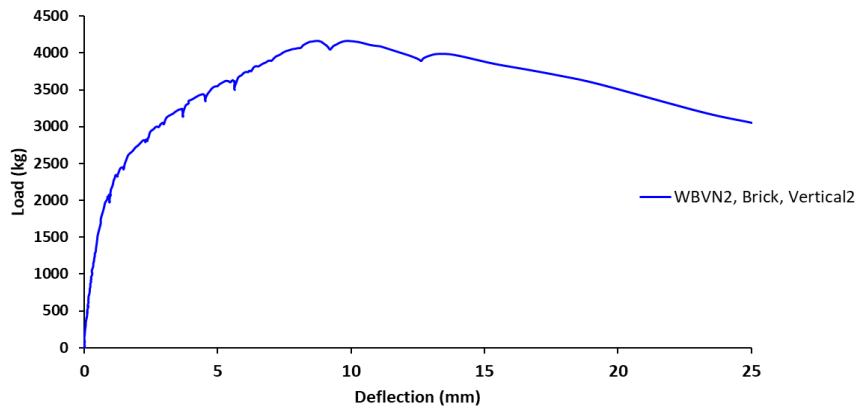


Figure 2.18. Load-Deflection Relation of Specimen WBVN2

2.5.4 Wall WBVW

Wall WBVW is built as a brick infill wall with a window opening and is shown without plaster in Figure 2.19. The model of the deflected shape and crack path of the wall WBVW are presented in Figure 2.20 and Figure 2.21, respectively. Figure 2.22 shows the load-deflection curve of wall WBVW.



Figure 2.19. Built WBVW Without Plaster on it

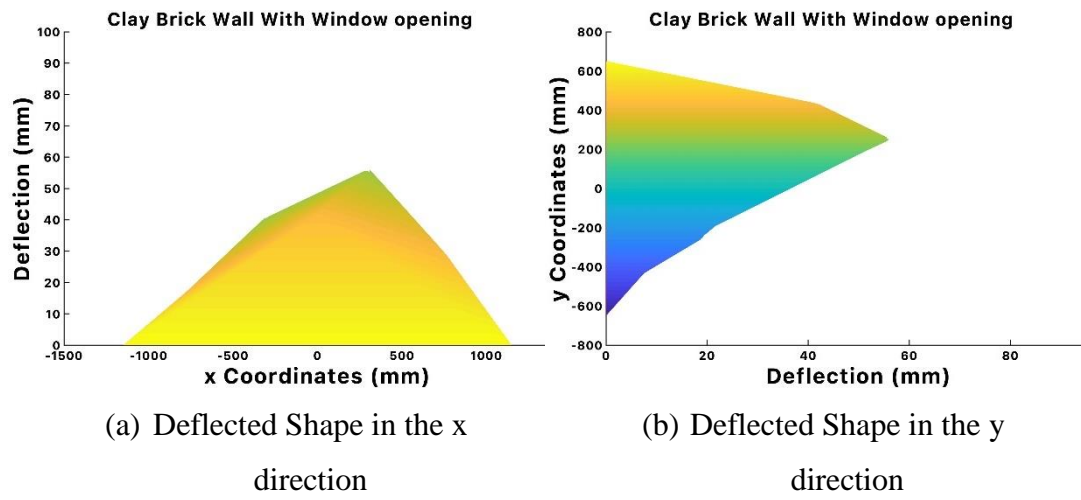


Figure 2.20. Deflected Shape of WBVW Before the Failure



Figure 2.21. Crack Path of WBVW Experiment

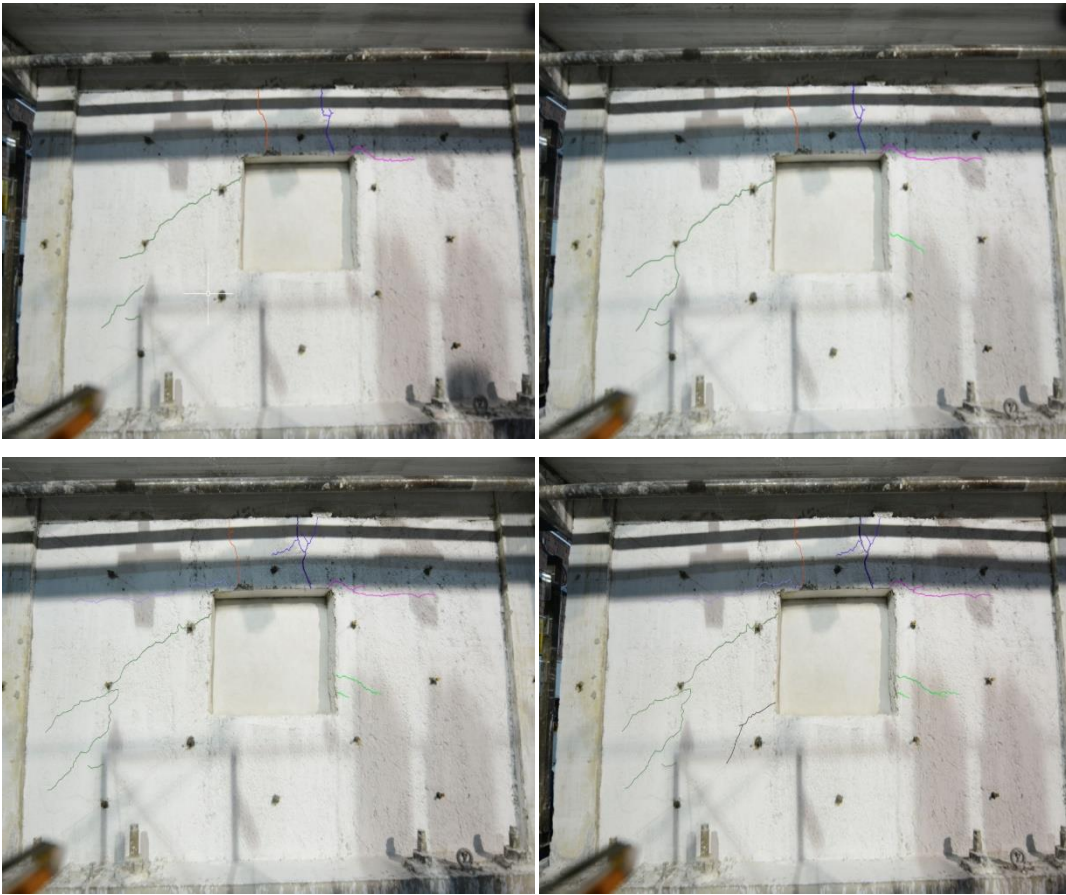


Figure 2.21. Crack Path of WBVW Experiment (continued)

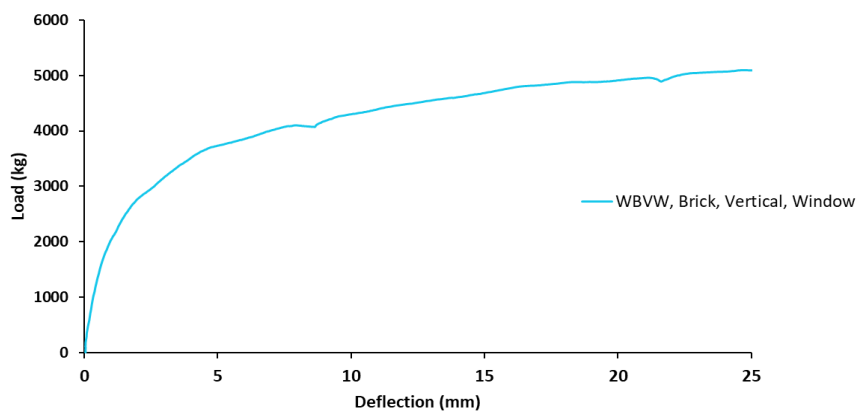


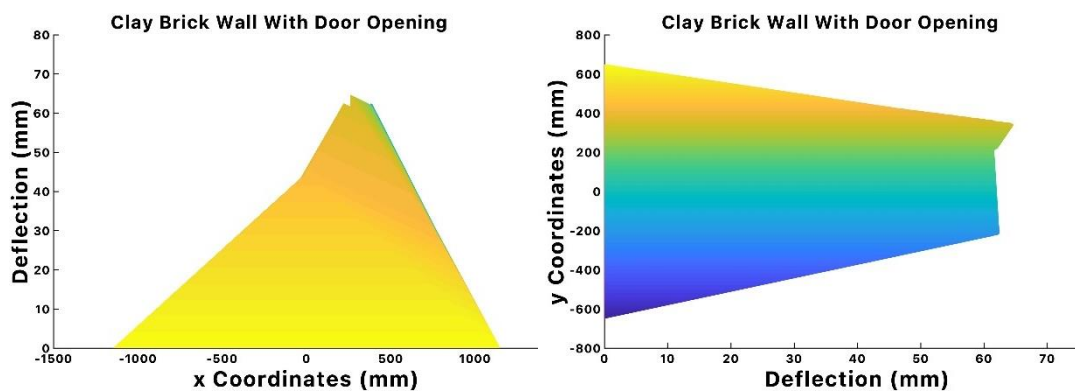
Figure 2.22. Load-Deflection Relation of Specimen WBVW

2.5.5 Wall WBVD

Wall WBVD was built as a brick infill wall with the door opening and is shown without plaster in Figure 2.23. The model of the deflected shape and crack path of wall WBVD are presented in Figure 2.24 and Figure 2.25, respectively. Figure 2.26 shows the load-deflection curve of wall WBVD.



Figure 2.23. Built WBVD Without Plaster on it



(a) Deflected Shape in the x direction (b) Deflected Shape in the y direction

Figure 2.24. Deflected Shape of WBVD Before the Failure

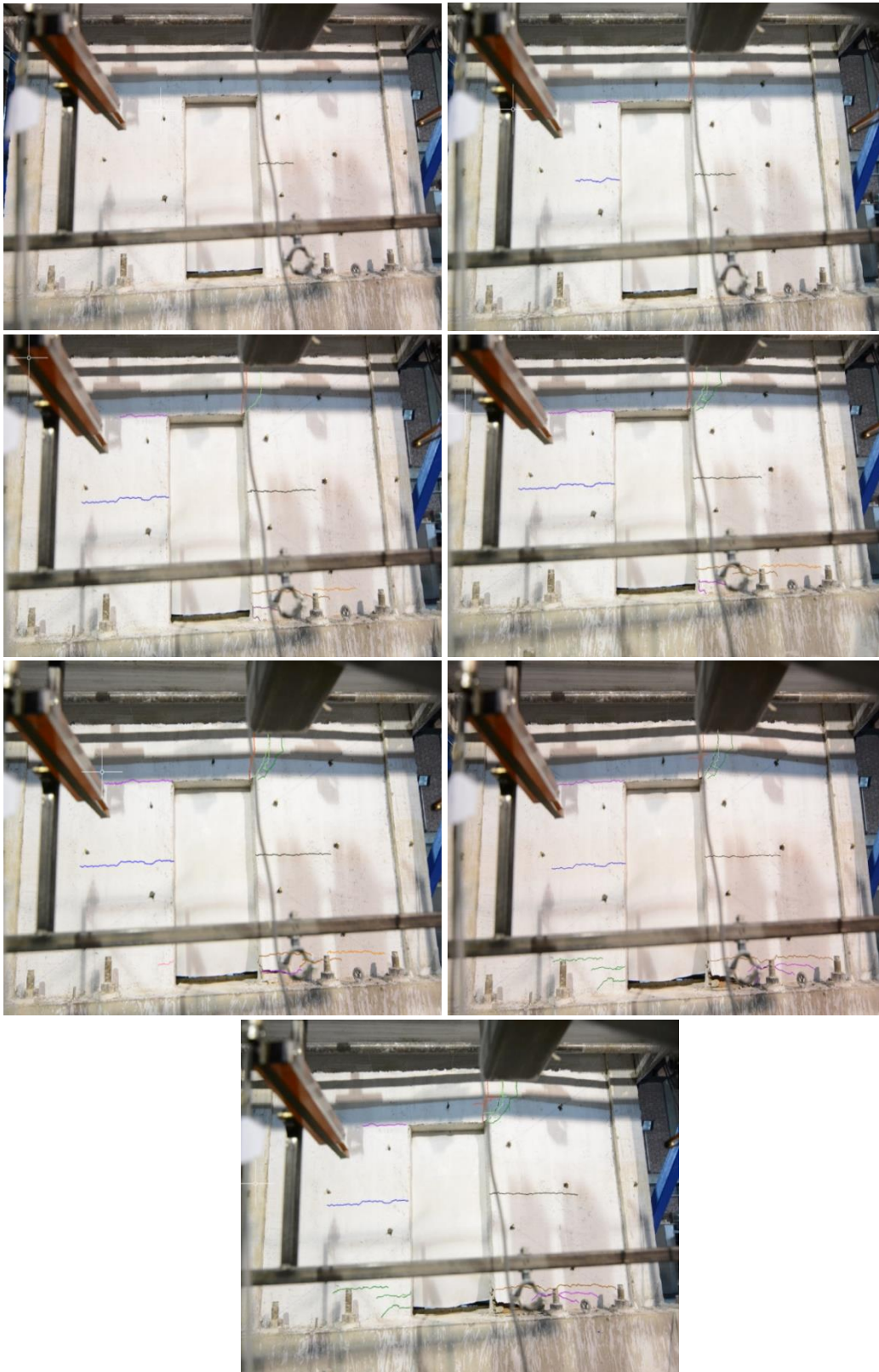


Figure 2.25. Crack Path of WBVD Experiment

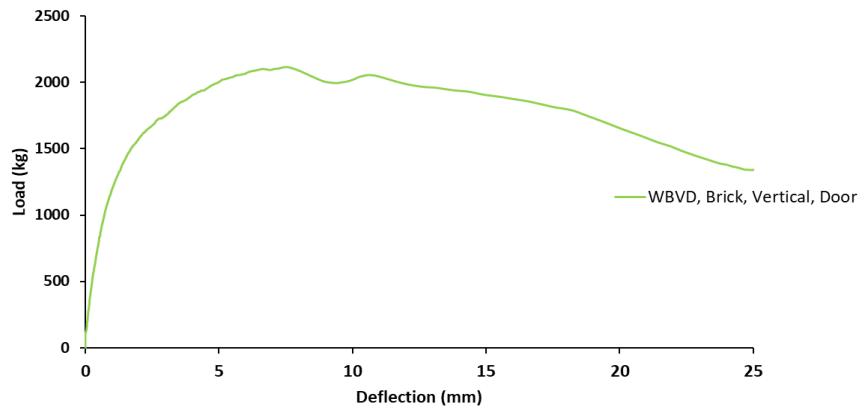


Figure 2.26. Load-Deflection Relation of Specimen WBVD

2.5.6 Wall WPVN

The wall WPVN was built without opening using pumice concrete as infill material. It is shown just before the plaster was covered on it in. The model of the deflected shape and crack path of wall WPVN are presented in Figure 2.28 and Figure 2.29, respectively. Figure 2.30 shows the load-deflection curve of wall WPVN.



Figure 2.27. Built WPVN Without Plaster on it

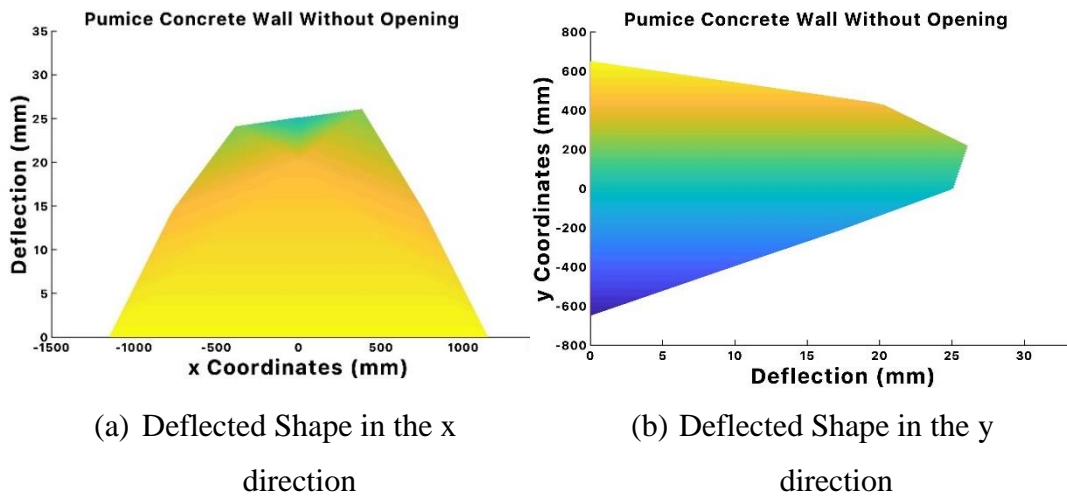


Figure 2.28. Deflected Shape of WPVN Before the Failure

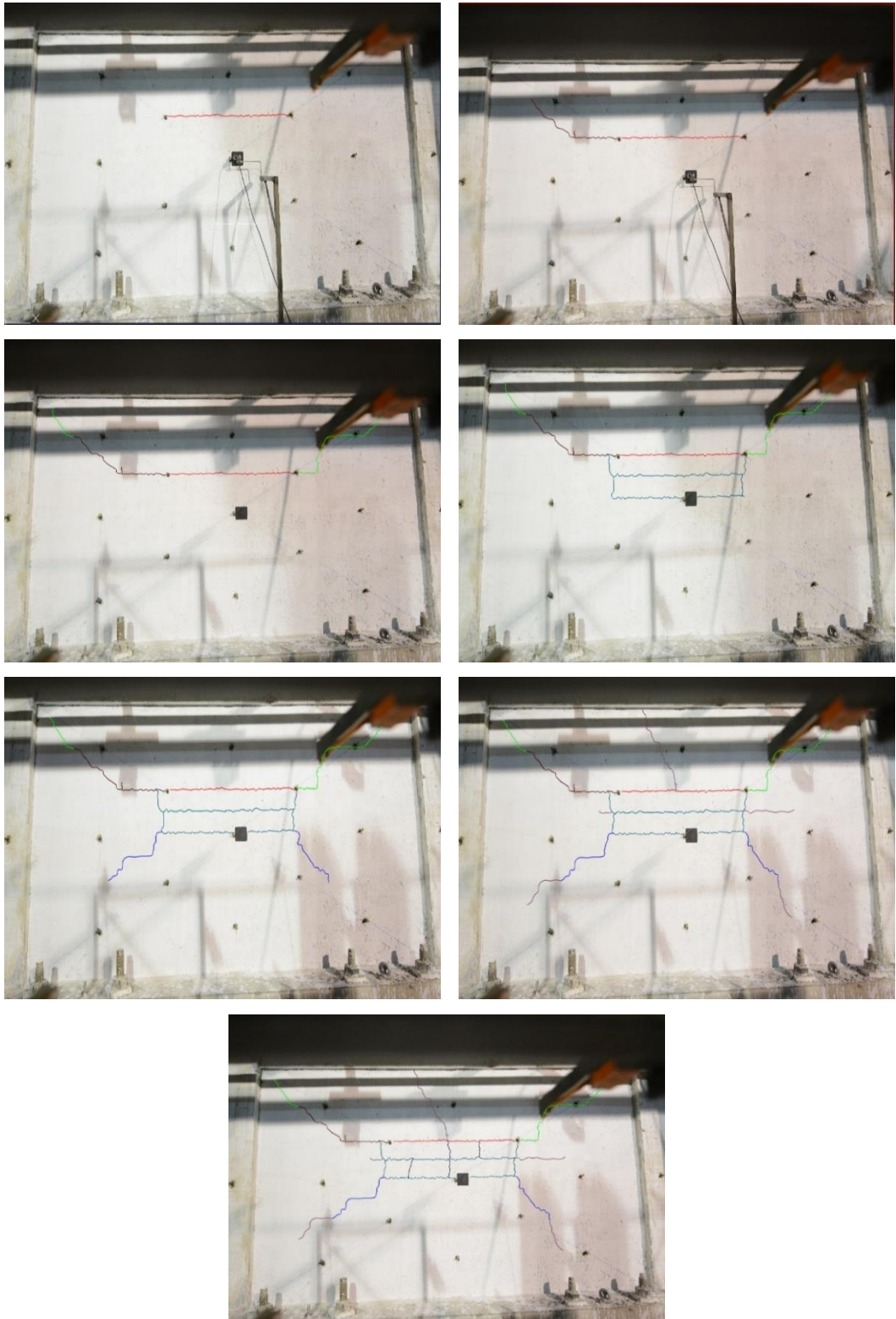


Figure 2.29. Crack Path of WPVN Experiment

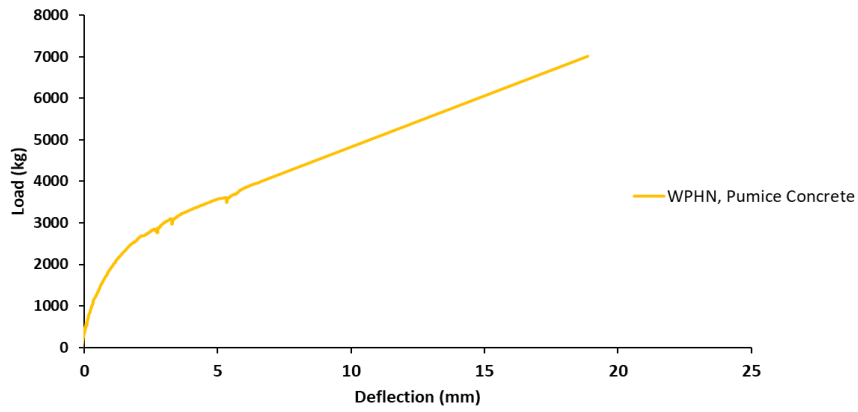


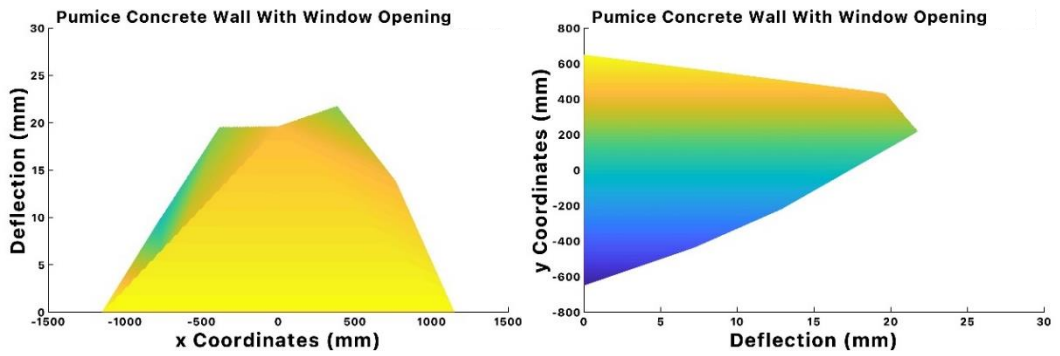
Figure 2.30. Load-Deflection Relation of Specimen WPHN

2.5.7 Wall WPVW

Wall WPVW was built with a window opening using pumice concrete as infill material and is shown without plaster in Figure 2.31. The model of the deflected shape and crack path of wall WPVW are presented in Figure 2.32 and Figure 2.33, respectively. The load-deflection curve of wall WPVW is shown in Figure 2.34.



Figure 2.31. Built WPVW Without Plaster on it



(a) Deflected Shape in the x direction (b) Deflected Shape in the y direction

Figure 2.32. Deflected Shape of WPVW Before the Failure

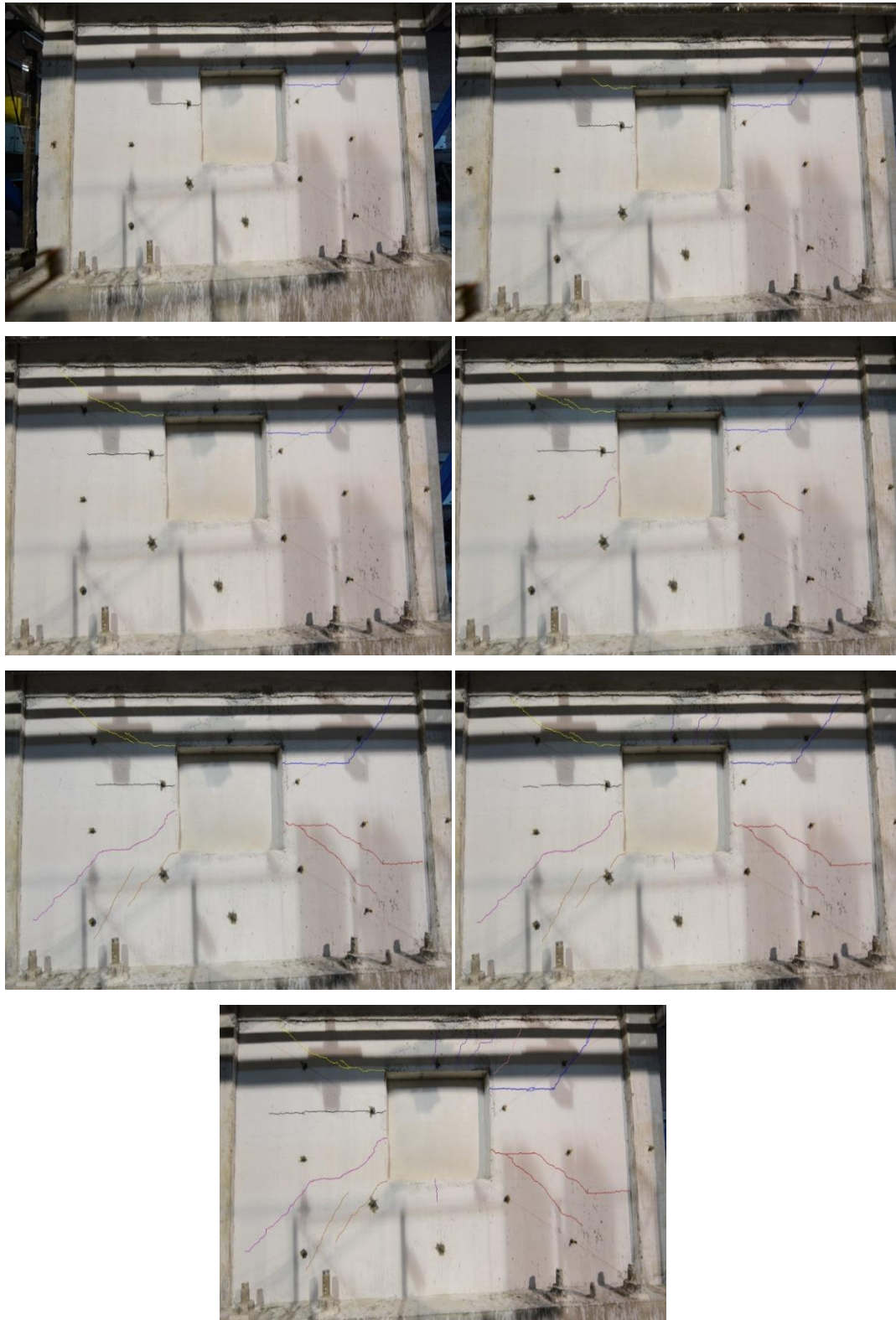


Figure 2.33. Crack Path of WPVW Experiment

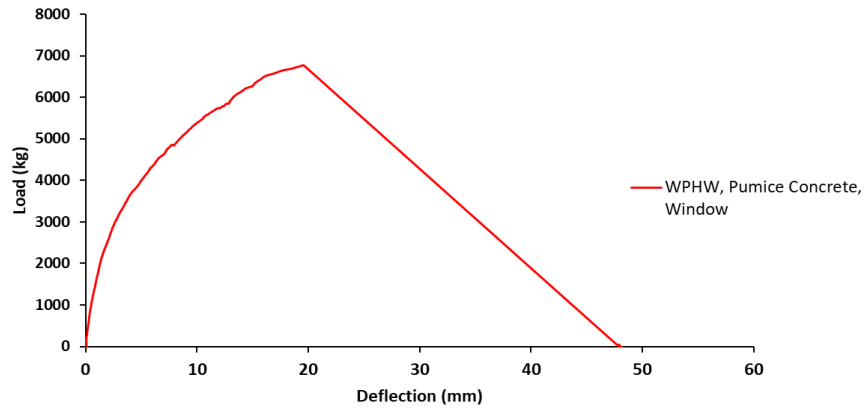


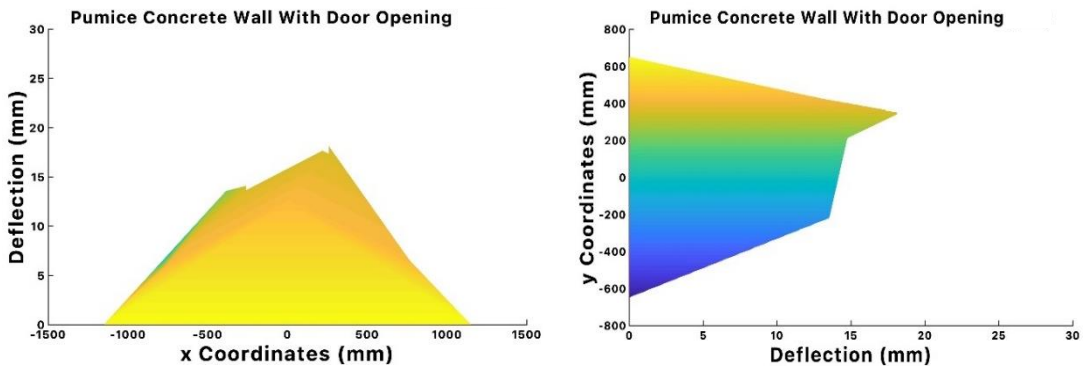
Figure 2.34. Load-Deflection Relation of Specimen WPHW

2.5.8 Wall WPVD

Wall WPVD was built with a door opening using pumice concrete as infill material and is shown without plaster in Figure 2.35. The model of the deflected shape and crack path of wall WPVD are presented in Figure 2.36 and Figure 2.37, respectively. The load-deflection curve of wall WPVD is shown in Figure 2.38.



Figure 2.35. Built WPVD Without Plaster on it



(a) Deflection Shape in the x direction

(b) Deflected Shape in the y direction

Figure 2.36. Deflected Shape of WPVD Before the Failure



Figure 2.37. Crack Path of WPVD

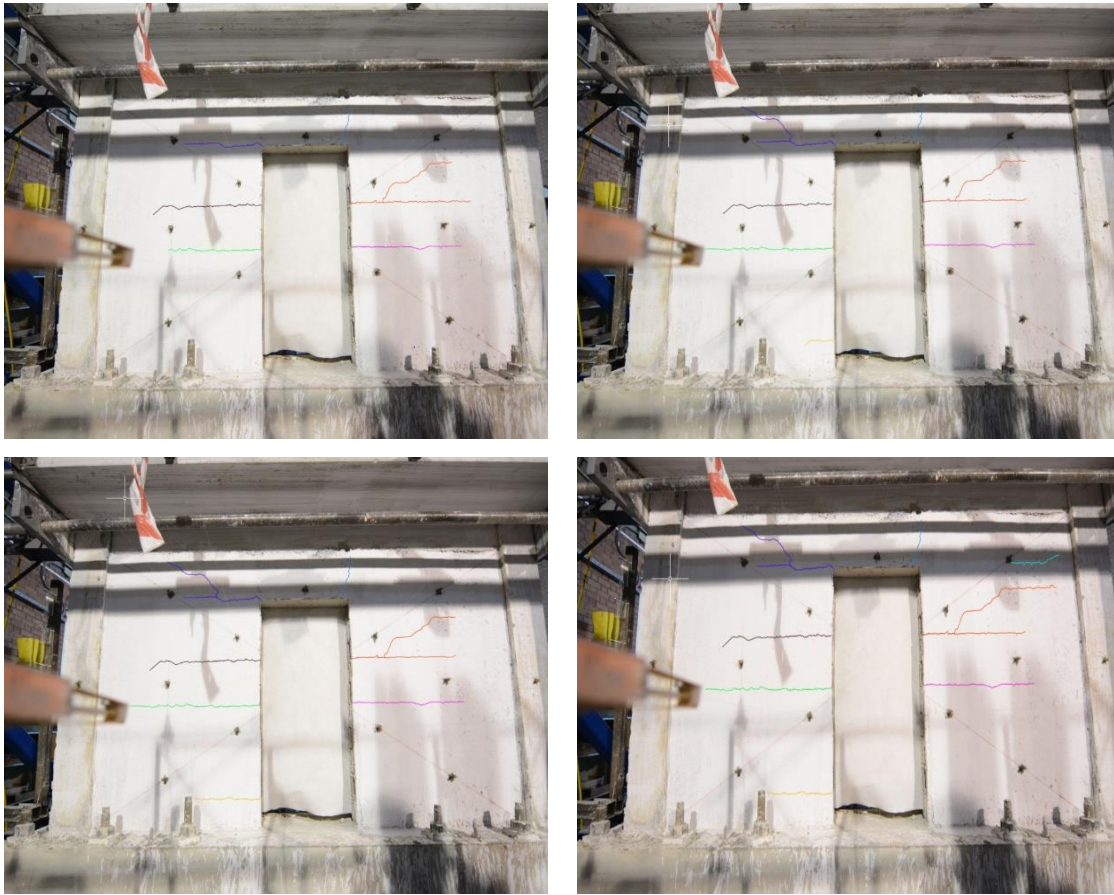


Figure 2.37. Crack Path of WPVD (continued)

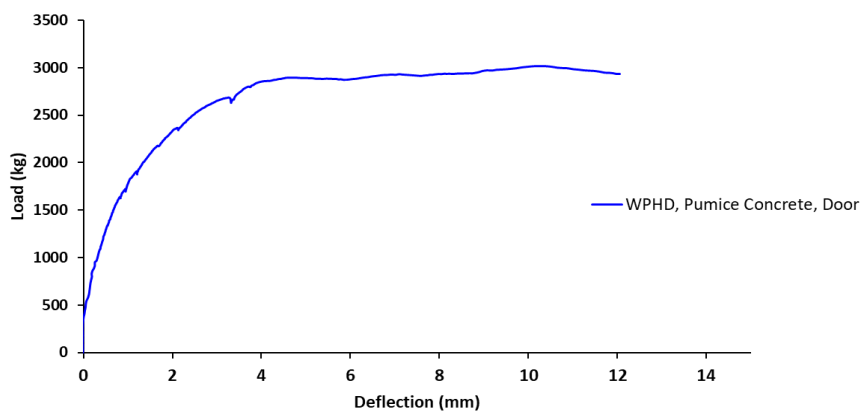


Figure 2.38. Load-Deflection Relation of Specimen WPVD

The following figure shows the failure crack states of each specimen. The corresponding out-of-plane forces which are observed when the cracks occurred are also specified in Figure 2.39, Figure 2.40, Figure 2.41, Figure 2.42, Figure 2.43, Figure 2.44, Figure 2.45.

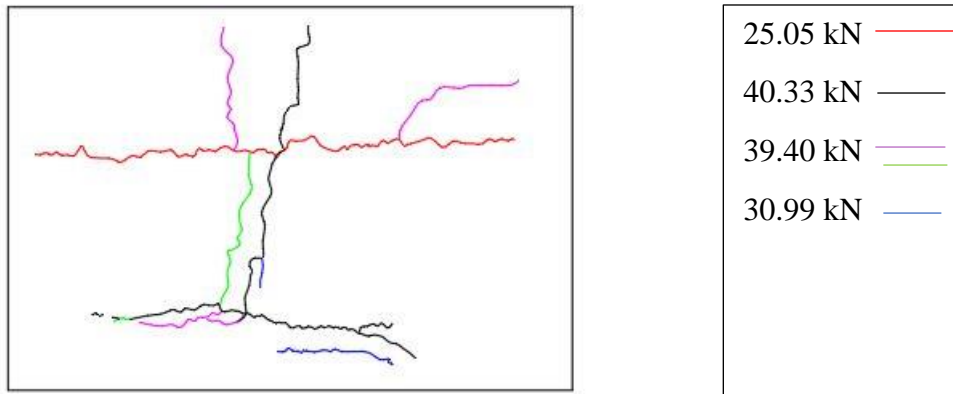


Figure 2.39. The Corresponding Loads of Cracks for WBVN1

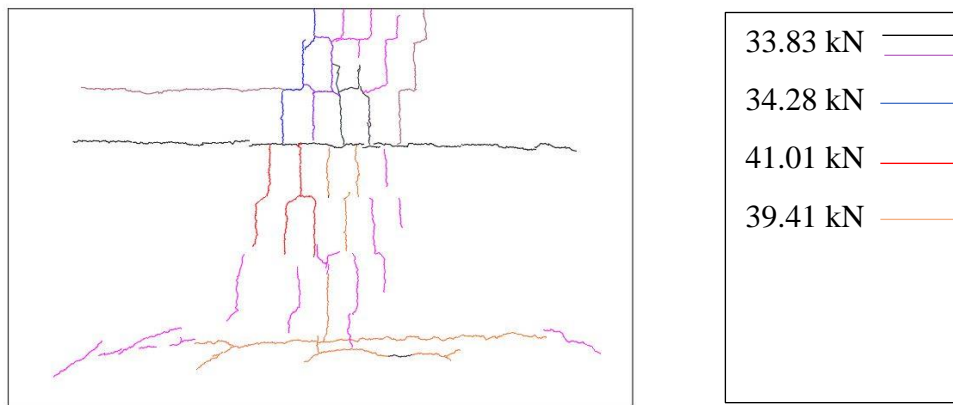


Figure 2.40. The Corresponding Loads of Cracks for WBVN2

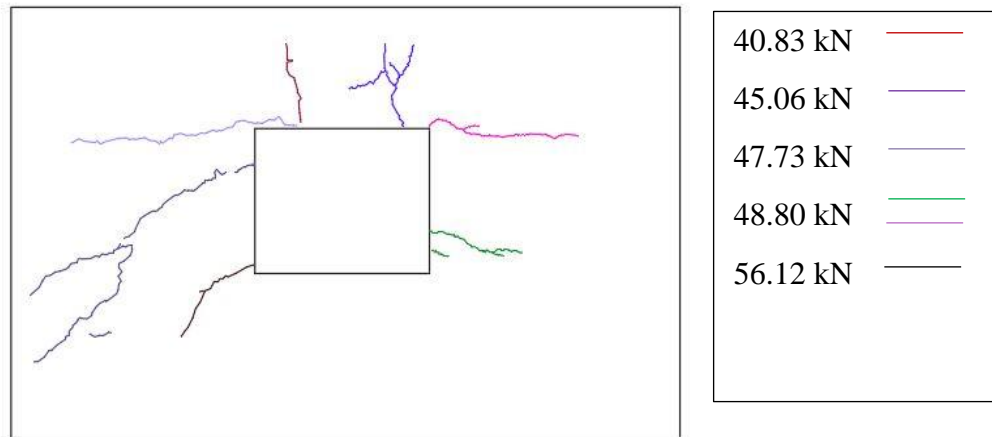


Figure 2.41. The Corresponding Loads of Cracks for WBVW

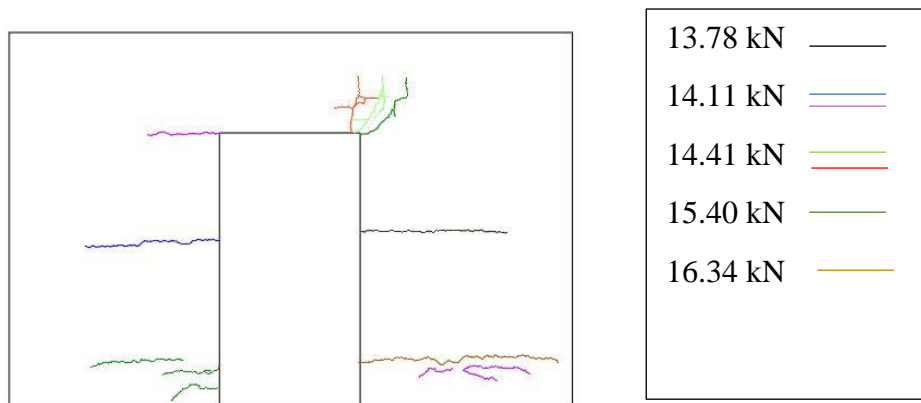


Figure 2.42. The Corresponding Loads of Cracks for WBVD

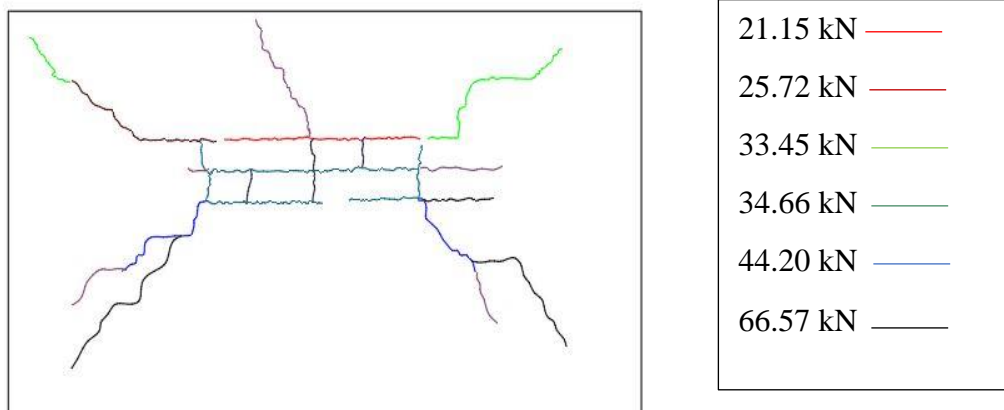


Figure 2.43. The Corresponding Loads of Cracks for WPVN

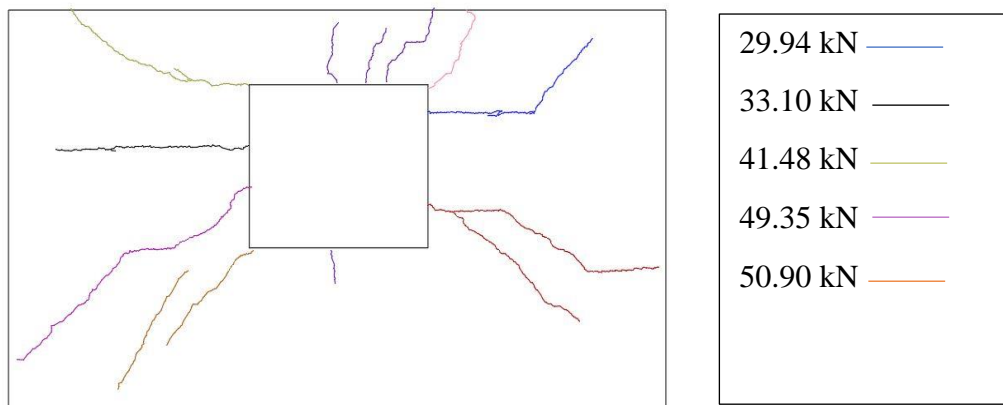


Figure 2.44. The Corresponding Loads Of Cracks for WPVW

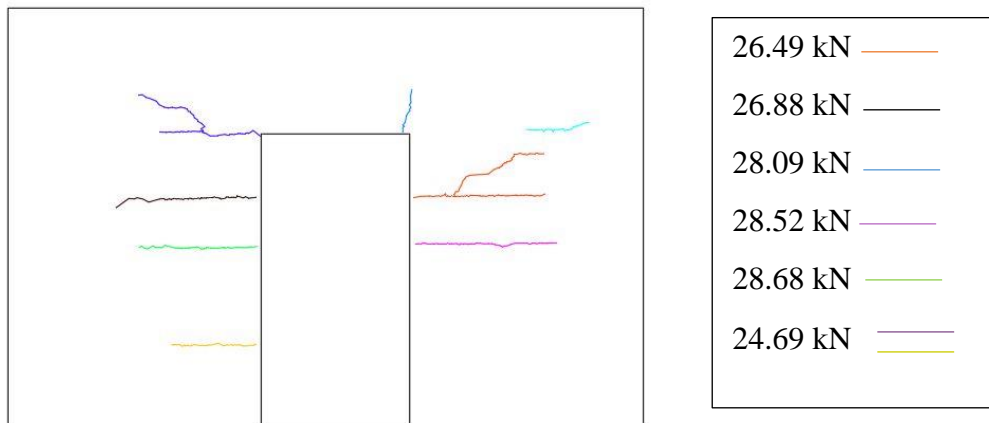


Figure 2.45. The Corresponding Loads of Cracks for WPVD

2.6 Comparisons of Test Results

The results and behavior of each tested specimen were given previously. In this section, the results are compared according to different parameters. These parameters are chosen as listed below.

- i. The infill material
- ii. The existence of the opening
- iii. The size of the openings

In that context, the following graphs presented in Figure 2.46, Figure 2.47, Figure 2.48, Figure 2.49, and Figure 2.50 show the difference in load-deflection capacities of the tested specimens.

The load-deflection relations of the infill wall specimens under out-of-plane loading show that the change of infill material also changes the out-of-plane capacity of the unreinforced infill wall, even if the same plaster and mortar mix is used. The infill walls built with pumice concrete blocks have more capacity with less deflection for all types of tested infill walls than the clay brick infill walls. This difference may be

due to the continuity provided by the tongue and groove at the side of the pumice concrete blocks.

Furthermore, the existence of openings is also another issue that affects the out-of-plane load-bearing capacity of infill walls. Infill walls with door openings have the lowest load capacity with the lowest deflection.

The presence of the window opening also affects the infill wall capacity. In light of the observations, it can be said that the failure loads and the deflections of infill walls with window openings are higher than the infill walls with door openings for both infill materials. This difference can be attributed to the smaller opening area of windows compared to the door opening area. However, the comparison of the infill walls with a window opening and without an opening show that the window opening does not cause a significant decrease in the load and the deflection capacity. Moreover, Figure 2.38 and Figure 2.39 show that the infill wall with a window opening has an even higher or equal capacity than the infill wall without an opening. According to some studies in the literature, the window opening may increase the two-way bending capacity of the unreinforced infill walls in the out-of-plane direction (Chang et al.,2022). In other words, the excess capacity of the infill walls with window openings is acceptable and justifiable according to the literature. Furthermore, it should be noted that there have been lintels above both the door and window openings. When a lintel is placed over the window, it causes additional yield lines to form and also improves the behavior of the arch action since there is not much distance from the top beam.

The infill wall, constructed by laying down the bricks horizontally, provided a higher load capacity than the specimen with vertical brick placement. The load-carrying capacity of the pumice concrete infill walls is higher than their counterparts, vertically aligned clay brick infill walls, as shown in Figure 2.48, Figure 2.49, and Figure 2.50. The tongue and groove of the pumice concrete blocks help resist failure, increase the out-of-plane load capacity, and decrease deflection.

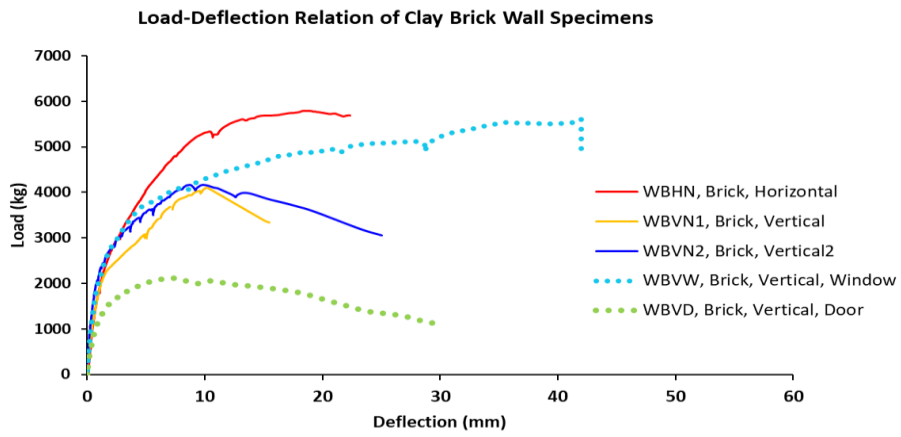


Figure 2.46. Load-Deflection Relation of Clay Brick Infill Walls

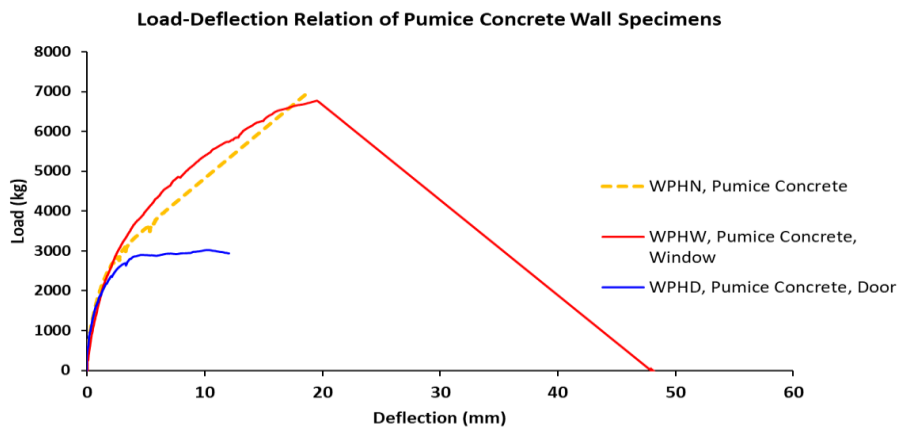


Figure 2.47. Load-Deflection Relation of Pumice Concrete Infill Walls

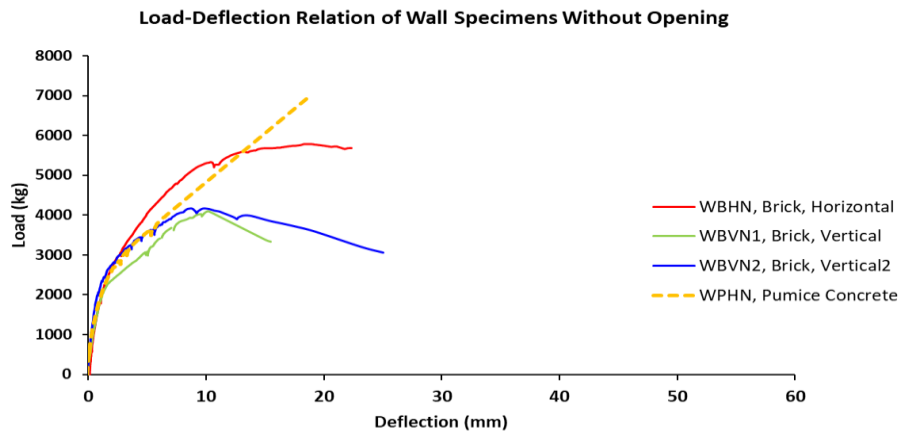


Figure 2.48. Load-Deflection Relation of Infill Walls Without Opening

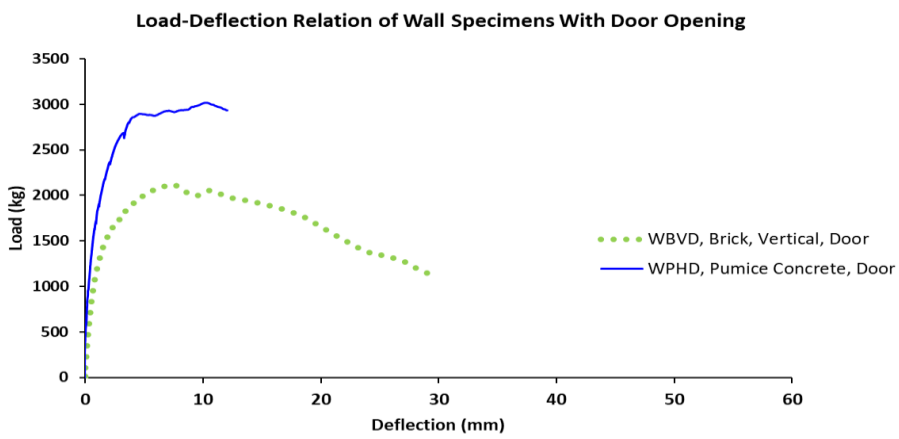


Figure 2.49. Load-Deflection Relation of Infill Walls With Door Opening

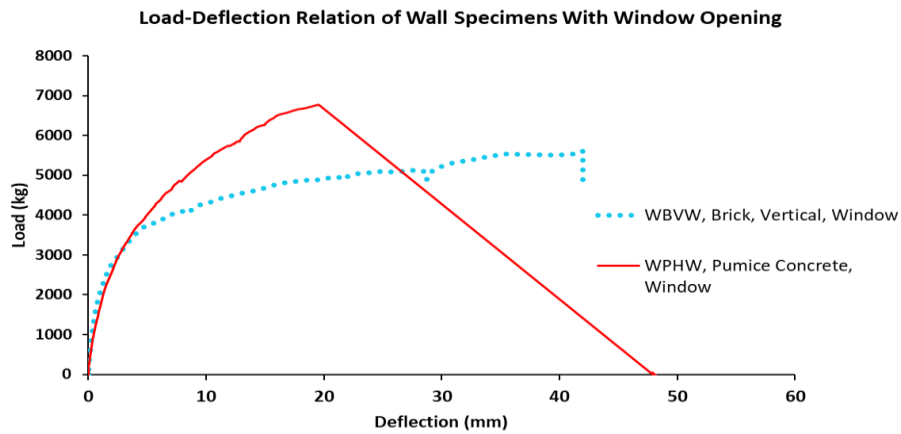


Figure 2.50. Load-Deflection Relation of Infill Walls with Window Opening

The maximum load capacities and the corresponding maximum deflections are summarized in Table 2.4.

Table 2.4 Maximum Load and Corresponding Deflections of the Specimens

Specimen Name	Maximum Load (kN)	Deflection (mm)	Deflection Place (LVDT)
WBHN	56.78	18.44	4
WBVN1	40.24	9.27	4
WBVN2	40.82	8.77	4
WBVW	55.07	38.72	14
WBVD	20.72	7.44	14
WPVN	70.05	18.87	4
WPVW	66.37	21.53	7
WPVD	30.15	10.15	14

CHAPTER 3

ANALYSIS

3.1 Out-of-Plane Capacity of Infill Walls

Out-of-plane behavior of the infill walls gained importance in the last few decades. Some studies showed that unreinforced infill walls carry a load in the out-of-plane direction and their load-carrying capacities make a difference during a seismic event. Therefore, it is important to properly determine the out-of-plane load-carrying capacity of infill walls. Eight out-of-plane tests were conducted in this scope. A one-bay, one-story, and half-scaled RC frame was used to fill with clay brick and pumice concrete infill.

3.1.1 Yield Line Analysis of Test Specimens

This section of the document presents the determination of the out-of-plane load-bearing capacity of unreinforced infill walls by means of yield line analysis, taking into account various parameters by applying the method of virtual work. Lawrence and Marshall [2000] suggested a new method for the out-of-plane design of unreinforced infill walls based on the knowledge of expected crack patterns by using the principle of virtual work, which is a theory that equates internal work and external work to each other in a system. The results of the numeric analysis were supported by the experimental studies. The methodology also permitted the existence of window and door openings [Solarino et al.,2019].

A virtual work method is an approach to calculate the load acting on the system or the deflection due to the load acting on the system using the law of conservation of energy. The work done through the virtual displacement and virtual force are equal according to the conservation energy rule. Briefly, the internal and external work of

the system is taken into account as equal, as shown in Equation 3.1. The external work is defined as the work done by the virtual displacement, while the internal work is the work done by the virtual force.

$$W_E = W_I \quad (3.1)$$

Yield line analysis is usually conducted to estimate the ultimate load of one-way and two-way slab failure. Four different support conditions for two-way slab failure and two different support conditions for one-way slab failure were chosen for the analysis. Four sides fixed-end supported and three sides fixed + one side simply supported boundary conditions were chosen for the failure of the two-way slab. Different yield patterns are obtained by different boundary condition assumptions (Vaculik, 2012; UFC, 2008). The support conditions and the assumed yield lines affect the internal work, and the occurred displacement produces the external work. One example is explained below for both one-way bending and two-way bending.

Two-way bending infill wall:

The assumed yield line pattern for the four sides fixed-end infill wall is shown in Figure 3.1. The load is assumed to be uniformly distributed over the area.

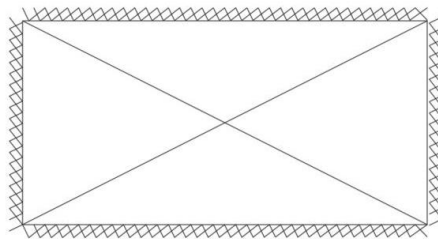


Figure 3.1. Assumed Yield Pattern for Four Sided fixed Supported Infill Wall

The internal work and the external work are equated to each other. The work done by the displacement is calculated as shown in Equation 3.2.

$$W_E = \Sigma A_i \cdot \delta_i \cdot w \quad (3.2)$$

Where, A_i is the area of the region i , δ_i is the deflection occurring in the center of the yield pattern, w is the acting uniformly distributed load.

The work done by the internal forces is calculated as shown in Equation 3.3:

$$W_I = \Sigma M_y l_y \theta_y + \Sigma M_x l_x \theta_x + \Sigma \alpha M_y l_y \theta_y + \Sigma \alpha M_x l_x \theta_x \quad (3.3)$$

where M_{ix} and M_{iy} are the ultimate moment capacities for unit length along the yield line in the x and y directions. l_x and l_y are the length of the yield lines projected in the x and y directions. θ_x and θ_y are the rotation of the yield line projected in the x and y axes. α is the ratio of support moments to mid-span moments (α values are taken as 1 in this study since the unreinforced infill walls are used as the system).

The unit-distributed load is obtained by equating external and internal work for unit displacement. The assumed yield line pattern is given for the one-way bending state in Figure 3.2.

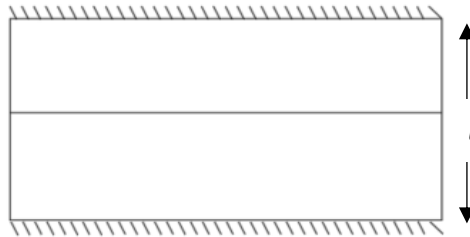


Figure 3.2. Assumed Yield Pattern for One-Way Bending for Infill Wall

The distributed load for the unit length is obtained as shown in Equation 3.4 by equating Equation 3.2 and Equation 3.3 to each other.

$$w = 8 \frac{M}{l^2} \quad (3.4)$$

The yield line patterns for unreinforced infill walls, which simulate window opening, door opening, and no opening conditions, were considered separately. Possible yield patterns for four sides fixed-end support and three sides fixed + one side simply supported boundary conditions for two-way slabs for two types of unreinforced infill

walls are presented in Figure 3.3 and Figure 3.4, respectively. In these figures, cross hatches represent fixed-end support, and diagonal hatch represents simply support.

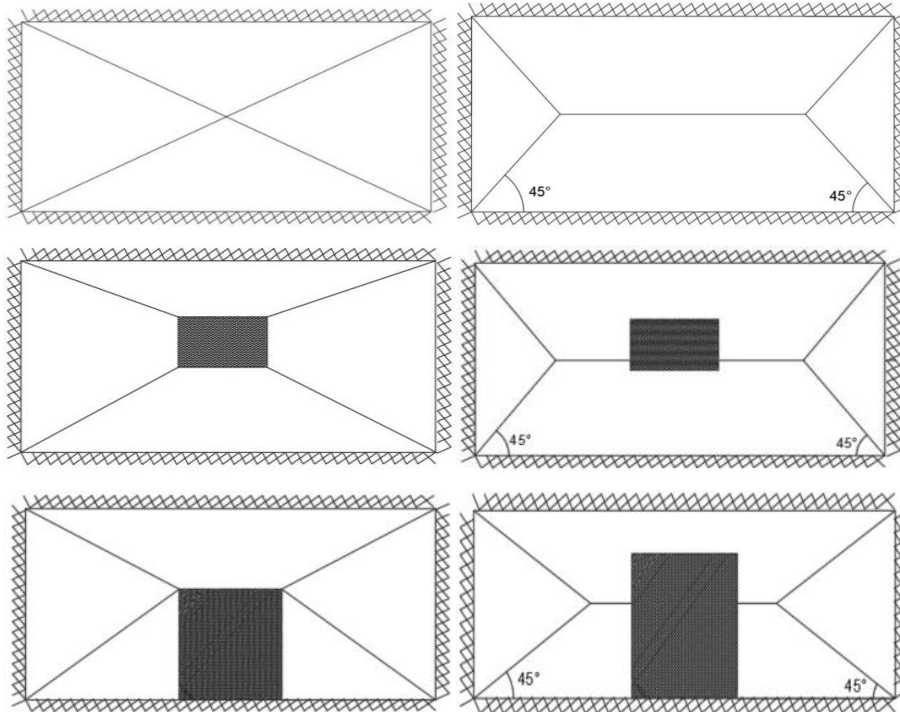


Figure 3.3. Yield Line Patterns for Four Sides Fixed-End Boundary Conditions

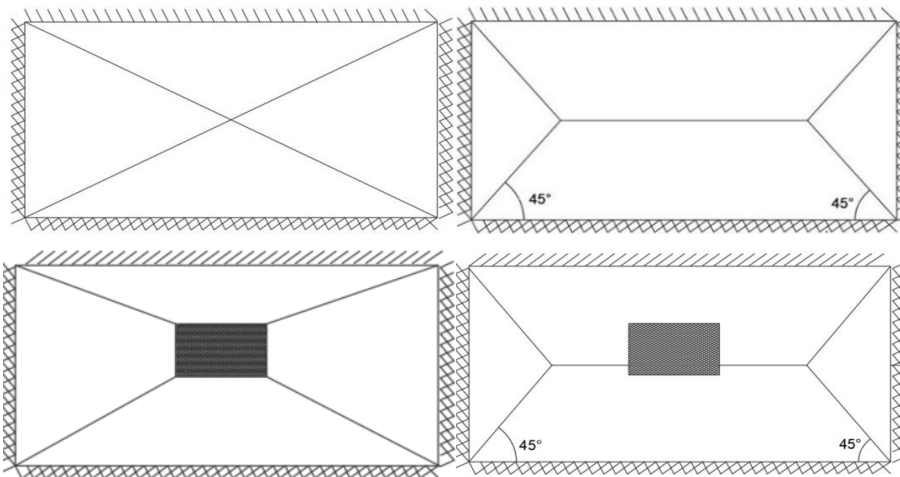


Figure 3.4. Yield Line Patterns for Three Sides Fixed + One Side Simply Supported Boundary Conditions

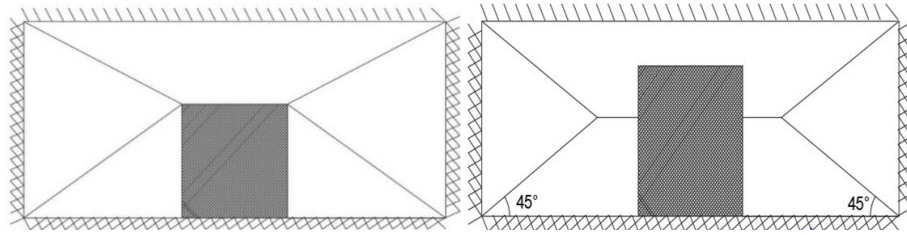
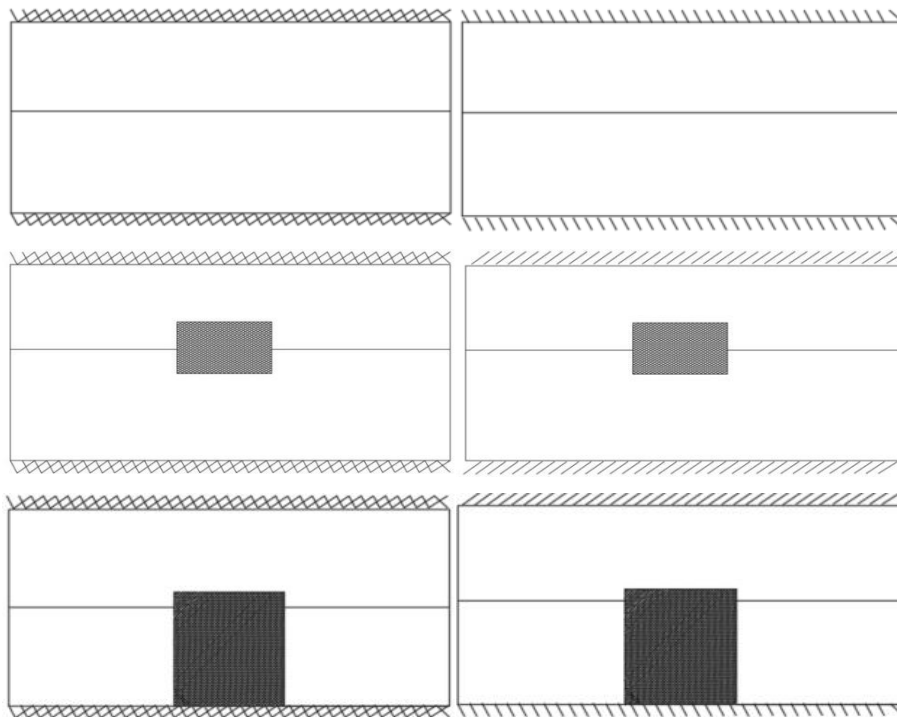


Figure 3.4. Yield Line Patterns for Three Sides Fixed + One Side Simply Supported Boundary Conditions (continued)

One-way failures were also examined for two different boundary conditions, fixed-end and simply supported for the infill walls' upper and bottom boundaries. The yield line patterns of simply supported and fixed-end boundary conditions for each infill wall type are shown in Figure 3.5.



a) Yield Line Patterns for One-Way Fixed-End Support Infill Walls b) Yield Line Patterns for One-Way Simply Supported Infill Walls

Figure 3.5. Yield Line Patterns for both Fixed-End and Simply Supported Boundary Conditions of One-Way Infill Walls

Yield line analysis was performed using the virtual work method for the tested infill walls mentioned in Chapter 2, using the theoretically possible yield patterns mentioned in Figure 3.3, , and Figure 3.5. The failure capacities of the infill walls were determined considering the flexural strength of the plaster, which is tested after each experiment. The reason for considering plaster in capacity calculations is that the flexural strength of plaster is the lowest among the infill wall materials. Cracking always starts at the plaster and reaches the failure state. In light of this observation, the virtual work method for yield line analysis was conducted with a specific flexural strength measured after each experiment. The measured and calculated capacities are compared, and accordingly, the best-match yield line pattern is determined. The calculations for the four sides fixed-end boundary conditions are shown in Appendix A. The compared results for each specimen and yield patterns are given in Table 3.1, Table 3.2 and Table 3.3.

Table 3.1 Comparison of Test Results with Yield Line Analysis for Infill Walls Without Opening

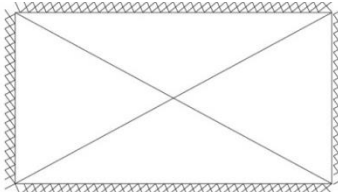
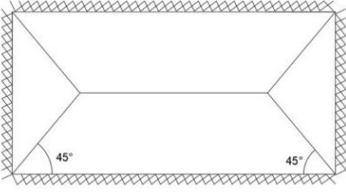
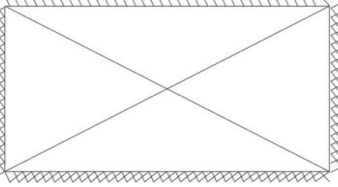
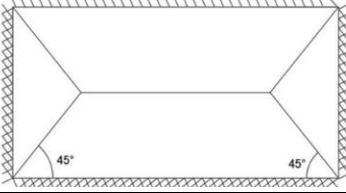
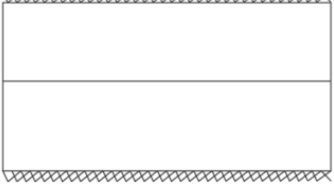

Yield Pattern	Specimen Name	Yield Line Analysis Results	Experiment Results
	WBHN	214.2 kN	57.9kN
	WBVN1	158.4 kN	41.0 kN
	WBVN2	242.2 kN	41.6 kN
	WPNV	339.9 kN	70.1 kN
	WBHN	188.5 kN	57.9 kN
	WBVN1	139.4 kN	41.0 kN
	WBVN2	213.4 kN	41.6 kN
	WPNV	299.2 kN	70.1 kN
	WBHN	165.6 kN	57.9 kN
	WBVN1	122.4 kN	41.0 kN
	WBVN2	187.2 kN	41.6 kN
	WPNV	262.9 kN	70.1 kN
	WBHN	148.6 kN	57.9 kN
	WBVN1	109.8 kN	41.0 kN
	WBVN2	168.0 kN	41.6 kN
	WPNV	235.8 kN	70.1 kN
	WBHN	73.2 kN	57.9 kN
	WBVN1	54.2 kN	41.0 kN
	WBVN2	82.8 kN	41.6 kN
	WPNV	116.2 kN	70.1 kN
	WBHN	36.6 kN	57.9 kN
	WBVN1	27.1 kN	41.0 kN
	WBVN2	41.4 kN	41.6 kN
	WPNV	58.1 kN	70.1 kN

Table 3.2 Comparison of Test Results with Yield Line Analysis for Infill Walls
With Window Opening

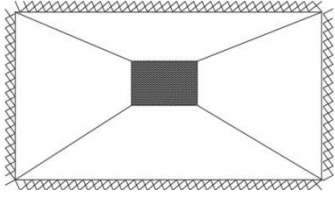
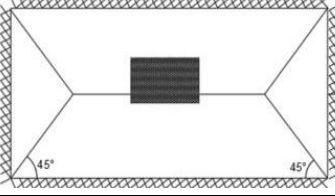
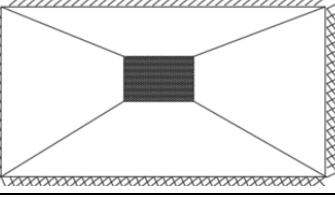
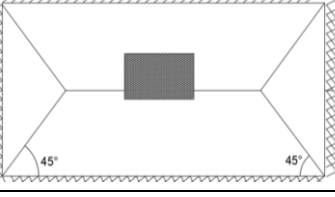
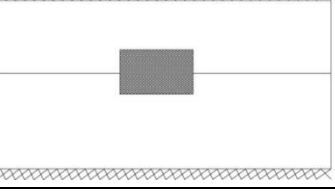
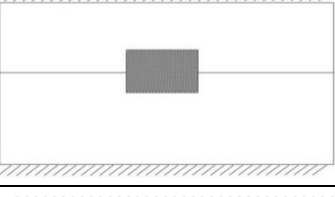
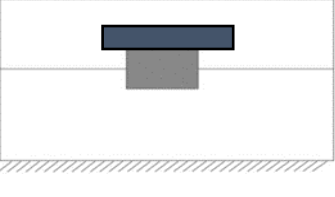
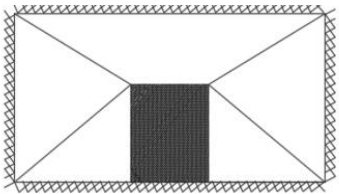
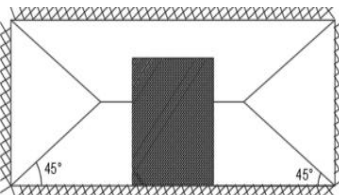
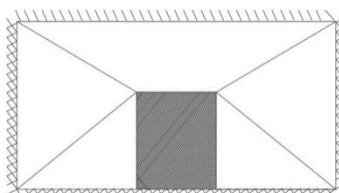
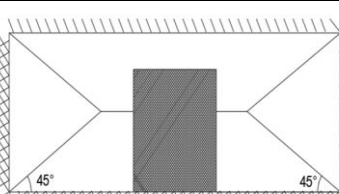
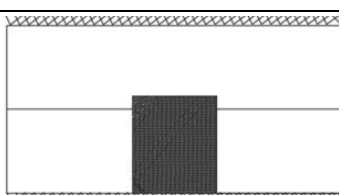
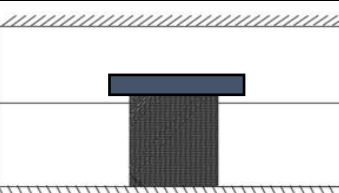
Yield Pattern	Specimen Name	Yield Line Analysis Results	Experiment Results
	WBVW	383.1 kN	56.1 kN
	WPVW	360.5 kN	67.7 kN
	WBVW	345.3 kN	56.1 kN
	WPVW	324.9 kN	67.7 kN
	WBVW	252.2 kN	56.1 kN
	WPVW	237.3 kN	67.7 kN
	WBVW	26.31 kN	56.1 kN
	WPVW	247.5 kN	67.7 kN
	WBVW	71.5 kN	56.1 kN
	WPVW	67.3 kN	67.7 kN
	WBVW	37.8 kN	56.1 kN
	WPVW	35.6 kN	67.7 kN
	WBVW	66.8 kN	56.1 kN
	WPVW	60.1 kN	67.7 kN

Table 3.3 Comparison of Test Results with Yield Line Analysis for Infill Walls with Door Opening

Yield Pattern	Specimen Name	Yield Line Analysis Results	Experiment Results
	WBVD	415.5 kN	21.1 kN
	WPVD	367.3 kN	30.1 kN
	WBVD	290.0 kN	21.1 kN
	WPVD	256.4 kN	30.1 kN
	WBVD	248.8 kN	21.1 kN
	WPVD	219.9 kN	30.1 kN
	WBVD	218.8 kN	21.1 kN
	WPVD	193.4 kN	30.1 kN
	WBVD	27.6 kN	21.1 kN
	WPVD	24.4 kN	30.1 kN
	WBVD	13.8 kN	21.1 kN
	WPVD	12.2 kN	30.1 kN

3.1.1.1 Discussion of Yield Line Analysis of Test Specimens

Compared results for the specimens give an idea of how the infill walls behave under out-of-plane loading. The comparison of different yield-line patterns with the measured experimental results shows that the failure state of the infill wall specimens matches the best with the one-way slab failure assumption. As expected, two-way yield patterns generate higher out-of-plane load-bearing capacity than one-way yield patterns. Moreover, the yield line analysis results of one-way yield patterns give acceptably accurate results as the experimental study. The comparison of experimental results with the yield line analysis results of the one-way failure assumption is given in Table 3.4

Table 3.4 One-Way Failure Assumption

Specimen Name	Description	Yield Line Analysis Results(kN)	Experimental Results (kN)	Experimental Results/Yield Line Analysis Results (%)
WBHN	Brick, Horizontal, Without Opening	36.6	57.9	158%
WBVN1	Brick, Vertical, Without Opening	27.1	41.0	152%
WBVN2	Brick, Vertical, Without Opening	41.4	41.6	100%
WPVN	Pumice, Without Opening	58.1	70.1	121%
WBVW	Brick, Vertical, Window Opening	37.8	56.1	148%
WPVW	Pumice, Window Opening	35.6	67.7	190%
WBVD	Brick, Vertical, Door Opening	13.8	21.1	153%
WPVD	Pumice, Door Opening	12.2	30.1	247%

It should, however, be noted that the lintel placed above the window and door openings affects the infill wall capacity considerably. The reinforcing effect of the lintel causes extra capacity during the out-of-plane loading due to the direct stiffening effect (Griffith and Vaculik,2007).

Both yield line analyses and the experimental results show that the capacity of the infill walls with door opening is the lowest. In contrast, the infill walls with window openings and without openings have higher out-of-plane load capacity.

While numerical comparisons justified one-way slab failure consideration, observed crack patterns of the specimens follow two-way slab behavior. However, despite the two-way slab crack pattern, the failure crack represented a one-way slab behavior at the ultimate stage. This situation highlights the alteration in infill wall behavior during out-of-plane loading. Figure 3.6 and Figure 3.7 show the failure state of the test specimens for clay brick and pumice concrete infill walls, respectively.

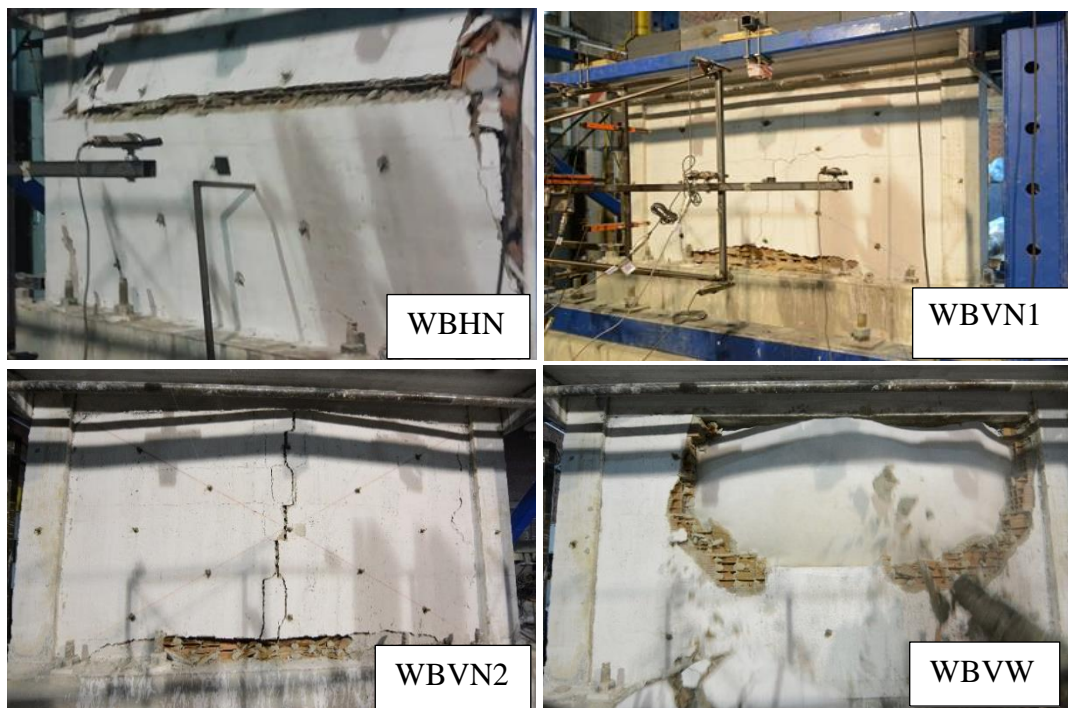


Figure 3.6. Failure State of Clay Brick Infill Walls



Figure 3.6. Failure State of Clay Brick Infill Walls (continued)

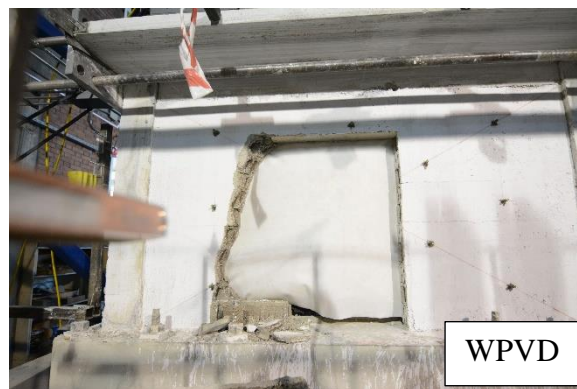
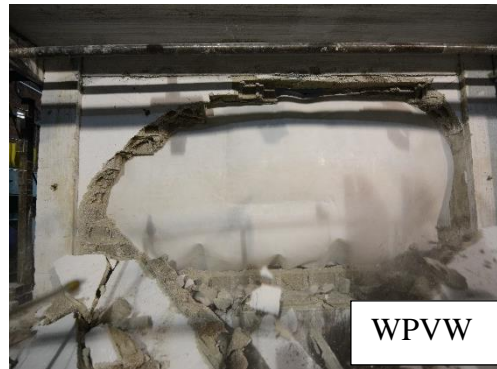


Figure 3.7. Failure State of Pumice Concrete Infill Walls

3.1.2 Demand Calculation of Infill Walls

This part of the document presents the determination of the out-of-plane (OOP) force demand of the infill walls according to an increased number of stories. The demand for the unreinforced infill wall, which is a non-structural element under out-of-plane loading, was determined as specified in TEC 2018. The demand of an infill wall is described as the equivalent seismic load acting on the element. The demand expression is given in Equation (3.5).

$$F_{ie} = \frac{m_e \cdot A_{ie} \cdot B_e}{R_e} \quad (3.5)$$

where m_e is the mass of the element, A_{ie} is the maximum total acceleration where the element or equipment is connected at the i^{th} floor during DD-2 ground motion, B_e and R_e are the importance and the reduction factors, respectively. These factors can be chosen for the related system in Chapter 6.2 of TEC 2018. The absolute acceleration, A_{ie} can be calculated by Equation (3.6) which is given by the TEC2018.

$$A_{ie} = \left(\frac{R}{I}\right) \cdot \left(\frac{2\pi}{T_p}\right)^2 \cdot u_i \quad (3.6)$$

where T_p is the effective natural period of the structure in the considered direction, u_i is the horizontal displacement calculated according to reduced earthquake loads applied to the i^{th} floor of the structure in the considered direction, R and I are reduction and importance factors of the structure, respectively. These factors can be chosen for the related system in Chapter 4.3 and Chapter 3.1 of TEC 2018, respectively.

The demand for the unreinforced infill walls was calculated with two different displacement approaches, namely by using FEMA356 and TEC2018. The demand analysis of the infill walls was performed for two cities with three different soil classes, ZA, ZC, and ZE, using FEMA356 and TEC2018. Ankara and İstanbul are the chosen cities for this study. The response spectra parameters of the cities for

different soil classes were obtained with the help of the official government website www.thtd.afad.gov.tr. The difference between the two approaches is the determination of the displacement. The displacement was calculated with uniform drift assumption according to TEC 2018, as stated in Chapter 4.9, while it is the calculated coefficient method, which is a nonlinear static procedure used to obtain the maximum global displacement, according to FEMA 356, as stated in Chapter 3.3. According to TEC 2018, the displacement depends on the drift ratio, the total story height of the structure, the type of structure, and the earthquake ground motion ratio of the zone where the structure is built. However, the target displacement depends on the number of stories, spectral acceleration, and the period of the structure in FEMA 356. The displacement formulations are given in Equation (3.7) and Equation (3.8) for TEC 2018 and FEMA 356, respectively.

$$\lambda \cdot \frac{\delta_{imax}}{h_i} \leq 0.008K \quad (3.7)$$

where λ is the ratio of the elastic design spectral acceleration of DD-3 earthquake ground motion to the elastic design spectral acceleration of DD-2 earthquake ground motion. Ground motions are defined for the predominant vibration period of the structure in the considered direction. Detailed information about the earthquake ground motion is explained in Chapter 2.2 of TEC 2018. K is a coefficient defined as 1 and 0.5 for reinforced concrete and steel constructed structures, respectively. h_i is the height of the i^{th} floor and δ_i is the displacement of the i^{th} floor.

$$u_t = C_0 \cdot C_1 \cdot C_2 \cdot C_3 \cdot S_a \cdot \frac{T_e^2}{4\pi^2} \quad (3.8)$$

where T_e is the effective fundamental period of the structure in the considered direction and S_a is the spectral acceleration corresponding to the effective period of the structure. C_0 , C_1 , C_2 , and C_3 are the modification factors used to produce the estimated maximum global displacement by modifying the linear elastic response of the equal single-degree-of-freedom system. C_0 modifies the spectral displacement of an equal single-degree-of-freedom system to the maximum displacement of the building's multi-degree-of-freedom system. Table 3.5 shows the suggested C_0

values. C_1 modifies the expected maximum inelastic displacement to displacements calculated for the linear elastic response. C_2 is the modification factor applied to indicate how the maximum displacement response is affected by the pinched hysteretic shape, stiffness degradation, and strength deterioration. Table 3.6 shows the suggested C_2 values. C_3 is the modification factor applied to indicate increased displacements due to dynamic P- Δ effects.

The effective natural period (T_e) of the structure was calculated for different story numbers by using the equation defined in TEC 2018. The formulation is shown in Equation 3.9.

$$T_{pA}(T_e) = C_t \cdot H_N^{0.75} \quad (3.9)$$

Table 3.5 Suggested C_0 Values

Number of Stories	<i>Shear Buildings</i>		<i>Other Buildings</i>
	<i>Uniform Load Pattern</i>	<i>Triangular Load Pattern</i>	<i>Any Load Pattern</i>
	1	1.00	1.00
2	1.15	1.20	1.20*
3	1.20	1.20	1.30*
5	1.20	1.30	1.40*
10+	1.20	1.30	1.50*

*The bolded values are the coefficient values chosen for the analysis.

Table 3.6 Suggested C_2 values

Structural Performance Level	$T \leq 0.1$ second		$T \geq T_s$ second	
	<i>Framing Type 1</i>	<i>Framing Type 2</i>	<i>Framing Type 1</i>	<i>Framing Type 2</i>
	Immediate Occupancy	1.00	1.00	1.00*
Life Safety	1.30	1.00	1.10	1.00
Collapse Prevention	1.50	1.00	1.20	T1.00

*The bolded values are the coefficient values chosen for the analysis.

where C_t is the coefficient equal to 0.1 for the reinforced concrete structures, H_N is the total height of the upper section of the structure above the basement floors.

Although the equations were used during the demand determination of the infill walls, the definition of the parameters was also concerned in each step of analysis since two different codes were combined. Thus, some of the formulas needed to be modified.

The absolute acceleration given in Equation (3.2) is calculated with the horizontal displacement calculated according to reduced earthquake loads that affect the i^{th} floor of the structure in the considered direction. However, the calculated displacements by using FEMA356 and TEC2018 are the maximum total displacements. In light of this situation, the absolute acceleration was calculated without a reduction factor. The modified equation is shown in Equation (3.10):

$$A_{ie} = \left(\frac{2\pi}{T_p} \right)^2 \cdot u_t \quad (3.10)$$

Since the value of λ gives almost the same result regardless of the soil type, the use of Equation 3.1 as given was not reasonable. Instead of analyzing uniform drift according to different soil types, a drift ratio was chosen. Uniform displacement calculated by TEC2018 was determined with a 2% drift ratio assumption. Thus, Equation 3.11 was modified, as shown below.

$$\frac{\delta_{imax}}{h_i} \leq 0.02 \quad (3.11)$$

The demand calculation was performed for the simulated infill wall types by the experimental study that is mentioned in Chapter 2. Since the specimens of the experimental study are $\frac{1}{2}$ scaled walls, the demand calculations were performed for the fully scaled infill walls. The outcomes of the demand calculations based on the number of stories of the reinforced concrete building are shown for each type of infill wall according to FEMA356 for both Istanbul and Ankara in Figure 3.8 and Figure 3.9, respectively.

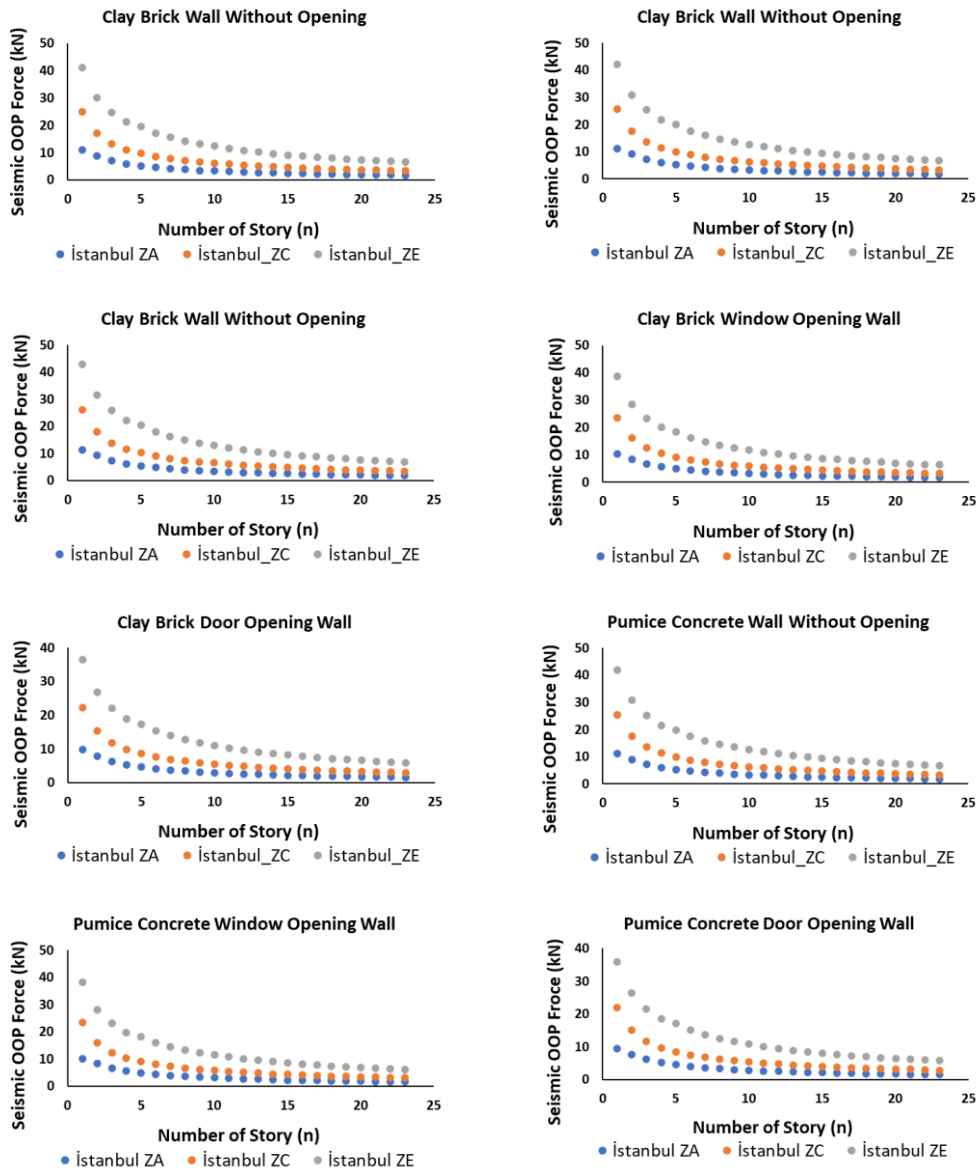


Figure 3.8. Demand and Story Number Relation of İstanbul Using FEMA356

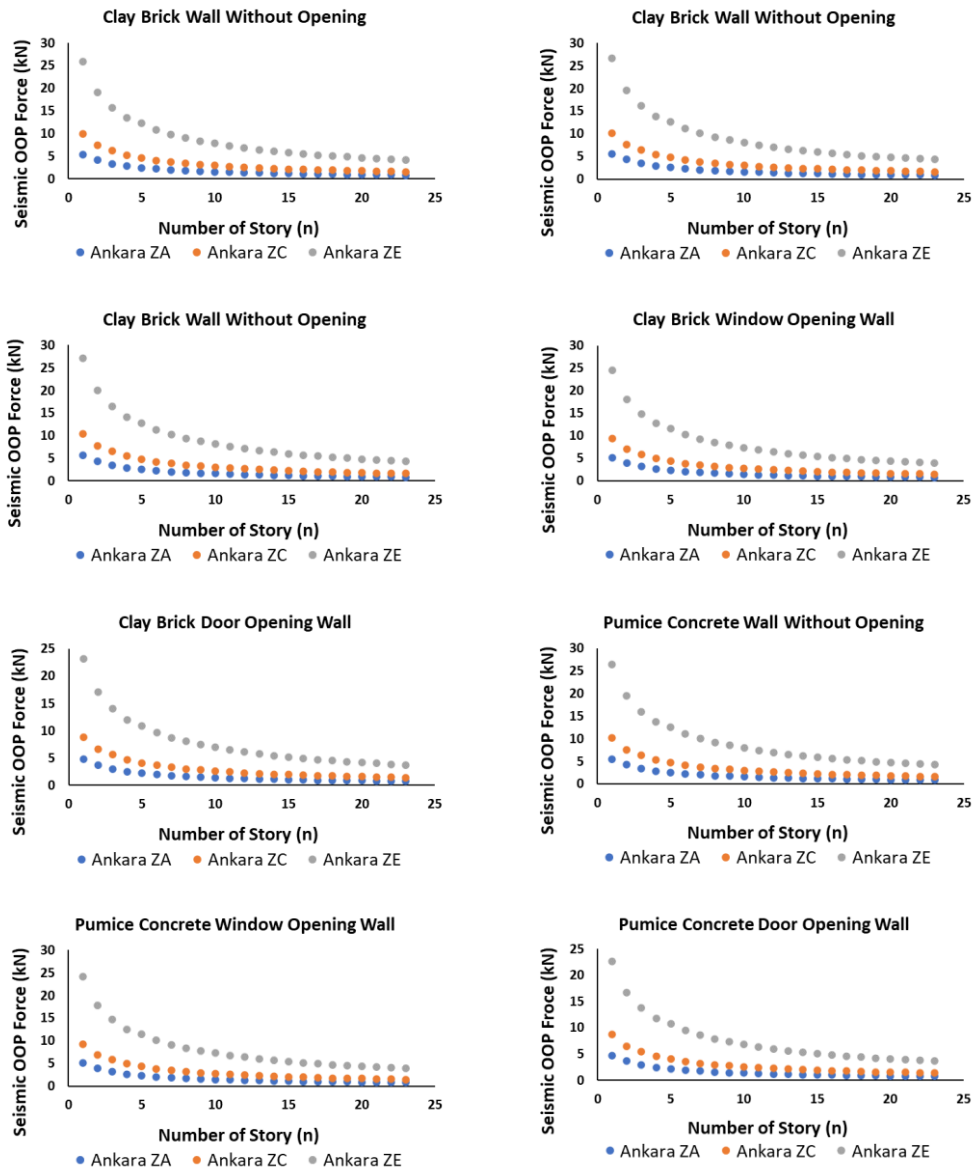


Figure 3.9. Demand and Story Number Relation of Ankara Using FEMA356

The calculated demand values of infill walls with a uniform drift approach using TEC2018 for each specimen type were also calculated for İstanbul and Ankara. The demand values of infill walls with two different displacement approaches are compared according to the number of stories of the structure. The comparisons are presented in Figure 3.10 and Figure 3.11 for İstanbul and Ankara, respectively.

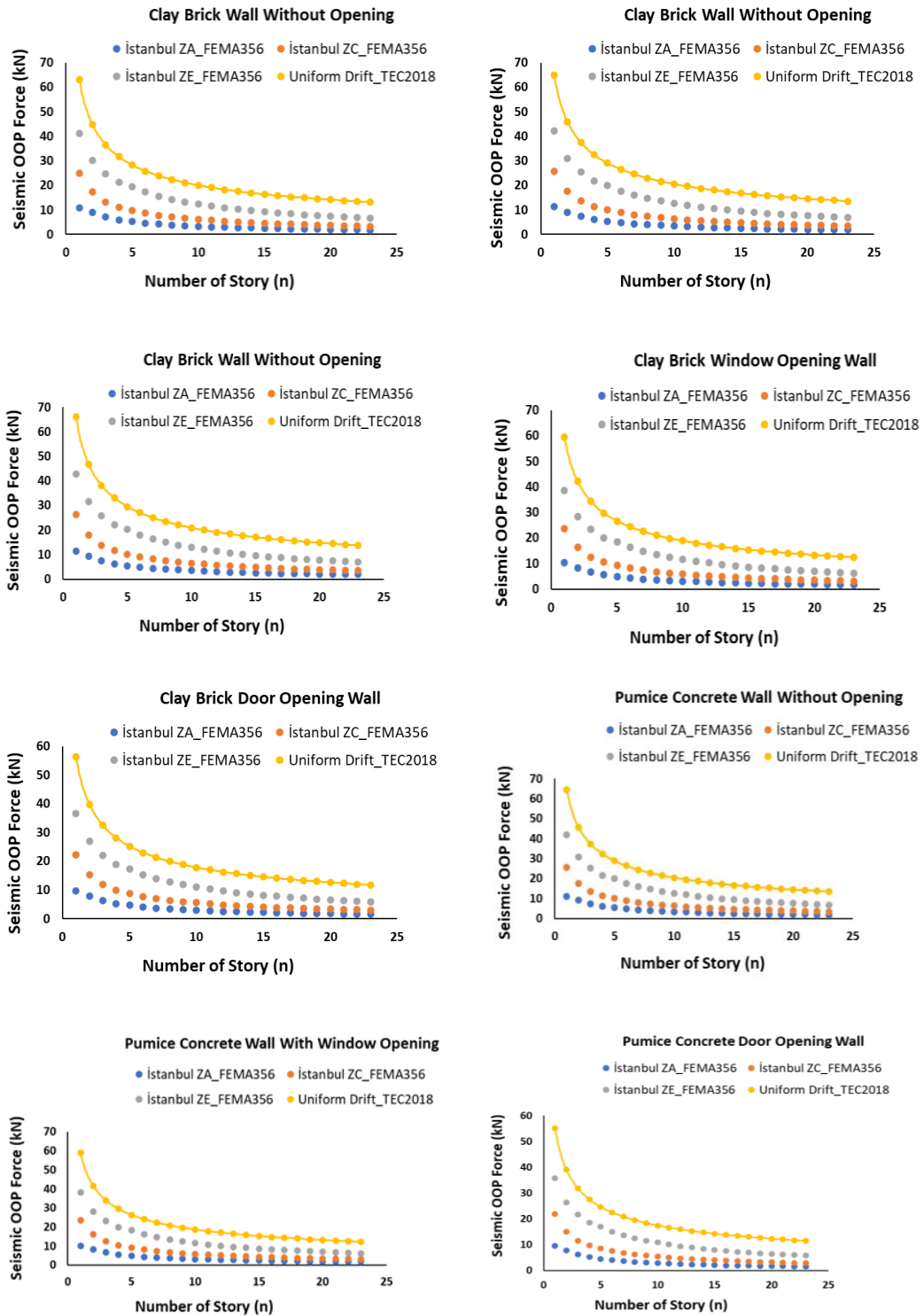


Figure 3.10. Comparison of Demand Capacities Using FEMA356 and TEC2018 for İstanbul

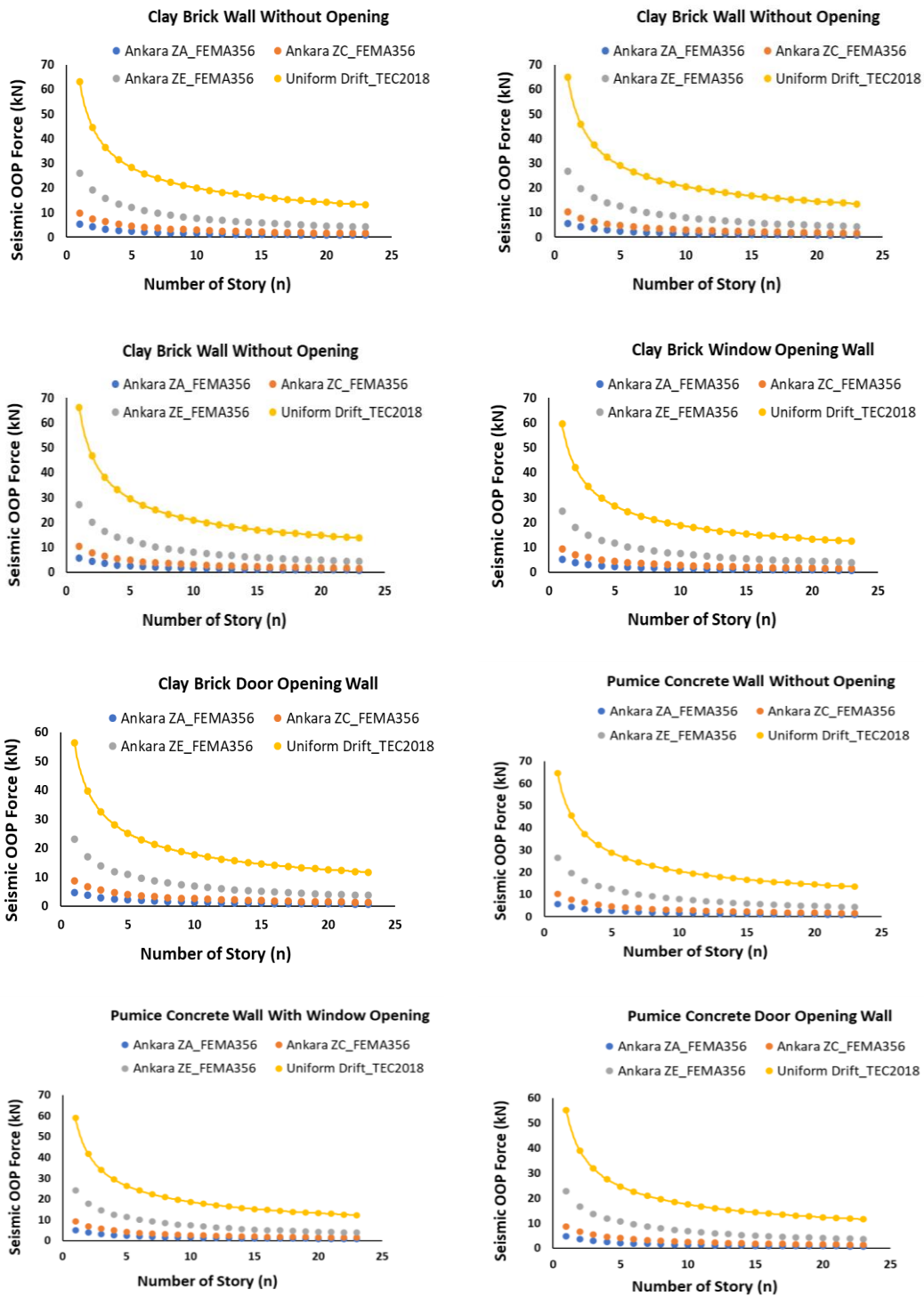


Figure 3.11. Comparison of Demand Capacities Using FEMA356 and TEC2018 for Ankara

In addition to comparing the demand calculations as the last step of calculations, another comparison was conducted for two cities. Considering the performed experimental study, the determined demands of the infill walls were compared to the fully scaled experimental results to get an idea of whether or not the infill wall requirements are sufficient as the number of stories of the structure increases. Since the uniform drift approach resulted in higher demand values, the test results are compared with the demand calculated with the uniform drift approach, according to TEC 2018. The results of the fully scaled specimens are reduced by 15% (0.85 Vu), so the highest force demand (seismic OOP Force) is compared to the lower load carrying capacity to stay on the safe side. The comparison is presented in Figure 3.12

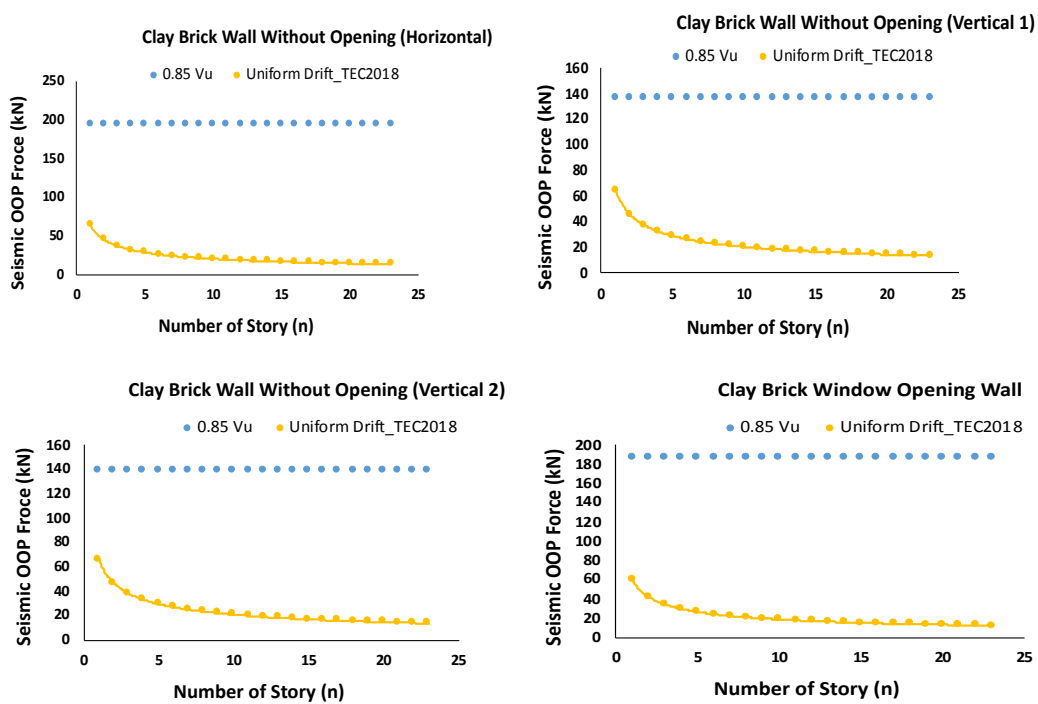


Figure 3.12. Demand and Capacity Comparison of the Infill Walls

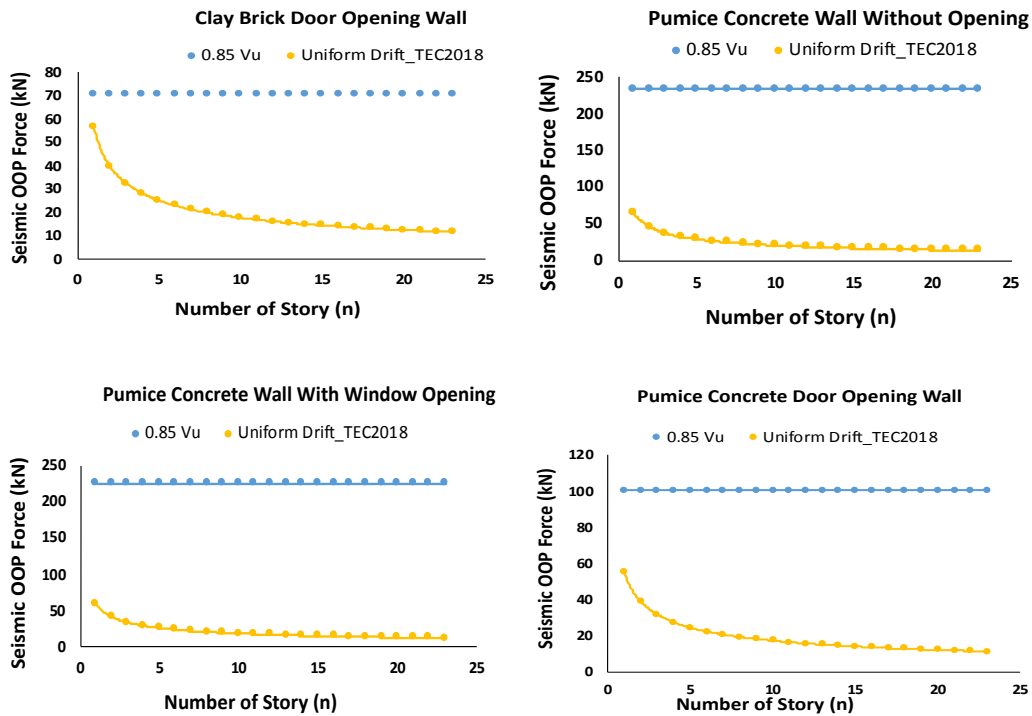


Figure 3.12. Demand and Capacity Comparison of the Infill Walls (continued)

3.1.2.1 Discussion of the Demand Calculation of Infill Walls

The demand calculations of infill walls, according to TEC 2018, were performed for two cities to understand the difference between high and low seismic zones. İstanbul and Ankara were chosen for high and low seismic zones, respectively. Two different approximations were used to estimate the displacements: the target displacement according to FEMA 356 and the uniform drift according to TEC 2018.

The outcomes of the demand analysis using target displacement according to FEMA 356 shows that as the occurrence probability of a seismic event increases, the demand value of the infill walls also increases. The comparison of Figure 3.8 and Figure 3.9 indicates that the demand value of İstanbul is much higher than Ankara. The reason for having higher ground acceleration leads to higher maximum displacement. Higher displacement causes higher absolute acceleration, and this workflow resulted in higher demand.

As the number of stories increases, since the shear force decreases on each floor, the demand and the absolute acceleration also decrease for the infill walls, although the maximum displacement demand increases. This situation is observed for all three soil types. The corresponding effective ground acceleration decreases as the soil gets stiffer (from ZE to ZA). Thus, less acceleration creates less displacement. These are the reasons for obtaining different demand values due to the difference in seismic zones and soil types. However, the demand calculations with uniform drift approximation are the same for the two cities. Demand calculations with the uniform drift depend on the same displacement regardless of the ground acceleration because the calculated displacement depends on only the drift ratio and the total story height. The demand estimations with two different displacement approximations show that uniform drift displacement approximation results in higher demand values which are more conservative considering the demand values calculated using FEMA 356, as shown in Figure 3.10 and Figure 3.11.

It is important to observe whether the estimated demand on the infill walls corresponds to the capacity of these members. Consequently, the experimental results of the $\frac{1}{2}$ scaled infill walls were modified for full-scale infill walls, and the expected capacities of the infill walls under out-of-plane loading were determined. Since infill walls were produced perfectly in laboratory conditions, the capacities of the infill walls are reduced by 15%. The reduced capacities and the estimated maximum demand values were compared to simulate the most hazardous conditions. As shown in Figure 3.12, even the highest demand estimation satisfies the reduced capacities for all types of infill walls tested with two different infill materials.

3.2 Design Thickness of Infill Walls

The height-to-thickness ratio of the unreinforced infill walls is an important issue that should be considered due to the high risk of damage and collapse in a failure state. The effective acceleration on a wall is found as the most influential factor. In

this context, many experimental and numerical studies have been performed on different kinds of infill walls by the related disciplines (Dave and Seah,1989; Calvi and Bolognini,2001; Edri and Yankelevsky, 2017; Oliiae and Magenes,2016; Ricci et al., 2018; Di Domenica et al. 2019). This part of the study specifies the design thickness of unreinforced infill walls for different spectral accelerations. Thus, a minimum thickness of infill walls can be chosen for different regions at different seismic levels.

The previous section presented that different earthquake regions have different demands due to differences in spectral acceleration. Moreover, the demand analysis conducted in Chapter 3.12 showed that the demand for the infill walls also depends on the story number. The number of stories and the effective spectral acceleration acting on the structure are some of the most important parameters affecting the out-of-plane demand of the infill walls. However, more important is the ability of the infill wall capacity to meet demand. The unreinforced infill walls should be designed considering the related demand in the direction of consideration.

Furthermore, the performed design of the infill wall shout not only meets the demand but also be economical from the engineering point of view. In this part of the work, the design of the infill wall was studied. Additionally, the thickness of the infill walls was associated with the capacity of the wall to satisfy the demand. In other words, the thickness of the infill wall is designed and specified according to its expected demand. In that spirit, the capacity of the simply supported infill wall with one-way failure mode and the estimated out-of-plane demand, according to TEC 2018, are associated. As a result, a formula was obtained and presented in Equation 3.12.

$$\left(\frac{L}{t}\right) = \frac{4 \cdot R_e \cdot f_t}{3 \cdot \gamma \cdot B_e \cdot L \cdot S_a \cdot C_0 \cdot C_1 \cdot C_2 \cdot C_3} \quad (3.12)$$

where L is the length of the infill wall, T is the thickness of the infill wall, γ is the unit weight of the infill material, B_e and R_e are the importance and the reduction factors, respectively, as mentioned in Equation 3.1. C_0 , C_1 , C_2 , and C_3 are the modification factors used to produce the estimated maximum global displacement,

as mentioned in Equation 3.4. f_t is the flexural strength of the plaster on the infill wall. S_a is the spectral acceleration corresponding to the effective natural period of the structure.

As shown in Equation 3.8, the slenderness of an infill wall is related to the spectral acceleration of the structure, length of the infill wall, and unit weight of the infill material. The formula contains modification factors obtained from FEMA 356. During the derivation of Equation 3.8, the target displacement approach was used.

The design thickness of the infill walls was determined for two different infill materials, namely clay brick and pumice concrete, considering different spectral acceleration levels with different flexural strength values of the plaster. As the unit weights 1500 kg/m^3 and 860 kg/m^3 are used for the clay brick and pumice concrete infill walls, respectively. It should be noted that the height (L) of the story was taken as 2.6 m.. The calculated design thicknesses for the infill walls considering the story number of the structure are given in Figure 3.13 and Figure 3.14 for the clay brick and the pumice concrete infill walls, respectively.

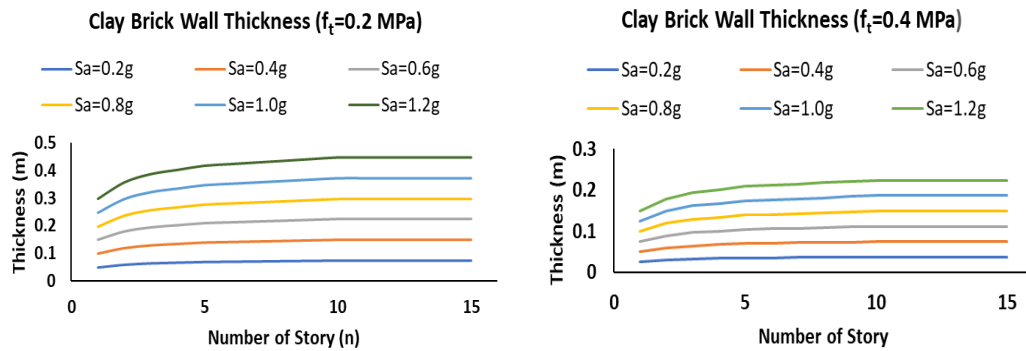


Figure 3.13. Design Thickness of Clay Brick Infill Walls

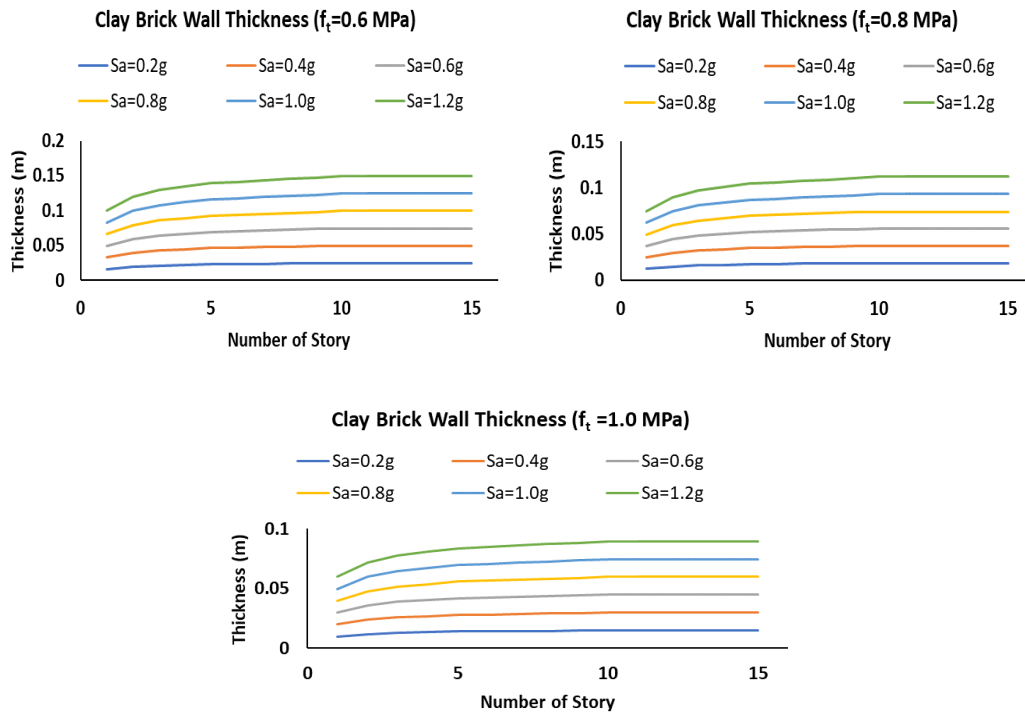


Figure 3.13. Design Thickness of Clay Brick Infill Walls (continued)

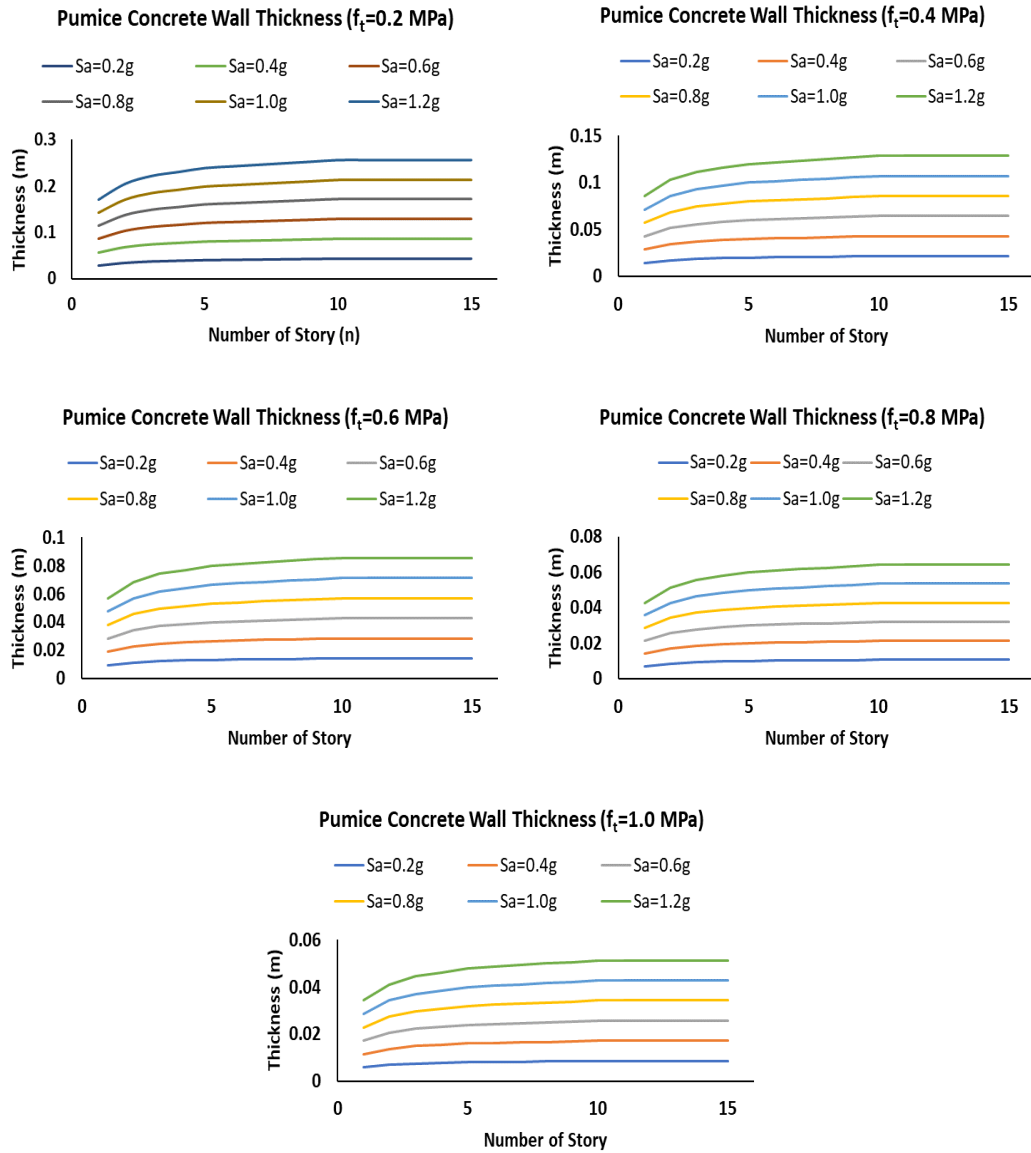


Figure 3.14. Design Thickness of Pumice Concrete Infill Walls

3.2.1.1 Discussion of the Design Thickness of Infill Walls

The design thicknesses of the infill walls were determined, taking into account the capacity of the infill wall and the demand acting on the member. First, the infill wall's slenderness was obtained by equating the infill wall capacity to the demand. In the second step, the thickness was determined using the obtained slenderness ratio

equation presented as Equation 3.8. The design thickness was calculated for different spectral acceleration levels and flexural strength capacities. The results are given for clay brick and pumice concrete infill materials in Figure 3.13 and Figure 3.14, respectively. As can be understood from the graphs, clay brick infill walls and pumice concrete infill walls have different design thicknesses with the same spectral acceleration and flexural strength. The infill walls with clay brick infill material require a thicker design than those with pumice concrete. The thickness of the clay brick infill wall is almost 1.7 times thicker than pumice concrete for the same spectral acceleration and flexural strength of the plaster used to build the wall.

Another result of estimating the design thickness is the noticeable change in thickness when the spectral acceleration, which corresponds to the effective natural period of the structure, changes. When it is assumed that the same flexural strength is used for the infill wall as the spectral acceleration increases, the demand on the wall also increases. Thus, the increased demand causes a thicker wall. On the other hand, when it is assumed that the same spectral acceleration is effective on the infill wall, as the flexural strength of the plaster increases, the capacity of the infill wall also increases. The increased capacity causes the wall to be thinner. This part presents the design thickness of the infill walls and how it changes due to different parameters such as spectral acceleration, flexural strength, and infill material. According to calculations, the thickness of the half-scaled infill wall is enough to bear the out-of-plane force of up to 1.8g spectral acceleration.

The analysis results of 10 and higher story numbers for different flexural strength values are given in Table 3.7, Table 3.8, Table 3.9, Table 3.10, and Table 3.11.

Table 3.7 Design Wall Thickness for 0.2 MPa Flexural Strength

Flexural Strength of the Plaster (MPa)	Spectral Acceleration (g)	Clay Brick Wall Thickness (cm)	Pumice Concrete Wall Thickness (cm)
0.2	0.2	7.5	4.5
	0.4	15.0	8.5
	0.6	22.5	13.0
	0.8	30.0	17.0
	1.0	37.0	22.0
	1.2	45.0	26.0

Table 3.8 Design Wall Thickness for 0.4 MPa Flexural Strength

Flexural Strength of the Plaster (MPa)	Spectral Acceleration (g)	Clay Brick Wall Thickness (cm)	Pumice Concrete Wall Thickness (cm)
0.4	0.2	4.0	2.0
	0.4	7.5	4.5
	0.6	11.0	6.5
	0.8	15.0	9.0
	1.0	19.0	11.0
	1.2	23.0	13.0

Table 3.9 Design Wall Thickness for 0.6 MPa Flexural Strength

Flexural Strength of the Plaster (MPa)	<i>Spectral Acceleration (g)</i>	<i>Clay Brick Wall Thickness (cm)</i>	<i>Pumice Concrete Wall Thickness (cm)</i>
0.6	0.2	2.5	1.5
	0.4	5.0	3.0
	0.6	7.5	4.5
	0.8	10.0	6.0
	1.0	12.5	7.0
	1.2	15.0	9.0

Table 3.10 Design Wall Thickness for 0.8 MPa Flexural Strength

Flexural Strength of the Plaster (MPa)	<i>Spectral Acceleration (g)</i>	<i>Clay Brick Wall Thickness (cm)</i>	<i>Pumice Concrete Wall Thickness (cm)</i>
0.8	0.2	2.0	1.0
	0.4	4.0	2.0
	0.6	6.0	3.0
	0.8	7.5	4.5
	1.0	9.5	5.5
	1.2	11.0	6.5

Table 3.11 Design Wall Thickness for 1.0 MPa Flexural Strength

Flexural Strength of the Plaster (MPa)	<i>Spectral Acceleration (g)</i>	<i>Clay Brick Wall Thickness (cm)</i>	<i>Pumice Concrete Wall Thickness (cm)</i>
1.0	0.2	1.5	1.0
	0.4	3.0	2.0
	0.6	4.5	3.0
	0.8	6.0	3.5
	1.0	7.5	4.5
	1.2	9.0	5.0

CHAPTER 4

CONCLUSION

The behavior and seismic performance of unreinforced infill walls under out-of-plane loads are reported within the context of this thesis. This study includes an experimental study, yield line analysis, seismic demand analysis, and determination of the design thickness of the infill walls. Infill walls were constructed with two different infill materials, namely clay brick and pumice concrete. The experimental study conducted in Uğur Ersoy Structural Laboratory at Middle East Technical University contains eight out-of-plane tests for infill walls. The infill walls were constructed within a one-bay, one-story, half-scaled RC frame and loaded by an airbag in the out-of-plane direction. The presence of the openings, size of the openings, and infill materials was chosen as parameters to study for the experimental part, yield line analysis part, and seismic demand analysis part. The yield line analysis was performed to estimate the behavior and the failure mode of infill walls by comparing them with the result of the experiments. The demand analysis was performed for two different cities in Turkey to simulate high and low seismic zone according to TEC 2018.

Additionally, two different displacement calculation approximations were used. The results were compared considering some specified variables. As the last step of the study, the design thickness of infill walls was obtained for clay brick and pumice concrete infill walls using TEC 2018. The highlighted outcomes are summarized below.

- The experimental study showed that the orientation of the infill material affects the out-of-plane capacity of infill walls. The specimen constructed with horizontally placed bricks (WBHN) behaved better than those with vertical brick alignment (WBVN1 and WBVN2).

- The specimens with door openings (WBVD and WPVW) have the lowest out-of-plane load-carrying capacity for both clay brick and pumice concrete infill walls. The reason is attributed to the massive opening in the wall.
- In contrast, although specimens with a window opening in infill walls (WBVW and WPVW) were expected to have lower capacity than those without an opening (WBVN1, WBVN2, and WPN), the experiments resulted in higher or equal out-of-plane load-carrying capacity for both infill materials.
- The out-of-plane load-carrying capacities of the pumice concrete infill walls for all specimens are higher than the companion specimens with clay brick infills. However, the pumice concrete has a lower unit weight. This difference can be attributed to the tongue-and-groove side connections between the pumice concrete blocks.
- Yield line analyses of the infill walls with one-way slab behavior assumption with simply-supports matched the best experimental results.
- The crack patterns at the failure stage of the tests also confirm the one-way yield line analysis results.
- The observed crack patterns during the tests and failure stages showed that the behavior of the infill wall under out-of-plane loading changed from a two-way behavior to a one-way behavior.
- According to TEC 2018, the demand analysis gives higher force demand with uniform drift displacement approximation. The target displacement approximation of FEMA 356 gives lower force demand when all the other parameters are the same.
- Infill walls constructed with pumice concrete blocks required lower force demand and higher load-carrying capacity. This tendency can be attributed to the tongue and groove at the side of blocks.
- As soil type changes from poor-bearing to strong-bearing (from ZE to ZA), effective spectral acceleration and demand decrease. Moreover, high seismic

zones require higher force demand than lower seismic zones for the same type of soil.

- The 15% reduced load-carrying capacities of the tests are sufficient compared with the demand calculations using the uniform drift approach for the different number of stories. Therefore, it can be said that the mortar and plaster wall components and infill wall material used have sufficient load-carrying capacity even for high seismic risk areas such as Istanbul.
- The calculation of the design thickness of the infill walls has shown that the infill materials, the spectral acceleration corresponding to the effective natural period of the structure, the number of stories of the structure, and the flexural strength of the plaster/mortar influence the demands and thus the design thickness of the infill walls.
- The minimum required thickness of the infill walls can be predicted by associating the capacity and the demand of the infill walls. Demand determinations were performed using the displacement approach of FEMA356. The capacity estimation was done by using a simply-supported one-way failure state to be on the safe side.
- Increased spectral acceleration causes infill walls to be thicker for the same flexural strength and number of stories due to increased demand. In contrast, increased flexural strength causes infill walls to be thinner for the same spectral acceleration and number of stories due to increased capacity.
- As the number of stories, up to 10 stories, increases, the minimum required design thickness of the infill walls increases since modification factors are constant after 10 stories, according to FEMA 356.
- The pumice concrete infill walls require a smaller thickness, considering the clay brick infill walls for the same conditions.

REFERENCES

Akhoundi, F., Vasconcelos, G., & Lourenço, P. (2020). Experimental out-of-plane behavior of brick masonry infilled frames. *International Journal of Architectural Heritage*, 14(2), 221-237.

American Society of Civil Engineers. (2017, December). *Seismic evaluation and retrofit of existing buildings*. American Society of Civil Engineers.

Anić, F., Penava, D., Abrahamczyk, L., & Sarhosis, V. (2020). A review of experimental and analytical studies on the out-of-plane behaviour of masonry infilled frames. *Bulletin of Earthquake Engineering*, 18(5), 2191-2246.

ASTM C109/C109M-16a Standard Test Method for Compressive Strength of Hydraulic Cement

Mortars (Using 2-in. or [50-mm] Cube Specimens), ASTM International, West Conshohocken, PA, 2016.

ASTM C348-18 Standard Test Method for Flexural Strength of Hydraulic – Cement Mortars, ASTM International, West Conshohocken, PA, 2018.

Binici, B., Canbay, E., Aldemir, A., Demirel, I. O., Uzgan, U., Eryurtlu, Z., ... & Yakut, A. (2019). Seismic behavior and improvement of autoclaved aerated concrete infill walls. *Engineering Structures*, 193, 68-81.

Brown, J. P., & Maji, A. K. (2002, June). Blast proofing of unreinforced masonry (URM) walls with GFRP. In *15th ASCE engineering mechanics conference* (pp. 1-8)

BS 5628-3: 2005. (2005). *Code of Practice for the Use of Masonry—Part 3: Materials and Components, Design and Workmanship*.

Calvi, G. M., & Bolognini, D. (2001). Seismic response of reinforced concrete frames infilled with weakly reinforced masonry panels. *Journal of Earthquake Engineering*, 5(02), 153-185.

Canbay, E., Binici, B., Demirel, I. O., Aldemir, A., Uzgan, U., Eryurtlu, Z., & Bulbul, K. (2018). DEGAS: An innovative earthquake- proof AAC wall system. *ce/papers*, 2(4), 247-252.

Canbay, E., Ersoy, U., & Ozcebe, G. (2003). Contribution of reinforced concrete infills to seismic behavior of structural systems. *ACI Structural Journal*, 100(5), 637-643.

Chang, L. Z., Rots, J. G., & Esposito, R. (2022). Influence of openings on two-way bending capacity of unreinforced masonry walls. *Journal of Building Engineering*, 51, 104222.

Da Porto, F., Guidi, G., Dalla Benetta, M., & Verlato, N. (2013, June). Combined in-plane/out-of-plane experimental behaviour of reinforced and strengthened infill masonry walls. In *12th Canadian masonry symposium* (pp. 2-5).

Dawe, J. L., & Seah, C. K. (1989). Out-of-plane resistance of concrete masonry infilled panels. *Canadian Journal of Civil Engineering*, 16(6), 854-864.

DEMİREL, İ. O., Yakut, A., & BİNİCİ, B. (2018). Dolgu Duvarların Düzlem Dışı Yönde Hava Yastığı İle Deneyi. *Eskişehir Teknik Üniversitesi Bilim ve Teknoloji Dergisi B-Teorik Bilimler*, 6, 133-140.

Derakhshan, H. (2011). Seismic assessment of out of plane loaded unreinforced masonry walls (Doctoral dissertation, University of Auckland).

Derakhshan, H., Griffith, M. C., & Ingham, J. M. (2013). Out-of-plane behavior of one-way spanning unreinforced masonry walls. *Journal of Engineering Mechanics*, 139(4), 409-417.

Di Domenico, M., Ricci, P., & Verderame, G. M. (2019). Experimental assessment of the out-of-plane strength of URM infill walls with different slenderness and boundary conditions. *Bulletin of Earthquake Engineering*, 17(7), 3959-3993.

Di Domenico, M., Ricci, P., & Verderame, G. M. (2020). Experimental assessment of the influence of boundary conditions on the out-of-plane response of unreinforced masonry infill walls. *Journal of Earthquake Engineering*, 24(6), 881-919.

Dizhur, D., Walsh, K., Giongo, I., Derakhshan, H., & Ingham, J. (2018, August). Out-of-plane proof testing of masonry infill walls. In *Structures* (Vol. 15, pp. 244-258). Elsevier.

Doherty, K., Griffith, M. C., Lam, N., & Wilson, J. (2002). Displacement- based seismic analysis for out- of- plane bending of unreinforced masonry walls. *Earthquake engineering & structural dynamics*, 31(4), 833-850.

Edri, I. E., & Yankelevsky, D. Z. (2017). An analytical model for the out-of-plane response of URM walls to different lateral static loads. *Engineering Structures*, 136, 194-209.

Ehsani, M. R., Saadatmanesh, H., & Velazquez-Dimas, J. I. (1999). Behavior of retrofitted URM walls under simulated earthquake loading. *Journal of Composites for Construction*, 3(3), 134.

Federal Emergency Management Agency (FEMA356) (2000) *Prestandard and Commentary for the Seismic Rehabilitation of Buildings*, Washington, DC.

Ferreira, T. M., Costa, A. A., & Costa, A. (2015). Analysis of the out-of-plane seismic behavior of unreinforced masonry: A literature review. *International Journal of Architectural Heritage*, 9(8), 949-972.

Furtado, A., Rodrigues, H., Arêde, A., & Varum, H. (2016). Experimental evaluation of out-of-plane capacity of masonry infill walls. *Engineering Structures*, 111, 48-63.

Griffith, M. C., Magenes, G., Melis, G., & Picchi, L. (2003). Evaluation of out-of-plane stability of unreinforced masonry walls subjected to seismic excitation. *Journal of Earthquake Engineering*, 7(spec01), 141-169.

Griffith, M. C., & Vaculik, J. (2007). Out-of-plane flexural strength of unreinforced clay brick masonry walls. *TMS Journal*, 25(1), 53-68.

Ghobarah, A., & El Mandooh Galal, K. (2004). Out-of-plane strengthening of unreinforced masonry walls with openings. *Journal of Composites for Construction*, 8(4), 298-305.

Navas-Sánchez, L., & Bravo, J. C. (2022). A theory-based simplified trilinear model for characterisation of the out-of-plane behaviour of URM walls. *Engineering Structures*, 259, 114058.

Hak, S., Morandi, P., & Magenes, G. (2014, August). Out-of-plane experimental response of strong masonry infills. In *2nd European conference on earthquake engineering and seismology (Vol. 1)*.

Lawrence, S., & Marshall, R. (2000, June). Virtual work design method for masonry panels under lateral load. In *12 th Int. Brick/Block Masonry Conf. Proc. (Vol. 2, pp. 1063-1073)*.

Liberatore, L., AlShawa, O., Marson, C., Pasca, M., & Sorrentino, L. (2020). Out-of-plane capacity equations for masonry infill walls accounting for openings and boundary conditions. *Engineering Structures*, 207, 110198.

Lönhoff, M., Dobrowolski, C., & Sadegh-Azar, H. (2017). Analysis of the out-of-plane capacity of unreinforced masonry infill walls. *Procedia engineering*, 199, 693-698.

Manual, F. P. (2008). *Unified Facilities Criteria (UFC)*.

Martini, K. (1998, May). Finite element studies in the two-way out-of-plane failure of unreinforced masonry. In *Proceedings of the 6th National Conference on Earthquake Engineering, Seattle Washington (Vol. 31)*.

Milanesi, R. R., Morandi, P., Hak, S., & Magenes, G. (2021). Experiment-based out-of-plane resistance of strong masonry infills for codified applications. *Engineering Structures*, 242, 112525.

Oliaee, M., & Magenes, G. (2016, June). In-plane out-of-plane interaction in the seismic response of masonry infills in RC frames. In *Proceedings of the 16th International Brick and Block Masonry Conference, Padova, Italy* (pp. 26-30).

Murty, C. V. R., & Jain, S. K. (2000, January). Beneficial influence of masonry infill walls on seismic performance of RC frame buildings. In *12th world conference on earthquake engineering*.

Pasca, M., Liberatore, L., & Masiani, R. (2017). Reliability of analytical models for the prediction of out-of-plane capacity of masonry infills. *Structural engineering and mechanics*, 64(6), 765-781.

Paulay, T., & Priestley, M. N. (1992). *Seismic design of reinforced concrete and masonry buildings* (Vol. 768). New York: Wiley.

Pradhan, B., Zizzo, M., Di Trapani, F., & Cavaleri, L. (2022). Out-of-Plane Behavior of URM Infill: Accuracy of Available Capacity Models. *Journal of Structural Engineering*, 148(3), 04021292.

Ricci, P., Di Domenico, M., & Verderame, G. M. (2018). Experimental investigation of the influence of slenderness ratio and of the in-plane/out-of-plane interaction on the out-of-plane strength of URM infill walls. *Construction and Building Materials*, 191, 507-522.

Sorrentino, L., D'Ayala, D., de Felice, G., Griffith, M. C., Lagomarsino, S., & Magenes, G. (2017). Review of out-of-plane seismic assessment techniques applied to existing masonry buildings. *International Journal of Architectural Heritage*, 11(1), 2-21.

Technical Guidelines for Engineering Assessment (2017), The Seismic Assessment of Existing Buildings– Part C7: Moment Resisting Frames with Infill Panels, New Zealand.

Turkish Earthquake Code (TEC 2018) Ministry of Public Works and Settlement, Ankara, Turkey.

Vaculik, J. (2012). Unreinforced masonry walls subjected to out-of-plane seismic actions (Doctoral dissertation).

Yu, J., Gan, Y. P., Wu, J., & Wu, H. (2019). Effect of concrete masonry infill walls on progressive collapse performance of reinforced concrete infilled frames. *Engineering structures*, 191, 179-193.

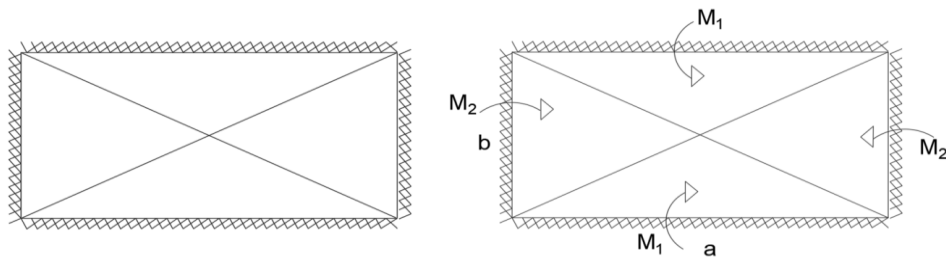
Xie, X., Qu, Z., Fu, H., & Zhang, L. (2021). Effect of prior in-plane damage on the out-of-plane behavior of masonry infill walls. *Engineering Structures*, 226, 111380.

APPENDIX

A. Yield Line Analysis Solutions for Infill Walls Without Opening

Load Carrying Capacity Calculation Four Sides Fixed-End Support Condition

Yield Pattern 1:



Assumed Yield Pattern and Corresponding Moments

Equating the external work to the internal work:

$$W_E = W_I$$

$$W_E = \Sigma A_i \cdot \delta_i \cdot w$$

$$W_I = \Sigma M_y l_y \theta_y + \Sigma M_x l_x \theta_x + \Sigma \alpha M_y l_y \theta_y + \Sigma \alpha M_x l_x \theta_x$$

$$\sigma = \frac{Mc}{I} \quad \rightarrow \quad M = \frac{\sigma I}{c} \quad \rightarrow \quad M_y = \frac{f_t \cdot b \cdot h^2}{6 \cdot a} \quad \& \quad M_x = \frac{f_t \cdot a \cdot h^2}{6 \cdot b}$$

Where h is the thickness of the wall and M_x and M_y are moment capacities per unit length.

$$W_{I,x} = \underbrace{2a \cdot \alpha M_x \cdot \theta}_{\text{Supports}} + \underbrace{2a \cdot M_x \cdot \theta}_{\text{slab}} \quad \text{and} \quad \theta = \frac{\delta}{b/2}$$

$$W_{I,x} = 4\delta \frac{a}{b} (\alpha M_x + M_x)$$

Similarly,

$$W_{I,y} = 4\delta \frac{b}{a} (\alpha M_y + M_y)$$

$$W_E = 2 \left[\frac{1}{2} b \frac{a \delta}{2 \cdot 3} w \right] + 2 \left[\frac{1}{2} a \frac{b \delta}{2 \cdot 3} w \right] = \frac{ab}{6} \delta w + \frac{ab}{6} \delta w$$

$$W_E = w \frac{ab}{3} \delta$$

$$4\delta \frac{a}{b} (\alpha M_x + M_x) + 4\delta \frac{b}{a} (\alpha M_y + M_y) = w \frac{ab}{3} \delta$$

The numeric values of the WBHN are given as follows:

$$a = 2300 \text{ mm}, b = 1300 \text{ mm}, f_t = 1.078 \text{ MPa}, h = 120 \text{ mm}$$

$$M_x = \frac{1.078 \times 2300 \times 120^2}{6 \times 1300} = 4577 \text{ Nmm/mm}$$

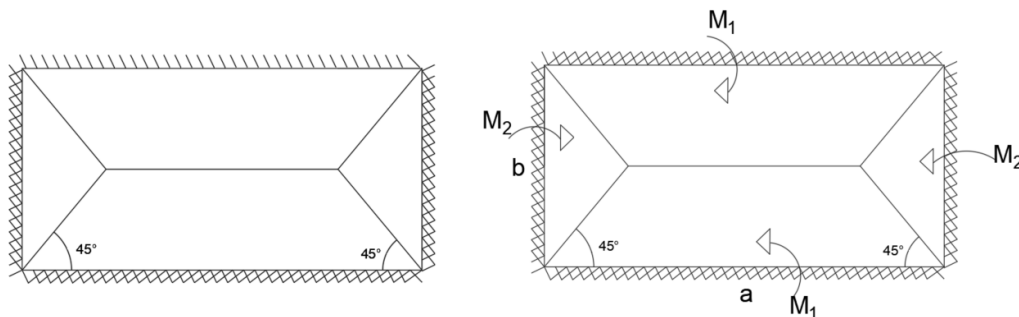
$$M_y = \frac{1.078 \times 1300 \times 120^2}{6 \times 2300} = 1462 \text{ Nmm/mm}$$

$$4 \frac{2300}{1300} (1 \times 4577 + 4577) + 4 \frac{1300}{2300} (1 \times 1462 + 1462) = w \frac{2300 \times 1300}{3}$$

$$w = 0.0716 \text{ N/mm}^2$$

$$W_{TOTAL} = w_{dist} Area = 0.0716 \times 2300 \times 1300 = 214.2 \text{ kN}$$

Yield Pattern 2:



Assumed Yield Pattern and Corresponding Moments

Equating the external work to the internal work:

$$W_E = W_I$$

$$W_E = \Sigma A_i \cdot \delta_i \cdot w$$

$$W_I = \Sigma M_y l_y \theta_y + \Sigma M_x l_x \theta_x + \Sigma \alpha M_y l_y \theta_y + \Sigma \alpha M_x l_x \theta_x$$

$$\sigma = \frac{Mc}{I} \rightarrow M = \frac{\sigma I}{c} \rightarrow M_y = \frac{f_t \cdot b \cdot h^2}{6 \cdot a} \quad \& \quad M_x = \frac{f_t \cdot a \cdot h^2}{6 \cdot b}$$

Where h is the thickness of the wall and M_x and M_y are moment capacities per unit length.

$$W_{I,x} = \underbrace{2a \cdot \alpha M_x \cdot \theta}_{\text{Supports}} + \underbrace{2a \cdot M_x \cdot \theta}_{\text{slab}} \quad \text{and} \quad \theta = \frac{\delta}{b/2}$$

$$W_{I,x} = 4\delta \frac{a}{b} (\alpha M_x + M_x)$$

Similarly,

$$W_{I,y} = 4\delta (\alpha M_y + M_y)$$

$$W_E = 2 \left[\frac{1}{2} b \frac{a \delta}{2 \cdot 3} w \right] + 4 \left[\frac{1}{2} \frac{b}{2} \frac{b}{2} \frac{\delta}{3} w \right] + 2(a-b) \left[\frac{1}{2} \frac{b}{2} \frac{\delta}{3} w \right] = \frac{b^2}{6} \delta w + \frac{b^2}{6} \delta w + \frac{(a-b)b}{6} \delta w$$

$$W_E = wb \left[\frac{a}{2} - \frac{b}{6} \right] \delta$$

$$4\delta \frac{a}{b} (\alpha M_x + M_x) + 4\delta \frac{b}{a} (\alpha M_y + M_y) = wb \left[\frac{a}{2} - \frac{b}{6} \right] \delta$$

The numeric values of the WBHN are given as follows:

$$a = 2300 \text{ mm}, b = 1300 \text{ mm}, f_t = 1.078 \text{ MPa}, h = 120 \text{ mm}$$

$$M_x = \frac{1.078 \times 2300 \times 120^2}{6 \times 1300} = 4577 \text{ Nmm/mm}$$

$$M_y = \frac{1.078 \times 1300 \times 120^2}{6 \times 2300} = 1462 \text{ Nmm/mm}$$

$$4 \frac{2300}{1300} (1 \times 4577 + 4577) + 4(1 \times 1462 + 1462) = w1300 \left[\frac{2300}{2} - \frac{1300}{6} \right]$$

$$w = 0.0630 \text{ N/mm}^2$$

$$= w_{dist} Area = 0.0630 \times 2300 \times 1300 = 188.5 \text{ kN}$$